UNIVERSITÀ POLITECNICA DELLE MARCHE

FACOLTÀ DI INGEGNERIA

Corso di Laurea magistrale in Ingegneria Edile-Architettura

WASTE-DERIVED NANOMATERIALS FOR SELF-CLEANING AND WATER PURIFICATION APPLICATIONS

NANOMATERIALI DERIVATI DA MATERIALI DI SCARTO PER APPLICAZIONI DI SELF-CLEANING E PURIFICAZIONE DELLE ACQUE INQUINATE

Advisor:

Prof. ssa Francesca Tittarelli

Coadvisor:

Dr. Qaisar Maqbool

Candidate:

Isabella Cavallini

A.A. 2022 / 2023

UNIVERSITÀ POLITECNICA DELLE MARCHE
Facoltà di Ingegneria
Corso di Laurea in Ingegneria Edile – Architettura
Via Brecce Bianche – 60131 Ancona (AN), Italy

Alla mia famiglia,

a chi c’è ancora e a chi non c’è più.

Contents

List of Figures

List of Tables

List of abbreviations

Advanced Oxidation Processes (AOPs)

Atomic layer deposition (ALD)

Bacterial Nano-Cellulose (BNC)

Carbon Nanotubes (CNTs)

Cellulose Nano-Crystals (CNCs)

Chemical vapor deposition (CVD)

Double Distilled water (ddH_2O)

Dymethylformalmide (DMF)

Dymethylsulfoxide (DMSO)

Electro-spun nanofiber membranes (ENMs)

Green Combustion (GC)

Green Synthesis (GS)

Heating, Ventilation, and Conditioning (HVAC)

Hydrochloric Acid Acid (HCl)

Indoor Air Quality (IAQ)

Iron Oxide (Fe_2O_3)

Methyl Orange (MO)

Methylene Blue (MB)

Nanocellulose (NCel)

Nanocomposites (NC)

Nano-Fibrillated Cellulose (NFC)

Nanoparticles (NPs)

Organo-halogenated Compounds (OA)

Polyacrylonitrile (PAN)

Polymerization Level (DP)

Reactive oxygen species (ROS)

Scanning Electron Microscopy (SEM)

Semi-Crystalline Nano-Cellulose (SCNC)

Sodium Hydroxide (NaOH)

Sulfuric Acid (H_2SO_4)

Titanium Dioxide (TiO_2)

Titanium Oxide Phosphate ($(TiO)_2P_2O_7$)

Titanium Oxide Phosphate ($Ti_2O(PO_4)_2$)

Titanium Oxide Phosphate (TiOP)

Trisodium Phosphate (Na_3PO_4)

Vapor deposition (PVD)

Volatile organic compounds (VOCs)

Water Contact Angle (WCA)

X-ray diffraction analysis (XRD)

Zinc Oxide (ZnO)

Abstract

The primary aim of this study is to employ green chemistry principles in the synthesis of Titanium Oxide Phosphate nanoparticles and Semi-crystalline Nanocellulose derived from waste, with the ultimate purpose of utilizing them for self-cleaning paints and water purification.

The first section of the research concerns the synthesis and characterization of the two nanoparticles (NPs) by comparing different methodologies to provide a greener and sustainable approach for the use of waste materials. Specifically, TiO_2 NPs are synthesized by processing titanium metal scrap through Green Synthesis (classical method) and Green Combustion (modified method). The obtained NPs are subjected to characterization through UV-vis spectroscopy, X-ray diffraction analysis (XRD), and Scanning Electron Microscopy (SEM), with a subsequent comparison of the results obtained from each of these methods. On the other hand, nanocellulose (NCel) is obtained from tissue paper waste through the acid hydrolysis method and characterized through SEM.

The second section refers to the application of the two NPs for self-cleaning applications and wastewater treatment. The main focus is on the effectiveness of the synthesized NPs and NCel regarding the adsorption and the photocatalytic degradation of pollutants in indoor and outdoor finishings (e.g., TiO_2-NPs) and water filtration nanoweb (e.g., NCel). Self-cleaning paint with TiOP NPs reached CV removal values of 91.56% in sunlight exposition and 61.86% in visible light exposition (GC 800 and GS 800). PAN/NCel nano-webs showed a maximum percentage of removal of 87.3% for PAN/NCel_10:01 and 94% for PAN/NCel_10:02.

Sommario

Lo scopo principale di questa ricerca è quello di applicare i principi della “Green Chemistry” nella sintesi di nanoparticelle a base di ossido di titanio e nanocellulosa ottenuti da materiali di scarto, con lo scopo ultimo di utilizzarli in applicazioni riguardanti l’Indoor Air Quality (IAQ) e il trattamento e depurazione delle acque.

La prima sezione della ricerca riguarda la sintesi e la caratterizzazione dei due nanomateriali confrontando diverse metodologie per fornire un approccio più green e sostenibile per l'utilizzo dei materiali di scarto. Nello specifico, le nanoparticelle di TiO_2 vengono sintetizzate a partire da trucioli di titanio provenienti dalla lavorazione del metallo tramite Green Synthesis (metodo classico) e Green Combustion (metodo modificato). Le particelle ottenute vengono sottoposte a caratterizzazione mediante spettroscopia UV-vis, analisi di diffrazione di raggi X (XRD) e microscopia elettronica a scansione (SEM), con successivo confronto dei risultati ottenuti da ciascuno di questi metodi. Mentre, la nanocellulosa è ottenuta da semplici fazzoletti di carta attraverso la tecnica più comunemente utilizzata di idrolisi acida, e viene successivamente caratterizzata mediante microscopia elettronica a scansione (SEM).

La seconda sezione si riferisce, invece, all'utilizzo dei due nanomateriali per applicazioni di self-cleaning e trattamento delle acque inquinate. Il focus è sull'efficacia dei materiali sintetizzati per quanto riguarda l'assorbimento e la degradazione fotocatalitica degli inquinanti nelle finiture interne ed esterne (TiO_2-NPs) e nelle membrane per il trattamento e depurazione delle acque (NCel). La vernice autopulente con TiOP NP ha raggiunto valori di rimozione di CV del 91.56% in esposizione alla luce solare e del 61.86% in esposizione alla luce visibile (GC 800 e GS 800). Le membrane PAN/NCel hanno riportato una percentuale massima di rimozione dell'87.3% per PAN/NCel_10:01 e del 94% per PAN/NCel_10:02.

Chapter 1
Introduction

In recent years, the significance of sustainable development has increased. This subject encompasses not only environmental sustainability but also social and economic aspects. The need for economically friendly growth has been recognized since the 1970s [1]. Now the international community acknowledges the reality of Planetary Limits. The rapid depletion of natural resources poses a long-term threat to the Earth's ecosystem. It is no longer feasible to adopt traditional development systems due to the associated risks. Consequently, the new development model must incorporate the concept of sustainability to ensure a future for our planet. Based on the information provided earlier, the use of materials sourced from organic and inorganic waste aim to offer a renewed perspective on waste regeneration.

In addition, the problem of pollution has gained relevance in the last decades. Environmental pollution, including water and air pollution, is a persistent problem that affects not only human beings but also the ecosystem [2], [3]. Organic dyes, characterized by their conjugated structures and photostability, are harmful to living organisms. Consequently, it is necessary to eliminate organic dyes from water sources and promote effective wastewater treatment. Several industries contribute to the release of synthetic dyes into the aquatic environment, with the textile industry being the largest culprit. Other industries, such as leather tanning, paper manufacturing, hair-colouring, and food production, also contribute significantly to this issue. Concerning water pollution, it has been estimated that globally, more than 800,000 tons of synthetic dyes are manufactured each year. Unfortunately, around 10−15% of these dyes are discharged into natural water bodies without undergoing proper treatment, primarily through industrial wastewater. To address these issues, various techniques have been developed, such as adsorption [4], biosorption [5], biodegradation [6], photodegradation [7], and electrochemical oxidation [8]. Among these, photodegradation stands out as one of the most widely employed methods, utilizing low-cost catalyst systems to break down the molecular structure of dyes [9], [10].

Nowadays, the Green Economy presents new opportunities, particularly in industrial production. There are new prospects for growth and investment that focus on sustainability. Innovative techniques enable the creation of new "recycled" materials that are both environmentally friendly and cost-effective. Moreover, nanotechnology offer intriguing possibilities in the industrial sector. By utilizing the unique properties of NPs, such as their composition, size, and shape, nanotechnologist can alter their characteristics. These processes can facilitate the production of novel nanocomposites (NC) with predetermined properties [11]. Nanotechnology enables the precise control of material properties by manipulating NPs. Through bottom-up or top-down approaches, NPs can be synthesized with specific compositions, sizes, shapes, and surface properties which allows the development of sustainable materials with tailored properties. This customizable nature of NPs makes them well-suited for a wide range of applications [11].

The actual interest in NC is particularly relevant for environmental remediation applications. Specifically, NPs can be engineered to efficiently remove pollutants from water or air, enabling the purification of contaminated environments. Additionally, NPs can serve as catalysts for degradation of harmful compounds or as sensors for environmental monitoring. NPs are also being investigated for water filtration and desalination processes. Nano-porous membranes or NC filters can effectively remove contaminants, bacteria, and salt particles from water, offering a sustainable solution for clean water supply [12].

It is worthwhile to note that while nanotechnology hold great promise for sustainable NPs, it is also essential to consider the potential environmental and health impacts of these materials during their life cycle. Proper risk assessment and responsible consumption are necessary to ensure the overall sustainability of NPs [13].

Considering the environmental aspects, two waste-derived nanomaterials are investigated in this research, with a focus on evaluating the sustainability impact of each process involved, from synthesis to application. By employing the principles of Green chemistry and Green synthesis, the process of synthesizing these nanomaterials becomes more sustainable. Green synthesis offers significant benefits over conventional methods, including cost-effectiveness, minimal pollution, and enhanced safety for both the environment and human health [14].

The main interest in this lies in the application of NPs and NC materials for self-cleaning paints and water decontamination. The NPs and NC selected for these applications are Titanium Oxide Phosphate (TiOP) NPs and NCel. Scientific research on these two materials is ongoing, and further studies are being conducted to explore their potential in different fields and optimize their performance for specific applications.

Particularly, the choice of using these two materials is due to the fact that both NPs and NCel exhibit high potential in the removal of pollutants in Self-Cleaning Paint and wastewater treatment. Numerous treatment technologies are available to address water pollution, each with varying degrees of success. However, many of these methods suffer from certain drawbacks, such as high operational and maintenance costs, the generation of toxic waste or by-products, and complex treatment procedures [15].

Photocatalytic removal of pollutants has gained importance in the last decades for its several advantages, including its non-toxic nature, high stability, absence of mass transfer limitations, the potential utilization of solar light for irradiation, and operation at room temperature [16]. Particularly, heterogeneous photocatalysis has gained significant attention as a promising technique among various Advanced Oxidation Processes (AOPs) for the effective treatment of water and wastewater. It has shown great efficacy in removing a wide range of pollutants, making it a highly promising method for water and wastewater treatment [17].

Among pollutants removal methods, use of semiconductor-based photocatalysts has also emerged as one of highly effective method applicable to both paint and water, even for contaminants present at very low concentrations. Among the various semiconductor materials suitable for this purpose, Titanium Dioxide (TiO_2) nanoparticles (TiO_2 NPs) has garnered extensive research and practical utilization as a photocatalytic material. Its exceptional catalytic activity, affordability, and photo-stability contribute to its popularity [10]. However, the practical implementation of TiO_2 as a photocatalyst faces a challenge due to its wide band gap, which mandates the use of ultraviolet (UV) radiation for photocatalytic activation. UV radiation, encompassing only 5% of the solar spectrum ($\lambda = 100 - 400$ nm), limits the effectiveness of TiO_2 NPs photocatalysis to this specific range. Consequently, there is a need to develop photocatalysts capable of being activated by visible light. This advancement would enable the utilization of the full solar spectrum or even common domestic lighting systems for efficient photoactivation [18].

The adsorption process is regarded as a efficient alternative in wastewater treatment due to its convenience, ease of operation, and simple design. Moreover, this process has the capability to effectively remove or minimize various types of pollutants, making it highly versatile and applicable in the realm of water pollution control [19]. Extensive research has been conducted on a wide range of low-cost adsorbents to assess their effectiveness in removing diverse pollutants from water and wastewater. Generally, a "low cost" adsorbent requires minimal processing, is readily available in nature, or is derived from industrial by-products or waste materials [20]. However, it has been observed that numerous low-cost adsorbents derived from various sources exhibit limited or inferior adsorption capabilities compared to commercial activated carbon when it requires removing pollutants from water. Indeed, activated carbon is widely recognized as a versatile adsorbent for treating effluents and is commonly employed for the removal of diverse pollutants from water [21]. Nonetheless, its extensive application in wastewater treatment is occasionally hindered by its higher cost. On the other hand, due to the environmental friendliness, cost-effectiveness, stability, and effective adsorption, natural biopolymer materials have gained more popularity. Among these biopolymers, cellulose stands out due to its numerous advantages, including high yield, non-toxicity, and a high content of hydroxyl groups that facilitate further modifications [22].

Considering above, it is obvious that nanotechnology offers the possibility to develop highly efficient materials that can overcome a wide range of unresolved challenges in environmental depollution.

The main objectives of this research are:

1. The development of waste-derived materials to offer environmentally sustainable alternatives to conventional technologies.

2. The evaluation of different synthesis methods to determine the optimal approach that combines both the efficiency of the synthesized material and the sustainability of the method.

3. The application of TiOP as additive in Self-Cleaning Paints for the photocatalytic removal of CV organic dye.

4. The addition of NCel to enhance the surface properties of PAN electro-spun nanowebs utilized in wastewater treatment for CV removal.

5. The evaluation of the removal efficiency and reusability of the synthesized materials.

6. The comparation of the applied methods with the currently available technologies.

7. The statement of the existing advantages and limitations on the application of the methods and synthesized nanomaterials.

Chapter 2
Literature review

2.1 Nanotechnologies and nanomaterials for environmental remediation

2.1.1 Introduction

Environmental pollution is a pressing global concern that accelerates each year, inflicting severe impacts on the Earth. The atmosphere, water and soil are contaminated with organic and inorganic substances stemming from different sources. Alongside, the rapid advancement of nanotechnology has developed significant interest in harnessing the potential of nanomaterials for enhanced monitoring and remediation systems.

The utilization of nanomaterials for environmental depollution, presents a challenging and novel approach that facilitates the rapid and effective elimination of pollutants from contaminated sites. The application of nanotechnology in pollution control, remediation, and prevention offers progressive solutions that bring clear benefits to public health and the preservation of natural ecosystems on Earth. Nano-remediation harnesses the distinctive characteristics of nanoscale particles or nanomaterials, such as their heightened reactivity and expansive surface area, enabling them to effectively eliminate a broad range of hazardous environmental pollutants. These pollutants encompass organo-halogenated compounds (OA), hydrocarbons, and heavy metals. Despite the increasing interest in nanotechnological solutions for pollution remediation and substantial global economic investment, there is ongoing debate regarding the environmental and human risk assessment linked to the use of engineered nanomaterials. Based on the aforementioned reasons, nano-remediation is acknowledged as an emerging technology, highlighting the necessity to provide sustainable approaches that utilize this significant potential through the application of green nanoscience [15], [23].

2.1.1 Nanomaterials and nanoparticles

Nanomaterials consist of particles that can be in an unbound state, as aggregates, or as agglomerates within the size range of 1 nm to 100 nm. These materials possess remarkable attributes as adsorbents, catalysts, and sensors, primarily attributed to their significant specific surface areas and heightened reactivity.

Nanoparticles possess distinct physicochemical properties as a result of their small size, chemical composition, purity, crystallinity, shape, and aggregation. These alterations in their morphological, structural, and chemical characteristics make them a unique and innovative option for a wide range of applications. Nanoparticles are composed of three distinct layers: a surface that allows for easy functionalization, a shell that can be incorporated to achieve desired properties in the final products, and a core that can be synthesized using different methods, reaction conditions, and precursor materials.

There are various types of nanoparticles (**Fig. 1**), each with its own unique properties and applications. Some common types of nanoparticles are:

1. *Metal nanoparticles*: These nanoparticles are composed of metals such as gold, silver, platinum, and copper. They exhibit excellent electrical conductivity, catalytic activity, and optical properties. Metal nanoparticles find applications in electronics, catalysis, sensing, imaging, and biomedical fields. Moreover, more metal NPs such as Gold (Au), Silver (Ag), Copper (Cu), Zinc (Zn), Platinum (Pt), Iron (Fe), Nickel (Ni) and Cobalt (Co) can be synthesized using plant [24].

2. *Metal oxide nanoparticles*: Metal oxide nanoparticles include materials such as titanium dioxide (TiO_2), zinc oxide (ZnO), iron oxide (Fe_2O_3), and many others. These nanoparticles exhibit properties such as high surface area, photocatalytic activity, and magnetic behaviour. They are used in applications such as solar cells, sensors, energy storage devices, and environmental remediation [25].

3. *Carbon-based nanoparticles*: Carbon-based nanoparticles include carbon nanotubes (CNTs) and graphene. CNTs are tubular structures composed of carbon atoms, exhibiting exceptional mechanical strength and electrical conductivity. Graphene is a single layer of carbon atoms arranged in a two-dimensional lattice, known for its excellent conductivity, mechanical strength, and transparency. Carbon-based nanoparticles find applications in electronics, energy storage, composites, and biomedical devices [26].

4. *Polymer nanocomposites*: Polymer nanocomposites are made of organic polymers, such as polyethylene, polystyrene, or polyvinylpyrrolidone, in nanoscale dimensions. They can be used for drug delivery systems, coatings, sensors, and nanocomposites [27].

5. *Lipid nanoparticles*: Lipid nanoparticles, including liposomes and solid lipid nanoparticles, are composed of lipid bilayers or solid lipid matrices. They are widely used in drug delivery, gene therapy, and cosmetic formulations [28].

The choice and synthesis method of nanoparticle type depends on the needed properties and applications required for a specific purpose.

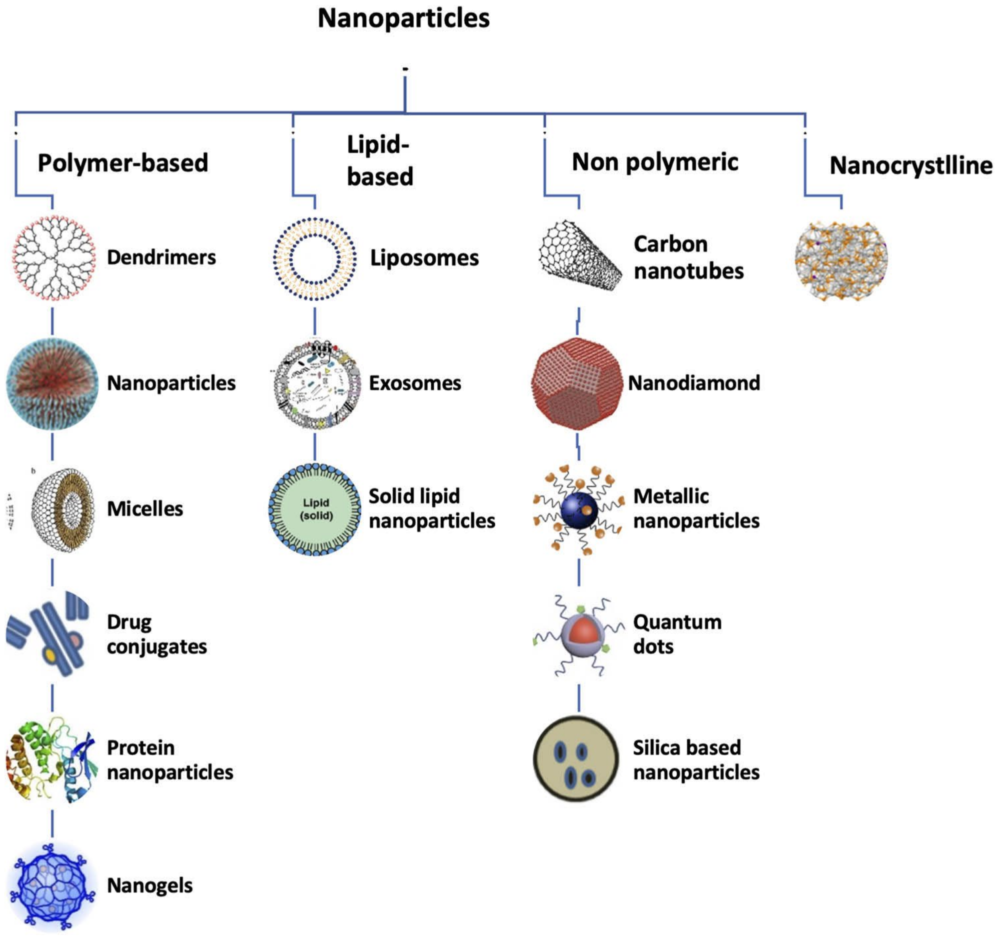

Fig. 1 – *Types of NPs* [29]

The synthesis of nanoparticles primarily follows two distinct methods: top-down and bottom-up approaches.

The top-down approach involves the reduction of larger materials or structures to nanoparticles through various techniques such as milling, grinding, or lithography. It relies on the mechanical or physical breakdown of bulk materials to achieve the desired nanoparticle size and shape. This approach allows precise control over particle size and offers scalability, but it may be limited in terms of achieving uniformity and purity [30].

On the other hand, the bottom-up approach involves the assembly or growth of nanoparticles from smaller building blocks or precursor molecules. This can be achieved through various techniques such as chemical synthesis, precipitation, sol-gel, or vapor-phase methods. The bottom-up approach enables precise control over nanoparticle composition, structure, and surface properties. It offers advantages in terms of uniformity, purity, and tailoring nanoparticles for specific applications. However, it may require more complex synthesis processes and may be limited in terms of scalability for large-scale production [30].

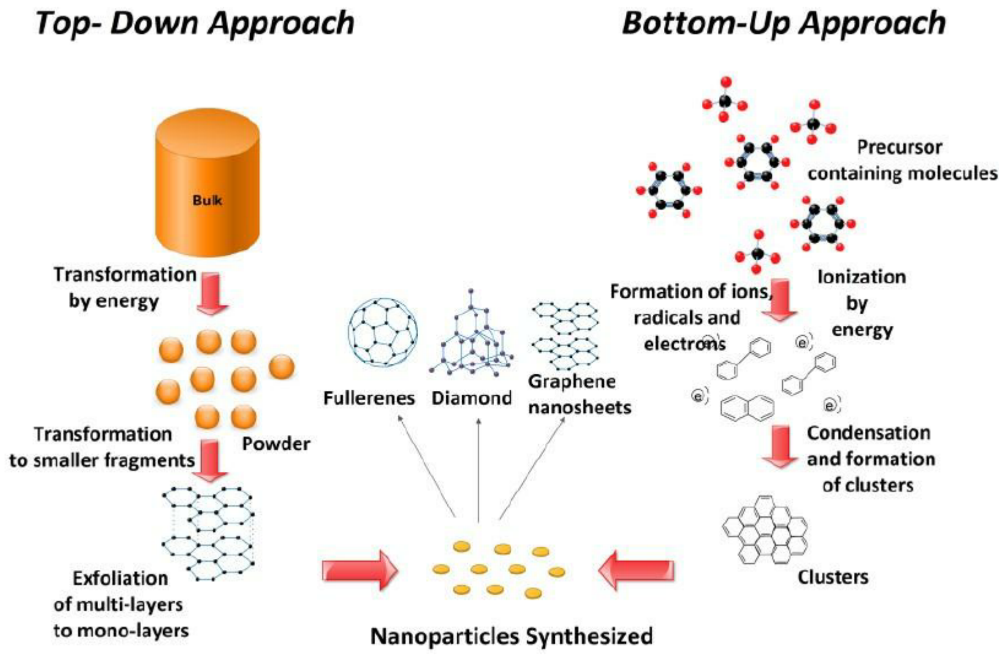

Fig. 2 - *Top-Down and Bottom-Up Approach schematization (Habiba, Makarov, Weinel, Morell. 2014)*

Both approaches have their advantages and limitations, and the choice of method depends on the specific requirements, desired properties, and intended applications of the nanoparticles [31].

Nowadays, there is a growing interest in the synthesis of nanoparticles. Many researches investigate the need for sustainable alternatives to these traditional synthesis approaches to provide greener solutions with low environmental impact. This is due to fact that the unique properties of nanoparticles also raise concerns about their potential environmental and health impacts. The behaviour and toxicity of nanoparticles can differ and careful consideration of their safety and proper handling is necessary. There is no universal mechanism of toxicity that applies to all nanoparticles. However, oxidative stress is commonly observed. In addition to oxidative stress, other significant mechanisms have been reported, including physiological impacts that can affect hormone regulation or the activity of hatching enzymes, leading to reproductive failure, among other effects [32]. Particularly, Green chemistry bases its principles in the reduction of the impact on human health as well as environment by the utilization of minimum amount of hazardous substances.

2.1.2 Green chemistry

Green chemistry, also known as sustainable chemistry, is an approach that focuses on designing and developing chemical processes and products that are environmentally friendly, economically viable, and safe for human health. It aims to minimize or eliminate the use and generation of hazardous substances throughout the life cycle of a chemical product, from its synthesis to its use and disposal.

The principles of green chemistry guide scientists and engineers in making decisions that promote sustainability and reduce the environmental impact of chemical processes.

The principles of green chemistry were established by chemists Paul Anastas and John Warner in 1998 as a guide for designing and developing sustainable chemical processes. These principles serve as a framework for promoting environmentally friendly and economically viable practices in the field of chemistry. Here are listed the 12 principles [33]:

1. *Prevention*: It is better to prevent waste generation and environmental pollution at the source by designing processes that are more efficient and produce minimal waste.

2. *Atom Economy*: Maximize the use of all atoms in a chemical reaction to minimize waste and reduce the consumption of raw materials.

3. *Less Hazardous Chemical Syntheses*: Design synthetic routes that use and produce chemicals that are less toxic, less hazardous, and have lower environmental impact.

4. *Designing Safer Chemicals*: Develop and use chemical substances that are non-toxic, non-persistent, and have minimal negative effects on human health and the environment.

5. *Safer Solvents and Auxiliaries*: Use safer solvents and auxiliary substances that are non-toxic, non-flammable, and have minimal environmental impact.

6. *Design for Energy Efficiency*: Optimize energy efficiency in chemical processes to minimize energy consumption and reduce greenhouse gas emissions.

7. *Use of Renewable Feedstocks*: Incorporate renewable raw materials and feedstocks, derived from sustainable sources, to reduce reliance on non-renewable resources.

8. *Reduce Derivatives*: Minimize or eliminate the use of unnecessary derivatization steps, which can lead to increased waste generation and environmental impact.

9. *Catalysis*: Utilize catalytic reactions whenever possible, as they can increase reaction rates, selectivity, and efficiency, thereby reducing energy consumption and waste production.

10. *Design for Degradation*: Design chemical products that are easily degradable, allowing them to break down into non-toxic substances after use, reducing environmental persistence.

11. *Real-Time Analysis for Pollution Prevention*: Develop and use analytical methods that enable real-time monitoring and control of chemical processes to prevent pollution and waste generation.

12. *Inherently Safer Chemistry for Accident Prevention*: Design chemical processes and products with a focus on minimizing the potential for accidents, releases, and explosions, thereby reducing risks to human health and the environment.

These principles provide guidance for researchers to make informed decisions and incorporate sustainable practices into their work, ultimately aiming to create a more sustainable and environmentally friendly chemical industry. By implementing the principles of green chemistry, scientists and engineers strive to develop sustainable alternatives, reduce waste, conserve resources, and minimize the environmental and health risks associated with chemical processes. The goal is to achieve a more sustainable and greener future for the chemical industry and its products [34].

2.1.3 Green synthesis of NPs

Green synthesis refers to the process of synthesizing various NPs using environmentally friendly and sustainable approaches. It aims to minimize the use of hazardous chemicals, reduce energy consumption, and generate less waste, thus promoting a more sustainable and eco-friendly method of production. The principles of green synthesis align with the broader concept of green chemistry, which focuses on designing chemical processes and products that have minimal impact on human health and the environment. Green synthesis techniques often employ renewable resources, non-toxic solvents, and mild reaction conditions to achieve desired synthesis outcomes [35].

One common aspect of green synthesis is the utilization of natural resources and bio-based materials as starting materials. This includes using plant extracts, agricultural waste, microorganisms, and biomolecules as precursors or catalysts in the synthesis process. By harnessing the inherent properties of these natural materials, green synthesis offers a more sustainable alternative to traditional synthetic routes. The creation of effective green chemistry methods for the synthesis of metal nanoparticles has drawn a lot of attention from researchers in recent years. The combination of chemical science, biological science, and industrial engineering is employed in the creation of nanoparticles that can be applied to commercial activities. In order to produce nanoparticles using an environmentally friendly method, the use of organisms is one of the approaches that is most discussed. Plants appear to be the most suitable for the production of nanoparticles on a large scale through biosynthesis. Compared to microbes, plants make nanoparticles that are more stable and can be synthesize at a faster rate. Biochemicals and metabolites, which are unique substances found in plants, are used as stabilizing and reducing agents in the creation of nanoparticles [14].

Metal NPs can be synthesized under certain circumstances, resulting in high-quality NPs that may even outperform those obtained through traditional chemical methods. The general procedure for green synthesis of various metal NPs involves obtaining a plant extract, mixing it with a synthetic metal salt solution under specific conditions, reducing the metal particles, and performing filtration and other necessary steps to obtain the desired nanoscale metal. However, it is important to note that customized technologies are required for different types of metals and plants, as the synthesis conditions depend on the specific metal being used. Further exploration and research are necessary to investigate and develop these tailored methods. Additionally, it is worth mentioning that different types of metal nanoparticles exhibit distinct properties related to the activity of the metal itself [36].

The green synthesis of metal oxide nanoparticles, in particular, leads to several advantages such as the reduced production of hazardous by-product and the better control of sizes and shapes of metal nanoparticles. Numerous methods using safe reducing agents are constantly being developed in order to avoid toxic chemicals and organic solvents. Moreover, using this technique, the necessity to purify the nanoparticles after their creation is removed, this reduces the need to employ different harmful organic solvents. Nevertheless, the development of this method still has several issues that need to be resolved. Therefore, further research is required to implement current techniques and procedures with more “green” approaches. Eliminating high energy consumption procedures and using different wastes are among the main researched issues.

Although green synthesis of metal NPs holds great potential, there are certain challenges that need to be addressed for its widespread adoption in industrial production and large-scale applications. These challenges include material selection, synthesis conditions, and quality control of the resulting products as well as energy consumption [37].

The main issues in the green synthesis research are about the availability of materials and the concerns regarding high energy consumption due to high processes temperature and prolonged reaction times. As a matter of fact, the required temperatures for green synthesis are sometimes excessively high, and the extended synthesis duration demands substantial energy input, potentially causing harmful environmental effects. Furthermore, the availability of certain organic materials used in green synthesis is often limited to specific localities, hindering the expansion of production to other regions. Several raw materials are also secondary products that necessitate additional processing before they can be utilized in the green synthesis of nanoscale metals. This additional processing adds to the overall cost and energy consumption of the synthesis process. Therefore, despite the use of eco-friendly natural materials, the process may not align with the principles of green synthesis [35].

2.1.4 Catalysis

Catalysis is a multidisciplinary field that combines principles from chemistry, physics, materials science, and engineering. It involves the study of catalyst design, synthesis, characterization, and the understanding of reaction mechanisms. Catalysis has also gained immense significance in industrial chemistry since the 1950s, with approximately $85-90\%$ of chemical processes incorporating at least one catalytic step. As mentioned earlier, catalysis plays a crucial role in green chemistry. The design and development of efficient catalysts are key to promoting sustainable practices in the field [38].

Catalysis is a fundamental process in chemistry that involves the acceleration or regulation of a chemical reaction by a substance known as a catalyst. A catalyst is a substance that remains unchanged at the end of the reaction and can facilitate the reaction by lowering the activation energy required for the reaction to occur. It increases the rate of reaction without being consumed in the process. More specifically, in a catalytic process, the reactant molecules interact with the catalyst, which facilitates the breaking and formation of chemical bonds. This interaction can occur through various mechanisms, such as adsorption of reactants onto the catalyst surface, formation of temporary bonds with the catalyst, or alteration of the reactant's electronic structure [39].

Catalysts can be classified into two main types: homogeneous catalysts and heterogeneous catalysts. Homogeneous catalysts are in the same phase as the reactants, while heterogeneous catalysts are in a different phase. Both types of catalysts have their advantages and applications, depending on the specific reaction and conditions.

The catalysis process plays a crucial role in various industries, including chemical production, pharmaceuticals, energy, and environmental applications. It enables the efficient production of desired products, reduces energy consumption, minimizes waste, and allows more selective and environmentally friendly processes. Researchers continuously strive to develop new and improved catalysts with enhanced activity, selectivity, and stability to drive more efficient and sustainable chemical processes [39].

The synergy between nanoscience and catalysis enables the emergence of sustainable materials that integrate the unique advantages of nanoscale materials in catalytic processes, addressing crucial aspects such as activity and selectivity. Progress in the synthesis and characterization of nanostructured materials has the potential to enable precise manipulation of these materials at the atomic level, resulting in the acquisition of desired catalytic properties [40].

Metal oxide catalysts have emerged as essential components in a wide array of industrial catalytic processes. Moreover, there has been a significant focus on harnessing the potential of metal oxide catalysts to resolve environmental challenges, particularly in the field of depollution. This involves minimizing the generation of waste byproducts by enhancing the selectivity of reactions.

The catalytic performance of metal oxides can be greatly improved by reducing their particle size to the nanoscale. This reduction leads to enhanced catalytic activity per unit weight. Initially, early research concentrated on exploring the impact of size, but investigations have now expanded to examine the influence of particle morphology, specifically in relation to the method used for catalyst preparation. Recent advances in catalysis science pertaining to metal oxides have facilitated the synthesis of catalysts with exceptional selectivity through innovative preparation and activation techniques. It is widely recognized that the effectiveness of a solid catalyst depends on various factors, such as the size and shape of its solid particles, which can favour specific facets and influence structure-sensitive reactions. Additionally, the catalyst's crystallinity, chemical composition (both internally and on the surface), and the methods employed for its preparation and activation all play crucial roles. Novel strategies for synthesizing metal oxide catalysts have led to the creation of catalysts with active single sites, theoretically offering 100% selectivity. Nanocrystals, characterized by dimensions on the scale of a few nanometres, exhibit remarkable catalytic efficiency due to their abundance of surface sites [38].

2.1.5 Photocatalysis

A particular form of catalysis has gained relevant interest for the removal of pollutants in both water and surface treatment applications. This type of catalysis is called Photocatalysis and involves chemical reactions taking place in the presence of light and a photocatalyst [41].

Photocatalysis is a process that utilizes light energy to drive chemical reactions. It involves the use of a photocatalyst, typically a semiconductor material, which can absorb light and promote a variety of reactions, such as oxidation, reduction, and decomposition.

Photocatalytic reactions can be classified into two categories based on the physical state of the reactants:

1. *Homogeneous photocatalysis* refers to a type of photocatalytic reaction where both the semiconductor and reactant are present in the same phase, which can be gas, solid, or liquid. This category encompasses a wide range of reactions, including mild or total oxidations, dehydrogenation, hydrogen transfer, metal deposition, water detoxification, and removal of gaseous pollutants [42].

2. *Heterogeneous photocatalysis* involves photocatalytic reactions where the semiconductor and reactant exist in different phases. In most cases, homogeneous photocatalytic reactions occur in the aqueous phase and employ a transition-metal complex as the photocatalyst. Homogeneous photocatalysts find extensive application in the production of clean hydrogen fuel, with cobalt and iron complexes being particularly noteworthy examples [43].

In photocatalysis, when the photocatalyst is irradiated with light of sufficient energy (typically ultraviolet or visible light), electrons in the valence band of the semiconductor material are excited to the conduction band, creating electron-hole pairs. These photoinduced electrons and holes can participate in redox reactions with adsorbed species on the catalyst surface or in the surrounding solution, leading to the transformation of pollutants or the generation of useful products [42].

The classification of materials can be done referring to the width of the band gap (unit = *eV*), that is obtained by the energy difference between the valence band and the conduction band. The valence band represents the energy levels occupied by electrons in their stable states, while the conduction band represents the energy levels that are available for electrons to move freely and participate in electrical conduction or optical processes. Band gap is a fundamental concept in solid-state physics and plays a crucial role in determining the electrical and optical properties of materials. Materials are classified into three types based on their band gap [77]:

1. *Insulators*: Insulating materials have a large band gap, which means there is a significant energy difference between the valence and conduction bands. Consequently, these materials do not conduct electricity easily and have limited optical activity (rubber, plastic, wax, and wood).

2. *Semiconductors*: Semiconductors possess a moderate band gap, making them capable of conducting electricity under specific conditions. By applying external energy (such as heat or light), electrons can be excited from the valence band to the conduction band, allowing for electrical conduction. Semiconductors are widely used in electronic devices, solar cells, and optoelectronics (gallium arsenide, germanium, and silicon).

3. *Conductors*: Conductors have a very small or nearly non-existent band gap, allowing electrons to move freely between the valence and conduction bands. As a result, these materials conduct electricity efficiently. Metals are a common example of conductors (gold, silver, aluminium, and copper).

The band gap directly influences the absorption and emission of light by a material. Materials with larger band gaps tend to absorb or emit light with higher energy (shorter wavelengths), while materials with smaller band gaps absorb or emit light with lower energy (longer wavelengths). The band gap can be also modified through doping (introducing impurities) or by applying external forces such as pressure. These modifications can alter the electrical and optical properties of materials, expanding their potential applications in various fields.

Based on the aforementioned information, it becomes evident that the process of photocatalysis is greatly facilitated when the photocatalyst is a semiconductor material. When a semiconductor is exposed to light, an electron within the valence band absorbs the energy carried by photons. As a result, a hole is created in the valence band as the electron gets excited to the conduction band. This photo-excitation state leads to the formation of an electron-hole pair. The excited electron can be utilized for reducing an acceptor, while the hole can participate in the oxidation of donor molecules [41].

The significance of photocatalysis lies in the fact that a photocatalyst provides both an environment for oxidation and a separate environment for reduction, carrying the two processes simultaneously.

Particularly, photocatalysis offers several advantages in environmental remediation and energy applications. It can effectively degrade a wide range of organic pollutants, including dyes, volatile organic compounds, and even certain persistent organic pollutants. Additionally, it can be used for water purification, air purification, self-cleaning surfaces, and hydrogen production through water splitting [44].

Recent advancements in photocatalysis research focus on improving the efficiency of photocatalysts, extending their light absorption range to visible light, enhancing their stability, and exploring novel materials with superior photocatalytic properties. Overall, photocatalysis has emerged as a promising technology for sustainable environmental remediation and energy conversion, harnessing the power of light to drive chemical transformations and mitigate pollution [44],[45].

2.2 Titanium Dioxide nanoparticles

The interest in studying titanium is due to its high availability and several properties. Therefore, in the last decades, titanium became a relevant element for many industrial applications. The metal is one of the ninth most abundant elements in the Earth's crust (0.63%). Particularly, TiO_2 NPs, shows excellent photocatalytic characteristics. This feature makes titanium dioxide an excellent photocatalyst for environmental purification [46].

TiO_2 NPs are hydrophilic and possess self-cleaning properties. When applied as coatings or incorporated into surfaces, they can help break down organic substances, prevent fouling, and resist the adhesion of pollutants, dirt, and microorganisms. This makes TiO_2 NPs beneficial for creating self-cleaning materials and surfaces in environmental applications.

The versatility of TiO_2 NPs allows for the creation of a multitude of hybrid TiO_2 NPs photocatalysts with distinct structural, chemical, and physical properties, each with its own specific applications. Hybrid TiO_2NPs can be generated by combining TiO_2 NPs with various materials, including metals, nonmetals, noble metals, and other photocatalysts. The incorporation of these materials into TiO_2 NPs enhances its properties, particularly its photocatalytic capabilities. The fabrication of hybrid TiO_2 NPs can be accomplished using a wide array of processes and technologies. Ongoing studies on processing techniques and material combinations, as well as their practical applications, will assist future researchers in selecting the appropriate materials for processing [35].

Above all, TiO_2 NPs are used in photocatalysis because of their unique electronic and optical properties. When exposed to light, TiO_2 NPs can generate electron-hole pairs, which can participate in various redox reactions. The photocatalytic activity of TiO_2 NPs is mainly due to their ability to absorb ultraviolet (UV) light, which promotes the electrons from the valence band to the conduction band. The excited electrons can then react with oxygen molecules, leading to the formation of highly reactive oxygen species (ROS), such as superoxide radicals, hydroxyl radicals, and singlet oxygen. These ROS can then oxidize organic and inorganic compounds, leading to their degradation into harmless products. This variation of particle's energy introduces a non-equilibrium condition which lead to oxidation or reduction of adsorbed species. This process led to the complete decomposition into CO_2 and H_2O of many organic and inorganic compounds. Hence, the application of TiO_2 NPs confers materials characteristics of self-cleaning and self-sanitization. Moreover, TiO_2 nanoparticles have high stability, are relatively low-cost, and can be easily synthesized in various sizes and shapes. These advantages make them a popular choice for photocatalytic applications [46].

Solar photocatalysis offers several advantages over traditional approaches, primarily due to its cost-effectiveness. By harnessing solar radiation as an energy source in real-time, the treatment costs can be significantly reduced. Additionally, the reusability of the photocatalyst is another valuable aspect. Moreover, the environmentally friendly nature of TiO_2 NPs, which is nontoxic, makes the solar photocatalysis approach even more appealing in terms of sustainability [25].

However, the application of solar photocatalysis still faces several limitations that need extensive research. Currently, traditional methods are still predominantly used worldwide instead of more advanced techniques like solar photocatalysis. To overcome the current limitations and promote the widespread adoption of solar photocatalysis with hybrid TiO_2 NPs, it is crucial to continue research and development efforts. This would involve exploring innovative techniques, optimizing performance, and addressing any remaining challenges to ensure the effective and practical implementation of solar photocatalysis in various real-world applications [25].

In summary, TiO_2 NPs hold great potential for environmental remediation applications. Their photocatalytic activity, self-cleaning properties, heavy metal adsorption capabilities, and compatibility with NC systems make them valuable tools in addressing pollution and improving environmental quality [15]. However, proper risk assessment and safety measures should be taken into account to ensure responsible and sustainable use of these nanoparticles in environmental remediation practices.

2.2.1 Titanium Oxide Phosphates

Titanium oxide phosphates NPs, also known as titanium phosphate oxides, are a class of materials composed of titanium, phosphorus, oxygen, and other elements. They have a layered or framework structure and exhibit unique properties that make them attractive for various applications. These materials possess excellent ion-exchange capabilities due to the presence of phosphorus and oxygen in their structure. This allows for the exchange of ions with the surrounding medium, making titanium oxide phosphates useful in catalysis, electrochemistry, and ion sensing.

In terms of catalytic applications, TiOP have shown promise in selective oxidation, hydrolysis, esterification, and Fischer-Tropsch synthesis. In particular, Fischer-Tropsch synthesis is a catalytic chemical process used to convert carbon monoxide (CO) and hydrogen (H_2) gases into hydrocarbon products, primarily liquid fuels. In Fischer-Tropsch synthesis, a mixture of carbon monoxide and hydrogen, often referred to as synthesis gas or syngas, is passed over a solid catalyst under specific reaction conditions. The catalyst used is typically based on iron, cobalt, or a combination of both metals supported on an inert material. The reaction proceeds through a series of complex steps involving adsorption, surface reactions, and desorption. Fischer-Tropsch synthesis is known for its ability to produce hydrocarbons with a wide range of carbon chain lengths, allowing the production of various petroleum-like products. The process is particularly valuable in situations where there is an abundance of carbon-rich feedstocks, such as coal or biomass, that can be converted into synthesis gas for subsequent conversion into liquid fuels. One advantage of Fischer-Tropsch synthesis is that it can produce cleaner-burning fuels compared to conventional petroleum sources, as the hydrocarbons produced have lower sulphur and aromatic content. Additionally, the process can be used to produce synthetic lubricants, waxes, and other chemical products. Although Fischer-Tropsch synthesis has been commercially used since the 1930s, it continues to be an area of active research and development to optimize catalysts, improve reaction efficiency, and explore new feedstocks. The process holds potential for sustainable production of liquid fuels and chemicals, offering alternatives to petroleum-based resources [47].

Titanium oxide phosphates also exhibit interesting electrochemical behaviour, making them suitable for energy storage and conversion. They can be utilized as electrode materials in lithium-ion batteries, supercapacitors, and other electrochemical devices [48].

Some titanium oxide phosphates display photocatalytic activity similar to titanium dioxide (TiO_2). They can absorb light energy and generate electron-hole pairs, enabling various photocatalytic reactions such as water splitting, pollutant degradation, and solar energy conversion [49].

Furthermore, these materials can be modified or functionalized to introduce specific properties or enhance their performance in areas such as sensors, membranes, and drug delivery systems. Surface modifications, doping with other elements, and structural engineering techniques can be employed to tailor their properties [50].

In summary, titanium oxide phosphates are versatile materials with unique properties and a wide range of applications. Their ion-exchange capabilities, catalytic activity, electrochemical behaviour, and potential for functionalization make them promising candidates for catalysis, energy storage, environmental remediation, and materials science. Ongoing research aims to further explore and optimize the properties and applications of titanium oxide phosphates [50].

2.3 Nanocellulose

Cellulose is the most abundant organic polymer on Earth and is commonly found in the cell walls of plants, where it provides structural support. The distinctive mechanical properties observed in various plant species can be attributed to the hierarchical structure of cellulose-based fibres, which are composed of nano-fibrilar components. Due to its hierarchical structure and semicrystalline characteristics, it is possible to extract nanoparticles from this naturally occurring polymer using a deconstructing strategy, which can be either mechanically or chemically induced, following a top-down approach [51].

Nanocellulose (NCel) refers to a group of nanoscale cellulose-based materials that exhibit unique properties due to their small size and high aspect ratio. It is derived from cellulose, a natural polymer found in the cell walls of plants, particularly in wood and certain agricultural byproducts. It can be divided into three classes based on their morphology and source:

a) Cellulose Nano-Crystals (CNCs):

b) Nano-Fibrillated cellulose (NFC):

c) Bacterial Nano-Cellulose (BNC).

CNCs and NFCs are produced via chemical or mechanical degradation of plant matter. The least crystalline materials will initially be weakened and destroyed by mechanical shearing or acid hydrolysis. These two methods lead to obtain different structures by mechanically shearing the cellulose fibres or subjecting them to controlled acid hydrolysis. Specifically, CNCs are produced as a result of acid hydrolysis [52].

Nanocellulose fibres are characterized by their small size, typically measuring less than 100 nm in diameter and several micrometres in length. These biodegradable nanofibers possess remarkable properties such as light weight and low density, with an approximate value of 1,6 g/cm^3 [53].

Nanocellulose materials possess several remarkable properties that make them attractive for a wide range of applications. Particularly, NCel exhibits exceptional mechanical properties, with high tensile strength (up to 10 GPa) and stiffness with an elastic modulus of up to 220 GPa. CNCs, in particular, have been reported to possess a higher strength-to-weight ratio than steel. Due to their nanoscale dimensions and high surface area-to-volume ratio, nanocellulose materials offer a large accessible surface area. This property is advantageous for interactions with other substances, such as gases, liquids, or polymers. Furthermore, its dispersions exhibit unique rheological behaviour, including shear-thinning and the ability to form stable gels or viscoelastic networks. These properties make them suitable for applications such as coatings, films, and 3D printing [54].

NCel is biocompatible, non-toxic, and has low immunogenicity, making it suitable for various biomedical applications, including drug delivery, tissue engineering, and wound healing. Moreover, it is derived from abundant and renewable sources, primarily plant biomass. It is biodegradable and has low environmental impact, making it an attractive alternative to synthetic materials [51], [55].

Presence of hydroxyl functional groups allows material modification through a large range of chemical reactions. This great flexibility of use makes possible to produce high-value products with low environmental impact. However, it is important to note that while nanocellulose holds great promise, further research is still being conducted to fully understand its properties, processing techniques, and potential limitations in different applications. As a matter of fact, ensuring the long-term sustainable success of nanocellulose requires a comprehensive understanding of its environmental impact throughout its entire life cycle. This understanding serves as the fundamental basis for assessing and mitigating any potential environmental effects associated with the production, use, and disposal of nanocellulose materials [56].

2.4 Electro-spun nanoweb for water treatment

2.4.1 Introduction

The global concern about clean water lack has grown during the last decades. The quality of water has rapidly decreased due to the exploitation of water resources for numerous industrial activities and population growth. Despite the Earth's surface being comprised of approximately 70% water, the availability of freshwater is limited. Only a small portion, approximately 3%, is deemed suitable for human consumption. Nowadays, the development of more effective filtration technologies is becoming a necessity to overcome this extended water contamination [57].

Pressure-driven membrane filtration processes are currently the prevailing water treatment technologies in widespread use. These systems have certain advantages and disadvantages and are open to development. In this scenario technology is a promising option to provide efficient water filtering devices at lower costs [58].

Among different available techniques, electrospinning of nanofiber membranes gathered significant attention from researchers due to its distinctive properties. Electro-spun nanofiber membranes (ENMs), are widely researched for the advantages in terms of reduced fouling issues and low cost of production. However, the commercialization of electro-spun nanofibrous membranes still presents limitations related to the low mechanical properties of the membranes. For these reasons, the implementation of membrane surface modification has gained significant importance as a means to enhance the performance of membrane processes [59].

2.4.2 Electrospinning

Electrospinning is a technique used to produce polymer fibres with diameters ranging from 2 nanometres to micrometres using polymer solutions of both natural and synthetic polymers. It involves the application of an electric field to a polymer solution or melt, which causes a thin jet of the polymer to be ejected from a spinneret. As the jet travels through the air, it undergoes stretching and whipping motions due to the electrostatic forces, resulting in the formation of ultrafine fibres that are collected on a grounded or oppositely charged collector [60].

Electrospinning has gained significant interest in various fields, including materials science, biomedical engineering, and nanotechnology, due to its ability to produce fibres with high surface area-to-volume ratios and unique properties. The technique allows for the creation of nanofibers that possess high porosity, large specific surface area, and potential applications in filtration, tissue engineering, drug delivery systems, sensors, and more. Over the last decades, a growing number of polymers, have been subjected to the process of electrospinning for a wide range of applications. This number continues to steadily increase as research progresses.

The electrospinning process can be summarized by the steps below:

1. *Polymer Solution Preparation*: A polymer is dissolved in a suitable solvent to create a polymer solution. The choice of polymer depends on the desired properties of the nanofibers.

2. *Electrospinning Setup*: The polymer solution is loaded into a syringe or reservoir, which is connected to a metallic needle or nozzle. A high voltage power supply is connected to the needle, creating an electric field.

3. *Jet Formation*: When the electric field is applied, the surface tension of the polymer solution overcomes the resistance, forming a droplet at the needle tip. As the voltage increases, the droplet elongates into a cone-shaped structure called a Taylor cone.

4. *Electrostatic Forces*: The repulsive electrostatic forces overcome the surface tension, resulting in the formation of a charged jet from the Taylor cone. The jet continues to elongate and thin down due to the electric field.

5. *Solvent Evaporation*: As the charged jet travels through the air towards a grounded or oppositely charged collector, the solvent rapidly evaporates. This solidifies the polymer into nanofibers.

6. *Fiber Collection*: The nanofibers are collected on a grounded or oppositely charged collector, such as a rotating drum, plate, or mesh. The collector's distance and speed can be adjusted to control the fibre alignment and density.

7. *Post-Treatment*: After collection, the nanofibers may undergo post-treatment processes such as heat treatment, crosslinking, or coating to further enhance their properties and stability.

Through electrospinning, various parameters can be optimized to control the characteristics of the nanofibers, including the polymer concentration, solution viscosity, applied voltage, distance between the needle and collector, and environmental factors like temperature and humidity. These adjustments enable the production of nanofibers with specific morphologies, such as aligned fibres, core-shell structures, or porous architectures, making electrospinning a versatile technique for diverse applications [61].

2.4.3 Fouling issues in membranes for water filtration

While nanofibrous membranes offer advantages in membrane technologies, fouling remains an inevitable occurrence during filtration processes. Membrane fouling occurs either on the membrane surface or within its pores, impacting the membrane's durability. The presence of fouling leads to a decline in membrane performance, hinders the efficient operation of membranes, and results in higher operational costs. Several factors influence the fouling phenomenon, including membrane properties, properties of the feed solution, and operating conditions [59].

This problem can occur due to various mechanisms [62], including:

1. *Particulate Fouling*: Suspended particles in the feed water can accumulate on the membrane surface, forming a cake layer that hinders water flow and reduces permeability.

2. *Scaling*: When the concentration of certain salts in the water exceeds their solubility limits, they can precipitate and form scale deposits on the membrane surface, causing pore blockage.

3. *Biofouling*: Microorganisms, such as bacteria, algae, and fungi, can colonize the membrane surface and create a biofilm. This biofilm can lead to pore blockage, decreased permeability, and altered membrane selectivity.

4. *Organic Fouling*: Dissolved organic compounds in the water, such as humic acids, oils, and proteins, can adsorb onto the membrane surface and form fouling layers, reducing membrane performance.

The remedies to address this particular phenomenon are various and include pre-treatment, membrane surface modification, backwashing and cleaning and advanced technologies such as ozonation, UV treatment or advanced oxidation processes.

Backwashing and chemical cleaning are frequently used to remove accumulated foulants and restore membranes' performance. However, despite its effectiveness, is unable to completely eliminate fouling that occurs during long-term filtration. For this reason, the fouling issue is a significant challenge in membrane-based water treatment processes that need to be exhaustively researched.

To overcome the issue, many researchers are investigating new combination of electro-spun fibres and methodologies that have the capacity to minimize the flouring controversy.

More specifically, considerable attention has been devoted to enhancing the durability and stability of the membrane through chemical and physical adsorption on its surface. Physical modifications such as etching, grit-blasting, and milling alter the surface topography or morphology with minimal to no chemical alteration. While, coating, deposition, and electrostatic attraction are normally used to introduce functional groups or chemical on the surface of the membranes. Unlike physical adsorption, chemical adsorption relies on a stable chemical bond between adsorbent materials and metal ions or an oxidation-reduction reaction for water treatment. Consequently, the surface chemical properties of adsorbents play a crucial role in chemical adsorption processes. By modifying the surface of an electro-spun nanofiber membrane (ENM), effective adsorbent materials can be obtained based on this principle [59].

2.4.4 Electro-spun PAN nanofibers membranes

Polyacrylonitrile (PAN) is a synthetic polymer derived from acrylonitrile monomers. PAN is known for its high tensile strength, excellent thermal stability, good chemical resistance, and high modulus of elasticity. It is a lightweight and durable material used in several applications.

PAN is commonly used in textile industry for producing acrylic fibers and yarns, which are used in clothing, upholstery, carpets, and industrial fabrics. It is also used as a precursor polymer for carbon fiber production, as it can be thermally stabilized and carbonized to obtain high-strength carbon fibers.

In addition, there has been a growing focus on affordable membrane materials for water filtration, specifically on nanofibers made of polyacrylonitrile (PAN). This is due to the high versatility of the polymer that can be chemically modified to enhance its properties [63].

Different researches deal with the topic of PAN membranes for removal of organic and inorganic contaminants in water treatment. Of particular interest are the research concerning PAN membranes application for removal of organic dye [12]and heavy metals [64] from aqueos solutions.

Despite the effectiveness of these membranes for the removal of different contaminants, a limitation is given by the impossibility of the simultaneous removal of both organic and inorganic pollutants.

Furthermore, the mechanical strength properties of PAN nanofibers are relatively low due to the weak adhesion between the fibers. To overcome this limitation, the reinforcement of PAN nanofibers with other materials, such as cellulose nanocrystals (CNC), becomes necessary. Previous research has demonstrated the potential use of CNC as a reinforcement phase, primarily because it is insoluble in common organic solvents and water. Additionally, the molecular chains of CNC contain numerous hydroxyl groups, which enable the formation of intramolecular or intermolecular hydrogen bond interactions. These interactions contribute to enhancing the mechanical strength and structural stability of the nanofiber membranes, while also providing excellent chemical resistance [65].

More specifically, the addition of nanocellulose to PAN membranes brings several benefits. Firstly, nanocellulose improves the mechanical strength and stability of the PAN matrix, making it more resistant to fouling and enhancing its overall durability. This leads to longer membrane lifespan and reduced maintenance requirements, ensuring consistent and reliable water filtration performance.

Secondly, nanocellulose acts as a pore size modifier, allowing for precise control over the membrane's pore structure. The nano-sized dimensions of nanocellulose fibers contribute to the formation of a porous network within the PAN matrix, which helps in achieving desired pore sizes for efficient filtration.

Additionally, nanocellulose possesses unique surface properties that enhance the adsorption and separation capabilities of PAN membranes. The high specific surface area and functional groups on the nanocellulose surface facilitate the adsorption and removal of dissolved substances, such as heavy metals and organic compounds, from water. This enables PAN membranes with nanocellulose additives to exhibit enhanced selectivity and improved water purification performance.

The incorporation of nanocellulose into PAN membranes reduces also the reliance on synthetic materials and introduces a renewable and eco-friendly component, aligning with the growing demand for sustainable water treatment solutions.

Despite the numerous advantages, challenges remain in optimizing the integration of nanocellulose into PAN membranes. These challenges include achieving homogeneous dispersion of nanocellulose within the PAN matrix, controlling the nanocellulose loading to maintain the balance between performance and permeability, and addressing potential issues related to membrane fouling and cleaning.

Lastly, the commercialization of nanofiber membranes has been hindered by the high production cost, which remains a significant limitation. The complex process involved in enhancing the performance parameters has limited its adoption on an industrial scale. A prime example is the overpriced cost of PAN, that poses a drawback to the potential of the polymer in various industrial applications [59].

In this context, this research explores the potential of nanocellulose as an additive for water filtration PAN-based membranes. By examining the underlying mechanisms, discussing recent advancements, and highlighting the challenges and opportunities associated with nanocellulose-based membranes, the goal is to provide valuable insights into the promising applications of this material in addressing water scarcity and advancing water treatment technologies.

2.5 Nano-coatings and Photocatalytic Paints

2.5.1 Introduction

The World Health Organization (WHO) has now acknowledged that air pollution poses a significant environmental risk to human health. Until recent times, there was limited investigation of indoor air quality issues in residential and non-industrial work settings. Currently, there is a growing concern about the health impacts of inadequate indoor air quality. This is due to the fact that a range of symptoms and illnesses showed a relation to non-industrial indoor air pollution. While this doesn't necessarily imply that indoor exposures will result in more severe health effects compared to outdoor air, evidence suggests that indoor concentrations of many pollutants are frequently up to 10 times higher than those typically found outside.

These indoor air pollutants originate from various sources such as indoor activities, products or materials. Additionally, in some cases, infiltration from the outside, whether through water, air, or soil, can serve as a notable source of certain contaminants [66].

For these reasons, indoor air quality (IAQ) has become a matter of great significance, impacting human health and overall well-being in all living and working environments. It is clear, that the problem necessitates deeper observation and monitoring. The examination of indoor sources and the potential for reducing emissions from these sources is fundamental.

Nanotechnologies have displayed significant promise in addressing challenges related to indoor air quality (IAQ). They offer innovative approaches for monitoring, filtering, and purifying the air, as well as detecting and removing harmful pollutants.

It's important to note that while nanotechnologies offer exciting possibilities, safety considerations regarding the potential release and exposure to nanomaterials should be carefully addressed to ensure their responsible and safe implementation.

2.5.2 Nano-coatings

Nano-coatings are thin layers of material with nanoscale thickness that are applied to the surface of a substrate. These coatings utilize nanotechnology to provide enhanced properties and functionalities to the surface they are applied on. Nano-coatings can be made from various nanomaterials, such as nanoparticles, nanocomposites, or nanofilms [67].

The application of this technology offers several advantages over traditional coatings. They can significantly improve the surface properties of materials, including enhanced durability, scratch resistance, corrosion resistance, water repellency, and UV protection. Additionally, nano-coatings can impart specific functionalities, such as self-cleaning, antimicrobial, anti-fogging, anti-reflective, or anti-static properties, depending on the desired application [68].

The common use of nano-coatings covers a wide range of industries and applications. In the automotive industry, nano-coatings can protect the paintwork, providing resistance to scratches and maintaining a glossy appearance. In the electronics industry, they can be applied to electronic devices to improve their performance and longevity by providing protection against moisture, dust, and corrosion. In the medical field, they are utilized on medical devices and implants to prevent bacterial adhesion and improve biocompatibility. They can also be used in textiles and clothing to provide water repellency or stain resistance. Furthermore, nano-coatings find applications in aerospace, energy, construction, and other industries where surface protection and performance enhancement are essential.

The fabrication of nano-coatings involves various techniques, including physical vapor deposition (PVD), chemical vapor deposition (CVD), atomic layer deposition (ALD), sol-gel process, and dip coating, among others. These techniques enable the precise deposition of nanomaterials onto the substrate surface, ensuring uniformity and control over the coating properties [67].

Ongoing research and development in nano-coatings aim to further expand their capabilities, such as the development of self-healing coatings or coatings with specific sensing functionalities.

2.5.3 Photocatalytic Paints

Photocatalytic paints are a type of coating that contains photocatalysts, typically titanium dioxide (TiO_2), which can react with sunlight or artificial light to catalyse chemical reactions. When exposed to light, photocatalytic paints can initiate the breakdown of organic pollutants, volatile organic compounds (VOCs), and certain inorganic compounds into harmless substances, such as carbon dioxide and water [69].

The photocatalytic process involves the absorption of photons by the TiO_2 particles, which then generates electron-hole pairs. These electron-hole pairs facilitate various oxidation and reduction reactions, leading to the decomposition of pollutants on the paint's surface. This self-cleaning property makes photocatalytic paints effective in reducing air pollution and maintaining cleaner surfaces. Besides their ability to decompose pollutants, photocatalytic paints also possess other desirable features. They are often used for their antimicrobial properties, as the photocatalytic process can inhibit the growth of bacteria, mold, and mildew on painted surfaces [70].

Photocatalytic paints find applications in various settings, including exterior walls, rooftops, and indoor surfaces, such as hospitals, public buildings, and residential spaces. Their use can contribute to improving air quality, reducing maintenance needs, and creating healthier and more sustainable environments [69].

Particularly, the field of materials science actively engages in researching the development of self-cleaning materials, investigating the relationship between their structure and functionality, and engineering artificial surfaces with adjustable wettability. These researches aim to create surfaces that can effectively repel contaminants and maintain cleanliness, catering to a wide range of commercial applications. The unique characteristics and practical uses of self-cleaning materials have garnered significant interest in the fields of energy and the environment. Recent studies have provided examples of various materials derived from titanium dioxide (TiO_2), shedding light on the underlying principles behind self-cleaning properties of both hydrophilic and hydrophobic surfaces. Indeed, self-cleaning properties of photocatalytic paints are based on the fundamental mechanism of hydrophilic and hydrophobic surfaces [71].

Titanium Dioxide exhibits superhydrophilic and oleophilic characteristics, meaning it has a strong affinity for water and oil, respectively. The superhydrophilic nature of TiO_2 surfaces allows them to readily attract and spread water droplets, resulting in a high degree of wetting. This property is attributed to the formation of a thin water film on the TiO_2 surface, which lowers the contact angle and promotes water adhesion. On the other hand, TiO_2 also possesses oleophilic properties, meaning it has a natural affinity for oil. This characteristic enables TiO_2 surfaces to attract and interact with oil droplets, leading to effective oil absorption and adhesion. These properties make TiO_2 a suitable material for applications such as oil-water separation, self-cleaning coatings, and environmental remediation. By combining both superhydrophilicity and oleophilicity, TiO_2 surfaces can exhibit excellent performance in various areas, including self-cleaning surfaces [71].

In contrast of superhydrophilic surfaces, superhydrophobic surfaces are defined by their low superficial energy and a water contact angle (WCA) greater than 150°. These surfaces can be created by manipulating the chemical composition and geometric structure of solid surfaces. However, there are relatively few instances of superhydrophobic surfaces that also exhibit photocatalytic properties. By introducing specific modifications in the development of TiO_2 surfaces, it is possible to achieve superhydrophobicity. For instance, a TiO_2 surface can be made superhydrophobic by adding a hydrophobic self-assembled monolayer or by creating a surface with a morphology with high cleaning action due to “lotus effect” [71]. These modifications or morphological characteristics result in TiO_2 surfaces exhibiting a high degree of water repellency because of the superhydrophobic − superhydrophilic conversion [72].

Still, the major limitation in developing self-cleaning materials based on TiO_2 is the wide band gap of the semiconductor, limiting its absorption to the UV region of sunlight, which comprises only 3–5% of the solar spectrum. Due to this wide band gap, utility of pure TiO_2 is restricted in fabrication of self-cleaning materials [73].

Chapter 3
Synthesis of nanoparticles

In the following sections, are presented the detailed experimental procedures, including the selection and preparation of green precursors, synthesis conditions, and characterization techniques. The obtained results will be discussed in the context of the synthesized TiO_2 nanoparticles' properties, such as size, morphology, crystallinity, surface chemistry, and photocatalytic activity. Finally, the potential applications are explored and discussed in the context of sustainable nanomaterial production. In order to obtain a fine metal powder, the metal shavings are processed through different procedures. The adopted synthesis procedures and methods are explained step by step below and summarized by the following image (**Fig.1**).

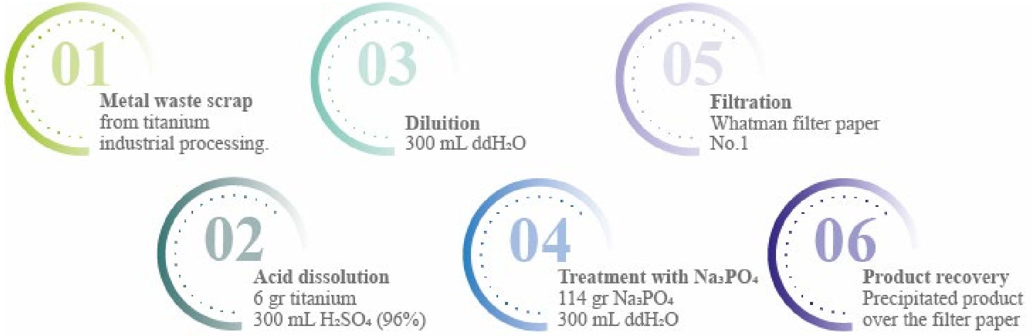

Fig. 3 - *Processing of metal*

3.1 Materials and Instruments

Titanium metal scrap (CALEFFI®, Modena, Italy), H_2SO_4 (96%), Na_3PO_4, methanol, sterile ultra-pure water (ddH_2O) by Milli-Q™, laurel powder, hotplate magnetic stirrer (RH basic, IKA™, Germany), water bath ultrasonication (FALC™, Italy), heating oven (LA PORTA™, Italy), grinder, centrifuge (ECCL31R Multispeed, Thermo Scientific™, USA), Whatman filter paper No.1.

3.2 Processing of metal

3.2.2 Acid dissolution

The titanium leaching allows to obtain a fine powder for the combustion reaction. The first step consists in the dissolution of titanium metal scrap in sulfuric acid. The sulphate process is the most effective method to process titanium and obtain TiO_2 nanoparticles.

Titanium metal scrap are put in a 500mL flask in which it is subsequently added concentrate H_2SO_4 (96%). The reaction ratio is 6g/300 mL (metal: acid). The process is carried out at room temperature.

The solution is allowed to rest until the metal is completely dissolved. After 24h sonication is used to speed up the reaction, the processing time is 1h at 50 degrees. This operation is repeated after 48h adopting time and temperature parameters used previously. After 24h sonication is repeated for 30 minutes at 50℃. The resulting solution is left to cool at room temperature. This operation is necessary to ensure that the leaching process has occurred correctly. Sonication uses an ultrasonic bath to apply sound energy to agitate particles in a liquid. Specifically, thousands of microscopic vacuum bubbles are formed in the solution due to cycles of pressure. These bubbles collapse into the solution in the process of cavitation. The released energy causes the disruption of molecular interactions. Hence, it separates clumps of particles and facilitates the dissolution process. In this case, ultrasonication it's also used to dissolve possible colloids in the scraps.

The dissolved $Ti_2(SO_4)_3$ is diluted with 100 mL of ddH_2O to allow the subsequent filtering. The addition of water in the acid solution causes an exothermic reaction and a consequent release of heat. Therefore, this procedure is made gradually pouring the required amount of water. The solution is left to cool at room temperature before proceeding further.

3.2.3 Treatment with Na_3PO_4

The next step consists in the addition of sodium phosphate (Na_3PO_4) to the $Ti_2(SO_4)_3$ solution. This step allows to achieve the precipitation of titanium particles and the pH neutralization. This leads to obtain more products left over the filter. In this case, the precipitation is a double-displacement reaction because of the displacement of SO_4 with PO_4.

In a 1000 mL flask 114g of Na_3PO_4 are dissolved in 300mL of ddH_2O. The dissolved $Ti_2(SO_4)_3$ solution is stirred at 180 degrees for 30 minutes at 480 rpm over hotplate magnetic stirrer. Subsequently, the diluted Na_3PO_4 is added to the dissolved $Ti_2(SO_4)_3$. The resulting solution is stirred for 15 minutes under room temperature. The composite is left to sit for extra 15 minutes before the filtration procedure.

The chemical reactions related to the previous steps are listed below:

(1) $6Ti + 3H_2SO_4 \rightarrow 3Ti_2(SO_4)_3 + 3H_2$

(2) $2Ti_2(SO_4)_3 + 2H_2SO_4 + O_2 \rightarrow 4Ti(SO_4)_2 + 2H_2O$

(3) $3Ti(SO_4)_2 + 4Na_3PO_4 \rightarrow Ti_3(PO_4)_4 + 6Na_2SO_4$

The previous composite is filtered using two foils of Whatman filter paper No.1 under room temperature. The process required 72h to be fully complete. The precipitated product is then recovered and put in a petri dish.

The mixture is subsequently stored at room temperature for further use. The filtered solution is collected and put through filtration again. The residue over the filter paper is then gently removed with a spoon and collected in the same jar of the previous product. The resulting product has a different colour compared to the first. This colour variation of the double filtered product is due to the different oxidation process. Therefore, the two mixtures are put together and mixed to have a homogeneous product.

To minimize the amount of phosphates in the TiO_2 NPs it is rinsed with ddH_2O. This involves placing 45 gr of the mixture into two 35 mL plastic tubes and adding ddH_2O to each tube. The tubes are then centrifuged at 9000 rpm for 10 minutes at 10℃. After completing the centrifugation, the water obtained is discarded and the tubes are refilled with ddH_2O. This cycle is repeated three times, following which the resulting composite is collected. To aid the recovery process, 15 mL of ddH_2O is added to each tube.

3.3 Green Combustion Method

To provide comparison data, the Green Combustion is carried out using both the traditional approach and the modified one. In comparison to the information obtained using the conventional approach, the efficiency of the new method is assessed. Therefore, the efficiency of the new approach is analysed comparing the traditional process data. The procedures of both classical and modified method are listed below.

3.3.1 Modified Green Combustion method

The modified Green Combustion is achieved by combining the previously obtained TiO_2 based composite (*3.1.4*) with fine grounded plant powder. The process steps are detailed below.

As said before, the green combustion is done on three different samples using laurel powder. Each sample is obtained by adding 12.5 gr of the TiO_2 composite and 0.4 gr of plant powder in a round bottom porcelain capsule. The components are weighted using a gravity balance in order to have a precise measurement of the materials quantity.

The prepared samples are then put in a heating oven to achieve the synthesis. The oven is switched on and the temperature is set to 200℃. The heating oven reaches the preset temperature after 15 minutes. Since that time, after 1h the first sample is taken out and the temperature is set to 500℃. The same steps above are done for the other samples. After 1h hour, the second sample is recovered, and the temperature is set to 800℃. The last sample is left in the oven for 1h after reaching the preset temperature. Then the heating oven is switched off and the 800℃ sample is collected the next day. The collected samples are stored in a dissicator for further use.

The samples are ground to a fine powder using a stone mortar in preparation for the second calcination step. To prevent cross-contamination between the samples, every tool used is thoroughly cleaned before use. Each powder is placed in the previously used porcelain capsule to undergo the second calcination step.

To achieve a more uniform result, the samples undergo a second calcination process. The fine powder form of the sample enables the heat to penetrate uniformly throughout, resulting in a more homogeneous product. The calcination is carried out using the same temperature and time parameters as the previously mentioned combustion process. The resulting products are grinded and subsequently stored in glass vials for further use.

3.3.2 Classical Green Synthesis Method

In green science, the reducing and capping agent is typically made from extracts of different plants. For this research, the previously utilised plant powder is used to produce the organic extract. As was previously said, the traditional method is carried out to get comparative data between the classical approach and the new green solid synthesis. The procedure described below refers to a previous research about the conversion of industrial and organic waste into a nanocomposite material consisting of titanium-doped activated carbon and cellulose [74].

On a hotplate stirrer 300 mL of ddH_2O are added in a 1000 mL flask. The water is stirred for 30 min at 135℃ and 360 rpm. After 30 minutes 3 gr of laurel powder are added and the solution is stirred for other 10 minutes. The solution is ready to undergo the filtration process after 5 minutes. The mixture goes through filtration for 45 minutes, after this step the residue on the filter paper is removed and the extract is collected.

Subsequently, the extract is transferred in a 500 mL flask and the volume is restored to 300 mL adding ddH_2O. The extract is stirred for 5 minutes at 135℃ and 360 rpm. In the flask are added 45 gr of the previously prepared TiO_2 solution (*3.1.4*). A sample of the extract is taken for testing before the addition of the TiO_2 solution.

The mixture of plant extract and TiO_2 composite is stirred for 45 minutes using the same parameters as before. The compound is let sit for 2h and then divided in 9 plastic tubes (35 mL). The tubes are centrifuged for 8 minutes at 10℃ and 8500 rpm. A part of the resulting water is collected for analysis. The solid particles are put in a 100 mL becker (adding in each tube 2.5 mL of ddH_2O to help the recovery process). The obtained product is set up for drying in a heating oven at 105℃ for 16 h. The process is repeated in order to have more material for the calcination process.

The material is collected in two 35 mL plastic tubes that are subsequently filled with ddH_2O. The tubes are put for centrifugation at 9000 rpm for 10 minutes at 10℃. The centrifugation process is repeated two times in order to reduce the presence of sulphates before calcination. The product is then dried at 105℃ and finely grinded.

Three samples made from 15 gr of the previously obtained material are prepared using the finely ground powder. The exact same stages from the GC method's paragraph *3.3.1* are applied to perform the procedure. Following that, the samples are extracted from the ceramic capsules and stored in glass vials.

Chapter 4
Synthesis of nanocellulose

The extraction of nanocellulose is done from small pieces of tissue paper waste. As said previously, this method modification allows to reduce extraction times and waste production. In fact, using a pigment-free product has the added benefit of being able to proceed directly to the NaOH treatment. The procedure refers to the classical preparation method by acid hydrolysis using sulfuric acid [75]. The following image (**Fig. 2**) summarizes the steps described afterwards.

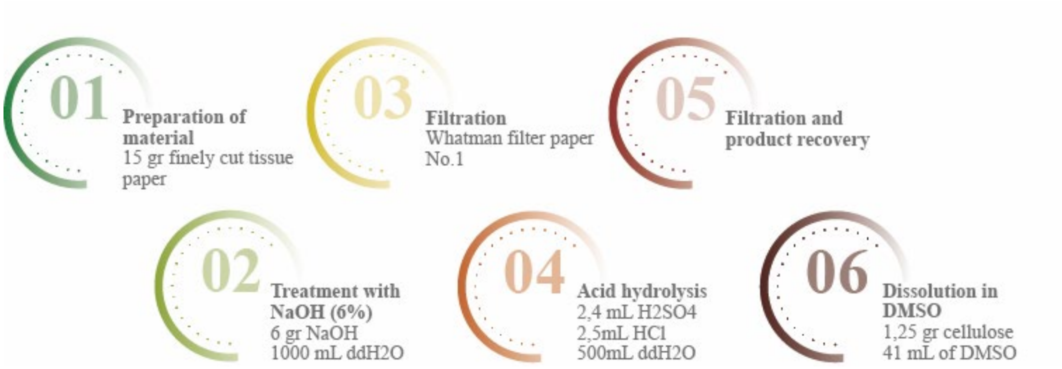

Fig. 4 - *Synthesis of nanocellulose process*

4.2 Process of synthesis

Tissue paper waste are finely chopped into small pieces (size of centimetres) using scissors. The used tissue paper is white with no pigment as said previously. The final product is then put in a 1000 mL flask to proceed with the next steps.

The next step consists in an alkaline treatment to break cellulose hydrogen bonds. The process modifies the natural cellulose structure by depolymerizing and generating short-length crystallites. Therefore, the alkaline treatment modifies the crystallinity, the unit cell structure, and fiber orientation. The disruption of hydrogen bonds results in an increase in surface roughness. Besides, alkaline treatment also exposes more cellulose on the surface of the fiber, increasing the potential number of reaction sites. The alkaline treatment is a chemical process in which natural fibers are submerged in a solution of sodium hydroxide (NaOH).

Aqueous solution of sodium hydroxide (6%) is obtained by adding 6 gr of NaOH and 1000 mL of ddH_2O in a 1000 mL flask. The solution is manually stirred until the hydroxide is completely dissolved. Subsequently, 15 gr of tissue paper pieces are added and the resulting mixture is left to sit for 12h under room temperature.

The obtained product is then filtered for 2 days under room temperature. The filtration is achieved using 2 foils of Whatman filter paper No.1 put in a glass funnel inserted in a 2000 mL flask. The residue is subsequently washed with ddH_2O to remove the remaining NaOH and stop the reaction. The whitish cellulose obtained from the process is then stored for further use.

4.2.1 Acid hydrolysis

Acid hydrolysis of native cellulose typically results in a sharp decline in the polymerization level (DP). The most common method of production is sulfuric acid hydrolysis, however hydrochloric acid (HCl) is also widely employed. Many of the acquired features of CNCs, such as the degree of crystallinity, the aspect ratio, dimensional dispersity, and the morphology, are influenced by both the reaction conditions and the cellulose supply. When sulfuric acid is applied as a hydrolysing agent, it combines with the hydroxyl groups on the surface of cellulose. This encourages the dispersion of the CNs in water and leads to obtain significant properties. Instead, the CNs produced by hydrolysis in hydrochloric acid have a limited ability to disperse and their aqueous suspensions have a tendency to flocculate.

The produced suspensions from hydrochloric acid and sulfuric acid displayed different rheological behaviours. When carried out under ultrasonic treatment, hydrolysis using a mixture of sulfuric and hydrochloric acids appears to produce spherical CNs rather than rod-like nanocrystals. This combination leads to obtain a reduced presence of sulphate groups on the spherical CNs.

The aim of this process is to obtain a Semi Crystalline Nano Cellulose (SCNC) by acid hydrolysis. This is achieved using a 5% solution of both sulfuric and hydrochloric acid in equal parts. The solution is obtained pouring 500 mL of ddH_2O in a 1000 mL flask in which are subsequently added 2.5 mL of H_2SO_4 and 2.5 mL of HCl. The solution is then stirred and the previously obtained white cellulose is added. In order to obtain a 5% acid solution, 500 mL of ddH_2O are then added in the flask.

The mixture is transferred in a 2000 mL round bottom flask to allow the stirring process. The composite is stirred on a hotplate magnetic stirrer for 2h at 80℃. After 2h the temperature is turned off and the stirring process is carried out for 30 more minutes.

The resulting solution is filtered using 2 foils of Whatman filter paper No.1 following the steps previously listed. The residue on the filter paper is collected carefully with a spoon and stored for further use.

4.2.2 Dissolution of cellulose in DMSO

There are several methods that have been developed to dissolve nanocellulose, including the use of solvents, surfactants, and ionic liquids. One of the most effective methods to dissolve nanocellulose is using a DMSO/ionic liquid mixture.

DMSO (dimethyl sulfoxide) is a highly polar solvent that has the ability to dissolve many types of compounds, including cellulose. Ionic liquids are another class of solvents that have shown promise for dissolving nanocellulose. Ionic liquids are salts that are liquid at room temperature and can dissolve a wide range of materials, including cellulose. However, ionic liquids are expensive and often toxic, which limits their use in large-scale applications. For the reasons listed above, the dissolution of cellulose is achieved using a DMSO/water mixture.

The dissolution of cellulose in DMSO can be achieved through a process called "regeneration." This involves dissolving the cellulose in a DMSO/water mixture, followed by precipitation of the cellulose out of the solution using a non-solvent.

There are several factors that can affect the dissolution of cellulose in DMSO, including the degree of polymerization of the cellulose, the concentration of the DMSO/water mixture, and the temperature of the solution. In general, higher degrees of polymerization and higher DMSO concentrations lead to better dissolution of cellulose.

The initial step in preparing cellulose for dissolution involves placing 5 grams of previously dried cellulose into a solution containing 15 mL of H_2SO_4, 15 mL of HCl, and 400 mL of ddH_2O. The mixture is stirred at a temperature of 180°C and a speed of 360 rpm for a duration of 1 hour. Subsequently, the solution is left undisturbed overnight and then subjected to filtration.

The filtered product is transferred to a 500 mL flask, to which 200 mL of ddH_2O is added. The mixture is stirred for 5 minutes, followed by the addition of 20 mL of HCl while continuing to stir. This process is carried out for an additional 10 minutes at a speed of 480 rpm under room temperature. Next, the solution is sonicated at a temperature of 70°C for 1 hour. The resulting product is dried using capillary action and stored for subsequent dissolution.

The dissolution process involves combining 1.25 grams of cellulose with 41 mL of DMSO. The mixture is then stirred and subjected to sonication at a temperature of 70°C until the cellulose completely dissolves. Following that, an additional 1,25 grams of cellulose are added, and the previous dissolution steps are repeated. The resulting cellulose is stored in a flask for further usage.

Chapter 5
Characterization and application of materials

5.1 Titanium Oxide Phosphate Nanoparticles

Nanoparticles are characterized using two samples obtained through the GC and GS methods. Specifically, samples obtained at a calcination temperature of 800 ˚C are chosen. This selection is based on the fact that titanium dioxide nanoparticles generally exhibit higher absorption and catalytic activity at higher calcination temperatures. In the case of titanium dioxide nanoparticles, higher calcination temperatures can lead to improved crystallinity, surface area, and porosity, which in turn enhance their absorption properties and catalytic activity. The improved crystallinity and surface area of the nanoparticles at higher temperatures provide more active sites for catalytic reactions. This can lead to enhanced performance in various catalytic processes, such as pollutant degradation, water splitting, and organic synthesis.

Specifically, the characterization of nanoparticles is conducted using three distinct methodologies: scanning electron microscopy (SEM), X-ray diffraction (XRD), and UV-visible spectroscopy (UV-vis). The obtained results are analysed in the following paragraphs.

The XRD measurements are achieved using X-ray diffraction (XRD) by X'Pert Powder-PANalytical™. The crystallographic structure and composition of the NPs samples are investigated by XRD analysis with angle range of 5˚÷90˚.

SEM observations provided a comprehensive understanding of the morphology exhibited by the samples.

UV-visible spectroscopy is conducted to obtain absorption data on a particle suspension. The used instrument is UV-vis spectrophotometer (UV-1900i by Shimadzu).

The results about the characterization of synthesized TiO_2 waste-derived nanoparticles are shown in chapter *6* paragraph *6.1*.

5.1.4 TiO_2 NPs application for self-cleaning applications

The experiment was conducted on five samples under both sunlight and visible light conditions. These samples include two specimens treated with nanoparticles obtained from the GC and GS processes, one comparative sample of a commercial UV resistant paint (SOL65), and two control samples (NC and PC).

In the case of sunlight exposition, the test is done in two cycles to evaluate the effectiveness of particles. The specimens are prepared on metal supports covered with a first layer of white paint. The second layer is composed differently for each type of specimen according to the following list:

1. *GC 800* – 2 gr white paint + 50 mg TiO_2-NPs from green combustion
2. *GS 800* – 2 gr white paint + 50 mg TiO_2-NPs from green synthesis
3. *SOL 65* – 2 gr Solarya 65 photocatalytic paint (25% TiO_2 NPs)
4. *NC* – 2 gr white paint (negative control)
5. *PC* – 2 gr white paint (positive control)

After complete drying, the specimens are immersed separately for 15 minutes in 100 mL of a dye solution containing Crystal Violet (CV) in the ratio of 37.5 mg/500 mL ddH_2O. After, this the specimens are taken out and left to dry for few minutes then the first scansion is done. The samples are subsequently subjected to sunlight exposure for a duration of 5 hours, with scanning measurements conducted at hourly intervals. The photocatalytic activity is investigated through UV-vis spectroscopy and image analysis, the results are discussed below.

The second cycle of test is done on the same specimens of the first analysis following the procedure described for the first cycle.

For the indoor case, the procedure for the preparation of samples is the same explained for the first cycle. In this case, the total exposure time is extended to 18 hours, as the photocatalytic activation of TiO_2 nanoparticles in visible light occurs gradually. Scansions are performed at intervals of 2 hours during this period.

5.*1.4 TiO_2 NPs application for self-cleaning and indoor air quality – analysis methods*

The absorption and removal data of CV on the specimens' surface are analysed through OriginPro software and ImageJ software. Different kinds of information are extracted and better explained in the results and discussion chapter. UV-vis spectra are exposed in graphs showing the absorption and wavelength of the samples through the different cycles of exposition.

In particular, the image processing through ImageJ software consists in the processing of the scansion images (600 dpi) by selecting an area of 4200x950 px for each sample. The area is then submitted to colour analysis through RGB spectra histogram. The RGB values are compared and the percentages of removal are calculated by doing simple math proportions with the NC sample. The maximum intensity of RGB values is obtained by considering a wavelength of λ=591 nm.

5.2 PAN-based electro-spun membranes

5.2.1 Formation of the membranes

In this study, PAN-based membranes are utilized, incorporating Semi-crystalline nanocellulose (SCNC), to investigate the changes in absorption data based on varying cellulose concentration within the membrane. The experiment is performed on three distinct membranes, each obtained from different solutions with their own specific composition as outlined below:

1. PAN_10.5% − 4 mL PAN-DMF (Dimethylformamide),
   solution ratio 4.87 gr PAN/ 50 mL DMF

2. PAN/NCel_10:01 − 4 mL of PAN-DMF and NCel,
   solution ratio 1 mL NCel /10 mL PAN-DMF

3. PAN/NCel_10:02 − 4 mL of PAN-DMF and NCel,
   solution ratio 2 mL NCel /10 mL PAN-DMF

The dissolution of PAN in DMF is achieved putting 50 mL DMF in a round bottom flask in which are added 4,87 gr of PAN. The process is carried out while stirring at 90 ˚C an 360 rpm under room temperature for 1 hour.

The two solutions of PAN-DMF mixed with NC are prepared by adding the quantities of NCel listed above to 10 mL PAN solution. The process is carried out through alternation of sonication and stirring processes every 5 minutes intervals for a total duration of 30 minutes.

The membranes are then formed through electrospinning process using the following parameters:

1. Flow rate: 0.02 μL/min

2. Target volume: 4 mL

3. Spin: 17.1 + kV

4. Distance: 24 cm

The obtained membranes are then stored in an airtight container with silica gel in order to prevent the absorption of moisture.

5.2.2 Absorption test

The objective of this research is to analyse the absorption data of PAN-based membranes when immersed in a dye solution with a specified concentration (3 mg CV/1000 mL ddH_2O). The study aims to investigate the absorption characteristics and behaviour of the membranes in response to the dye solution.

The absorption capacity is quantified for every membrane by UV-vis spectrophotometry. Additionally, the test is repeated for three cycles to asses the reusability of the membranes.

The membranes are square-shaped with edges measuring 6.5 cm, and they are obtained from the electrospinning support aluminium foil. The test is carried out by immersion of the three membranes in three different boxes containing 60 mL of a solution made by CV and ddH_2O (3 mg CV/1000 mL ddH_2O).

After a 10-minute interval, a volume of 3 mL from each solution is extracted to proceed with UV-vis spectroscopy, and then returned to their respective containers. This process is repeated for a total duration of 90 minutes, with UV scans performed at 10-minute intervals throughout the duration.

Upon completion of the procedure, the solution is removed from the containers, and the membranes undergo a cleaning process. The cleaning process involves immersing each membrane in different solutions in a sequential manner, comprising three distinct steps as follows:

1. NaOH 1% − 60 mL, immersion duration: 1 hour

2. HCl 1% − 60 mL, immersion duration: 30 minutes

3. ddH_2O − 60 mL, immersion duration: 5 minutes (3 cycles of washing)

The cleaning process is finalized by allowing the membranes to air dry at room temperature for a period of 12 hours. The dried membranes are then used to proceed with the next absorption cycle. The results of the cleaning processes are showed in the “performance efficient on reusability” paragraph.

5.2.3 Absorption test – analysis methods

The UV-vis data are processed through OriginPro software in order to acquire different types of information. For each cycle are provided information about UV spectra of absorption, effect of contact time, adsorption kinetics study, effect of initial concentration, adsorption isotherm study and performance efficient on reusability. The data are detailed and compared below to assess the most effective membrane in terms of absorption and reusability.

The absorption kinetics are investigated through pseudo-first-order (4) and pseudo-second-order (5) models, effect of initial concentration and absorption isotherm study.

The linearized expressions of the mathematical models are presented as follows:

$$\log(q_e - q_t) = \log q_e - \frac{(k_1 * t)}{2{,}303} \qquad (4)$$

$$\frac{t}{qt} = \frac{1}{k_2 * q_e^2} + \frac{1}{q_e} * t \qquad (5)$$

In which:

q_e = amount of dye adsorbed at equilibrium (mg/g)

q_t = amount of dye adsorbed at time t (mg/g)

t = adsorption time (min)

k_1 = pseudo-first order rate constant (min^{-1})

k_2 = pseudo-second order rate constant (g/mg/min)

Both models are applied to determine the absorption kinetics of each cycle. The image below shows the pseudo-first and pseudo-second order adsorption kinetics graphs.

The adsorption behaviour of CV dye was investigated at three different temperatures (300 K, 305 K, and 307 K) during a contact time of 90 minutes. The isotherm model is used to explain the adsorption behaviour of the PAN-based surface functionalized membrane.

The Langmuir isotherm model can be mathematically represented as follows:

$$\frac{C_e}{q_e} = \frac{1}{q_m k_a} + \frac{C_e}{q_m}$$

Where:

q_e = amount of dye adsorbed on the adsorbent surface at equilibrium (mg/g)

C_e = equilibrium concentration of adsorbate solution (mg/L)

q_m = maximum adsorption capacity of the adsorbent (mg/g)

k_a = Langmuir adsorption equilibrium constant

Chapter 6
Results and discussion

6.1 Titanium Oxide Phosphate Nanoparticles

6.1.1 Synthesis of TiO_2 NPs

The synthesized TiO_2 NPs from GC and GS method show different aspect in colour and consistency of the powder. Following the heating process, the appearance of the samples varies based on their carbon content. The sample heated to 200℃ has a high carbon content, resulting in a dark appearance, while the samples heated to 500℃ and 800℃ are lighter in colour due to the complete removal of sulphates and lower carbon content. Particularly, the samples of calcination temperature 800℃ results in a whitish colour.

The crystallographic structure, composition, optical and elemental analysis are better investigated in the following paragraphs using different methodologies.

6.1.2 X-ray Diffraction Analysis

The crystallographic structure and composition of the NPs samples are investigated by XRD analysis with angle range of $5^\circ-90^\circ$. The XRD pattern of TiO_2 NPs obtained from GC and GS method are shown in **Fig. 5** and **Fig. 6** below. The spectrum trend reveals the presence of major diffraction peaks at $2\theta = 26.9^\circ$ and $2\theta= 24.2^\circ$ and two minor peaks at $2\theta = 22.2^\circ$ and $2\theta = 34.3^\circ$. The peaks of the XRD patterns indicate the presence of Titanium Oxide Phosphate $Ti_2O(PO_4)_2$ and Titanium Oxide Phosphate $(TiO)_2P_2O_7$. Crystalline phosphates exhibit distinct diffraction peaks at specific 2θ angles, corresponding to the arrangement of atoms within their crystal lattice. These peaks are sharp and well-defined, indicating the presence of long-range order and crystalline structure. Whilst, amorphous phosphates lack a regular and repeating atomic arrangement, resulting in a diffuse scattering pattern without well-defined peaks. The absence of sharp peaks at specific 2θ angles suggests the amorphous nature of the phosphate material.

The presence of Titanium Oxide Phosphate is due to the specific synthesis method used to prepare TiO_2 nanoparticles. Referring to the present research, the formation of phosphates is caused by the treatment of metal with Na_3PO_4 (*3.1.3*). This process leads to the incorporation of phosphorus into the titanium oxide structure, leading to the formation of titanium phosphate compounds.

Titanium Oxide Phosphates can affect the optical, electronic, and catalytic properties of TiO_2 nanoparticles, making them suitable for specific applications. Particularly, it can enhance the photocatalytic activity of TiO_2 nanoparticles and promote the separation of electron-hole pairs generated upon exposure to light, reducing charge recombination and improving the overall photocatalytic efficiency.

Moreover, Titanium Oxide NPs typically exhibits good photocatalytic activity under ultraviolet (UV) light due to its wide bandgap. These phosphates can extend the response of TiO_2 nanoparticles to visible light due to its narrower bandgap. This expanded light absorption range allows for the utilization of a broader range of solar wavelengths, increasing the overall efficiency of photocatalytic processes.

Another effect of the phosphate's presence is the enhanced chemical stability. In fact, phosphates can enhance the chemical stability of TiO_2 nanoparticles, making them more resistant to degradation under harsh environmental conditions, including high temperature, humidity, and corrosive chemical environments. This improved stability can extend the lifetime and durability of TiO_2 - based materials, increasing their suitability for long-term applications.

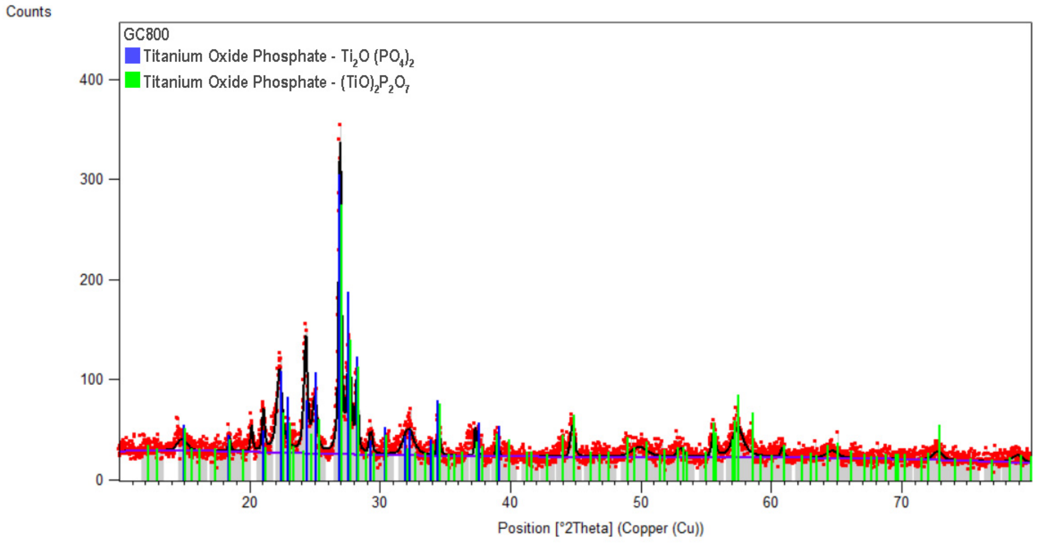

Fig. 5 - *XRD analysis of nanoparticles from Green Combustion method (2ϑ on x-axis and intensity on y-axis)*

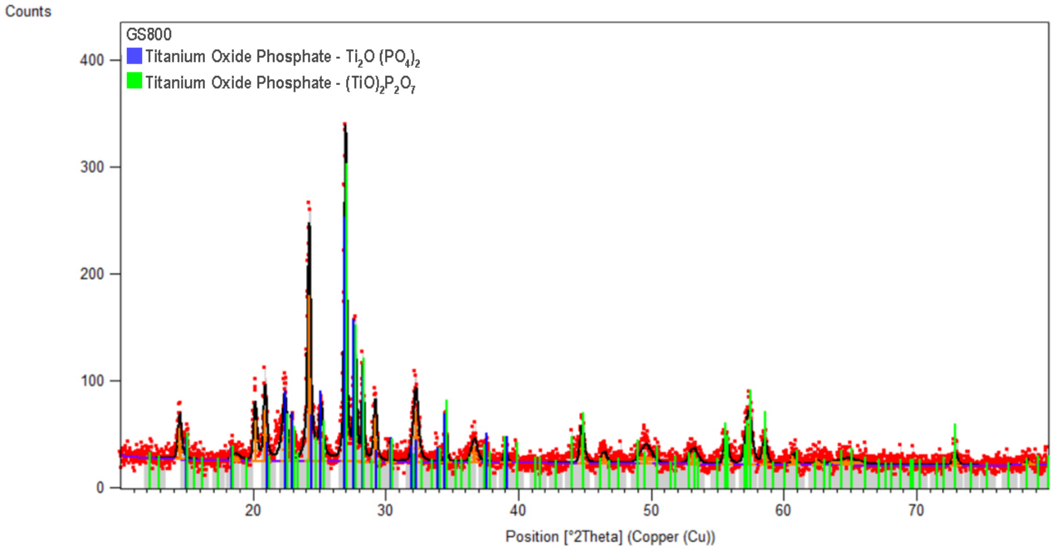

Fig. 6 - *XRD analysis of nanoparticles from Green Synthesis method (2ϑ on x-axis and intensity on y-axis)*

The difference plot of GS 800 and GC 800 in **Fig. 7** shows a pattern nearly flat except for the interval $2\theta = 20^\circ - 30^\circ$. These values correspond to the crystalline phosphates' phases of the two samples. More specifically, for 2θ around 20.8°, 24.2° and 27.1° the GS 800 specimen shows a higher content of titanium oxide phosphates compared to GC 800.

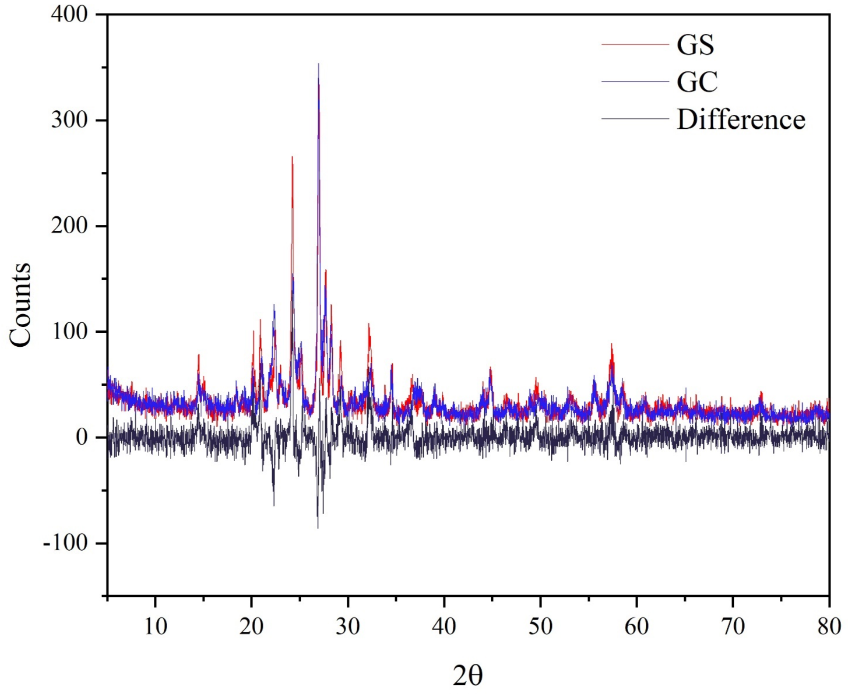

Fig. 7 - *XRD difference plot between GC 800 and GS 800*

6.1.3 UV-vis spectroscopy

The UV-vis spectroscopy is done to investigate the optical and elemental analysis, focusing on the absorption values. The test is done on both GC and GS samples obtained at the different calcination temperatures. The resulting spectra are displayed in **Fig. 6**.

The GC 200 and GS 200 maximum absorptions are registered for wavelengths between 200 – 300 nm while the curve tends to flatten from values around 400 nm. The absorption values are in the range of 0.3 – 0.6.

The absorption values of GC 500 and GS 500 nanoparticles exhibit differences, while the wavelength range for both remains constant at 250 – 350 nm. The maximum absorption range for GC 500 nanoparticles is from 0.9 to 1.1, whereas for GS 500 nanoparticles, it falls between 0.3 and 0.5.

The GC 800 and GS 800 show higher absorption value as compared to the other specimens. Specifically, within the wavelength range of 250 – 350 nm, the maximum absorption range for GC 800 nanoparticles is between 1.0 and 1.2, while for GS 800 nanoparticles, it lies between 0.7 and 0.8.

The maximum absorption values between wavelengths of 200 − 400 nm, means that the maximum absorption is done in the ultraviolet (UV) region of the electromagnetic spectrum.

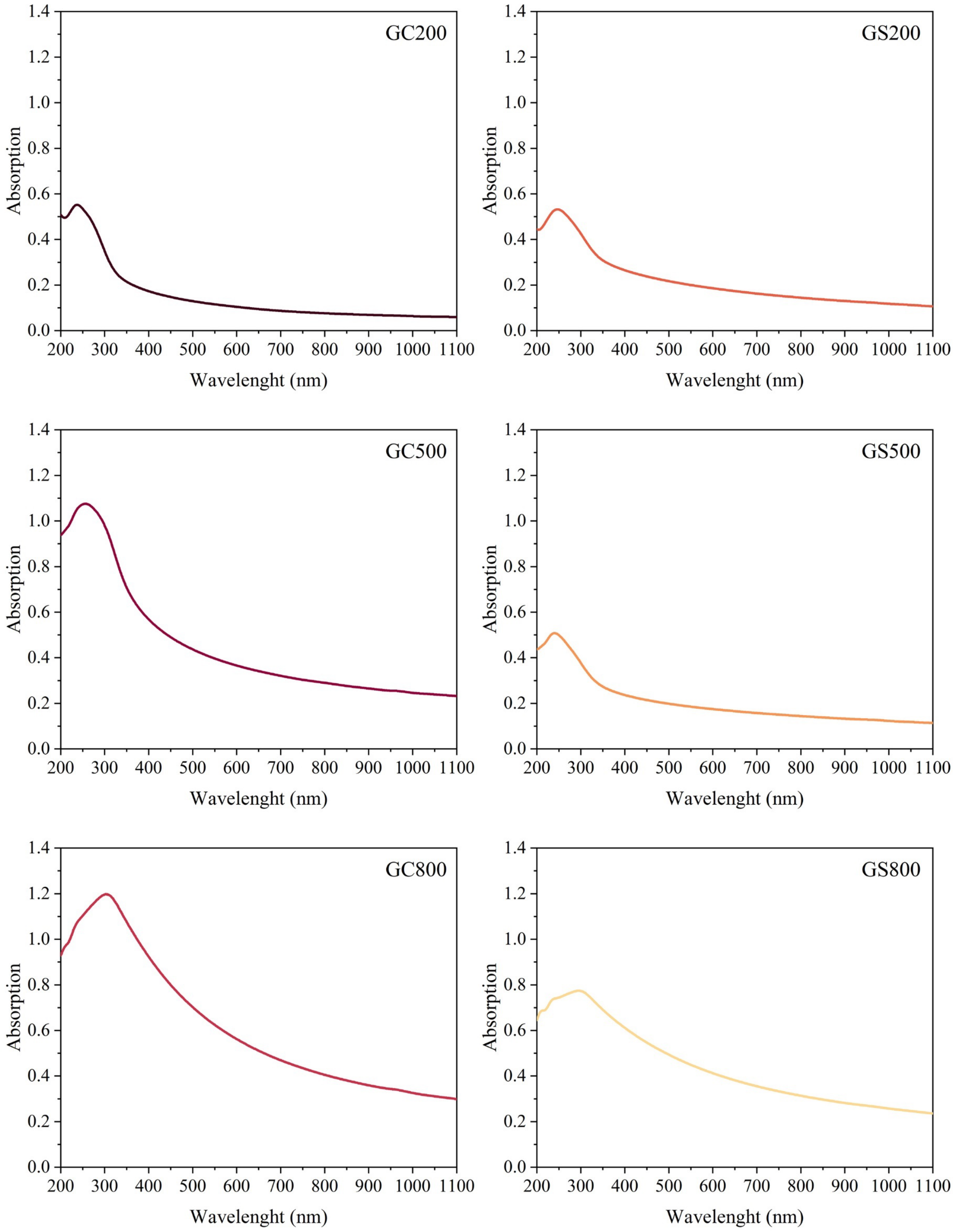

Fig. 6 - *UV-vis spectra of GC and GS samples*

6.1.4 Scanning Electron Microscopy (SEM) and Energy Dispersive X-ray Spectroscopy (EDS)

The structure of TiO_2 NPs from GC and GS is characterized by a well crystallized granular morphology as shown in **Fig. 8** and **Fig. 9** below.

The nanoparticles exhibit a spherical morphology, displaying minimal agglomeration and falling within a size range of 50–110 nm for GC 800 and 35−70 nm for GS 800.

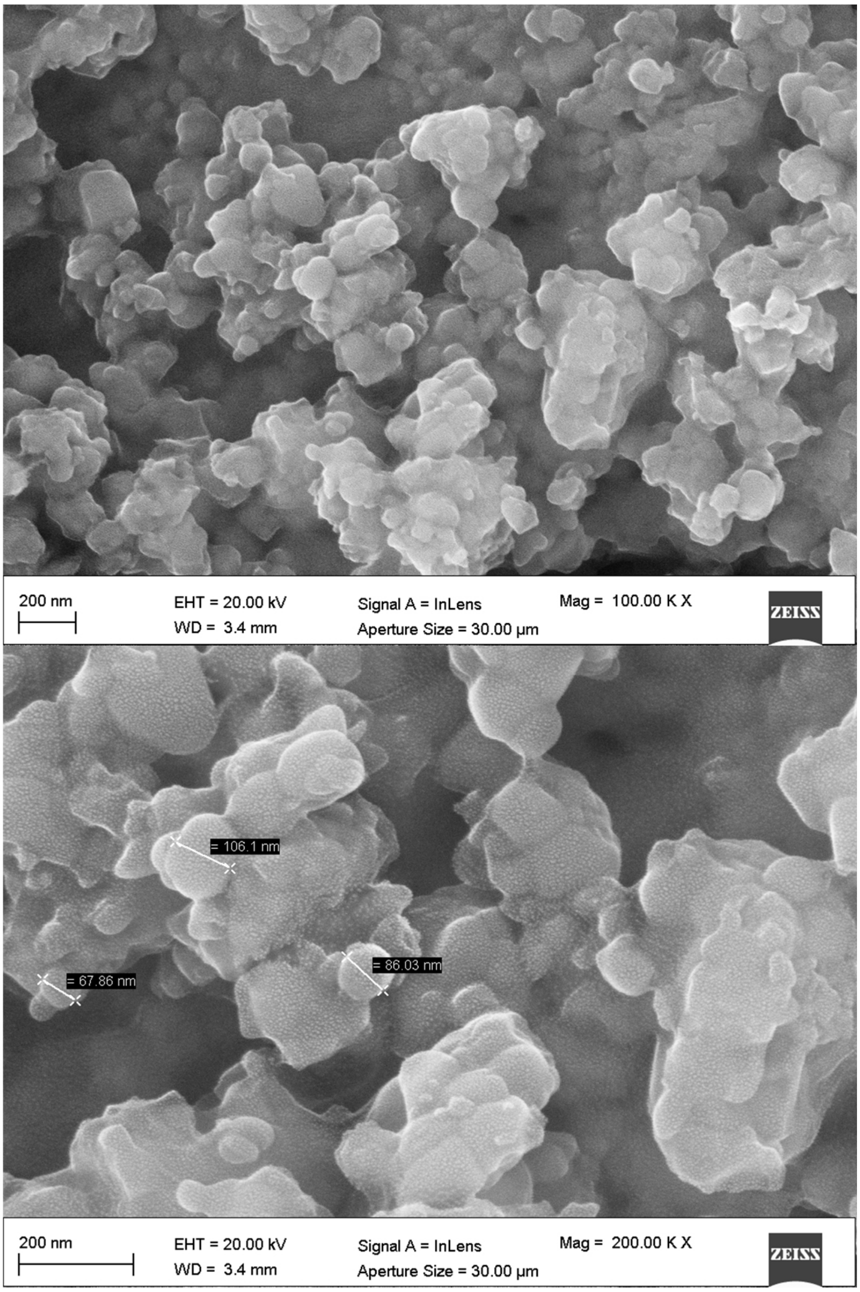

Fig. 7 - *SEM of GC800 sample*

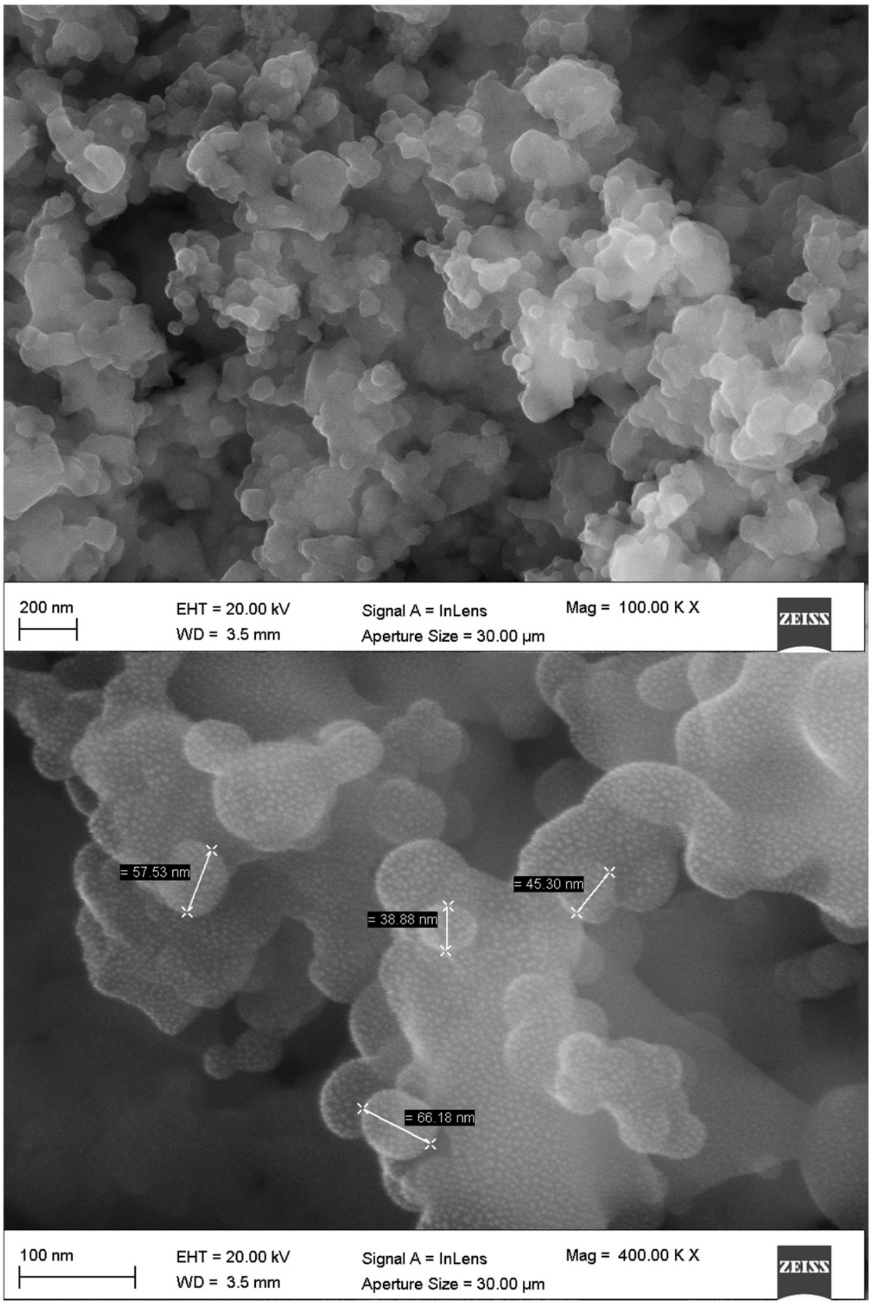

Fig. 8 - *SEM of GS 800 sample*

The EDS shown in **Fig. 10** and **Fig. 11** below provides information on the elemental composition of the samples. Specifically, it highlights the presence of carbon, phosphorus, and titanium in both samples. Particularly, GS 800 sample shows lower carbon content compared to GC 800.

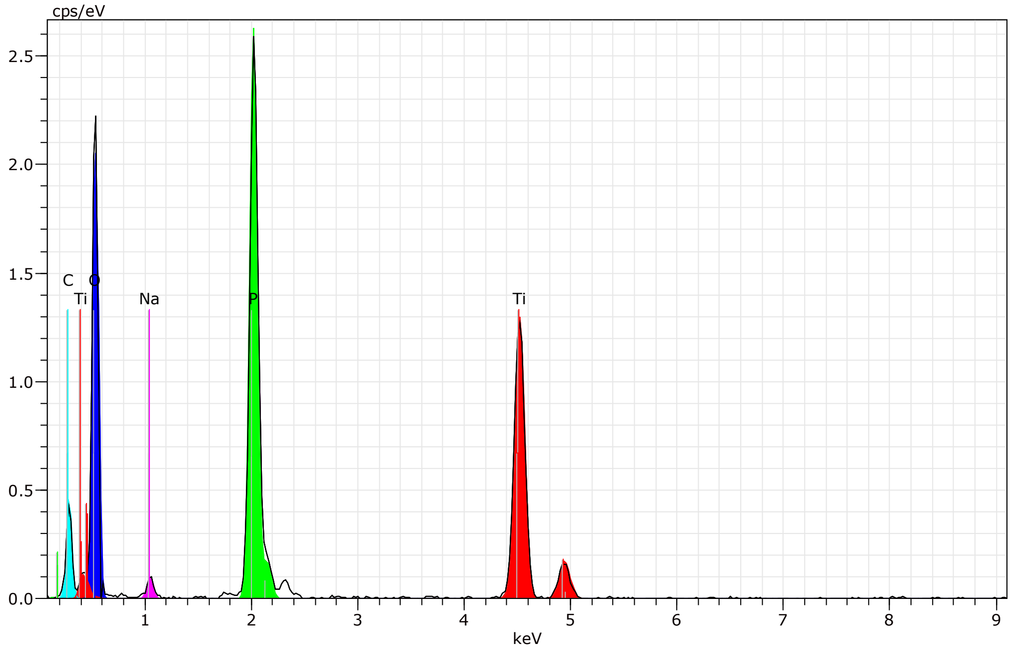

Fig. 9 - *EDS of GS 800*

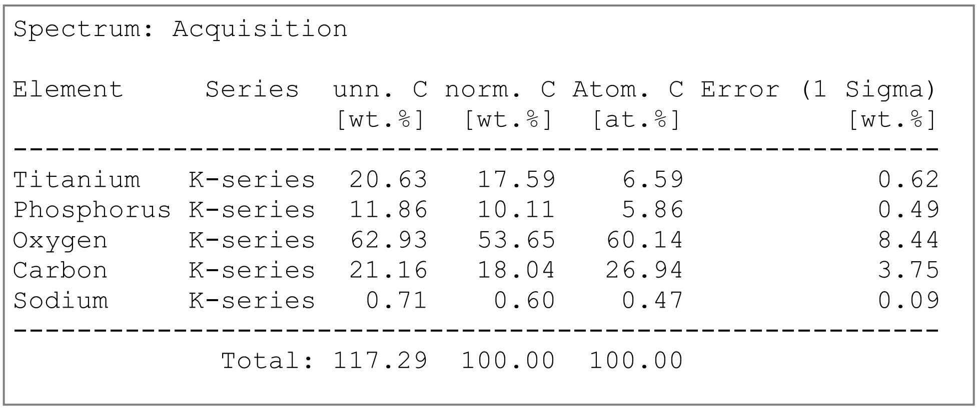

```
Spectrum: Acquisition

Element      Series   unn. C norm. C Atom. C Error (1 Sigma)
                      [wt.%]  [wt.%]  [at.%]           [wt.%]
-----------------------------------------------------------
Titanium   K-series   20.63   17.59    6.59              0.62
Phosphorus K-series   11.86   10.11    5.86              0.49
Oxygen     K-series   62.93   53.65   60.14              8.44
Carbon     K-series   21.16   18.04   26.94              3.75
Sodium     K-series    0.71    0.60    0.47              0.09
-----------------------------------------------------------
             Total:  117.29  100.00  100.00
```

Tab. 1 - *EDS data for GS 800*

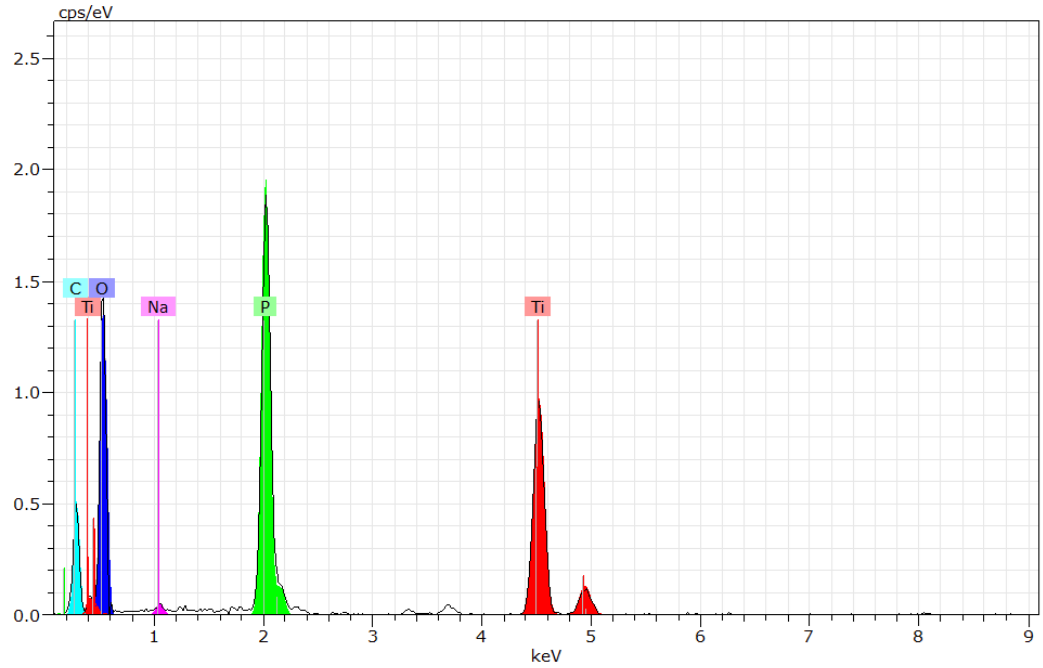

Fig. 10 - *EDS of GC 800*

```
                    Spectrum: Acquisition

Element      Series   unn. C norm. C Atom. C Error (1 Sigma)
                      [wt.%]  [wt.%]  [at.%]           [wt.%]
-----------------------------------------------------------
Titanium    K-series  16.07   14.55    5.23             0.50
Phosphorus K-series  12.20   11.05    6.14             0.51
Oxygen      K-series  54.17   49.04   52.72             7.68
Carbon      K-series  27.36   24.76   35.46             4.70
Sodium      K-series   0.67    0.60    0.45             0.09
-----------------------------------------------------------
                      Total: 110.47  100.00  100.00
```

Tab. 2 - *EDS data for GC 800*

6.1.5 Nanoparticles as paint additive for self-cleaning applications

The absorption test through UV-vis spectroscopy for both 1st and 2nd cycles under sunlight exposition are reported in **Fig. 12** and **Fig. 16**. The concentration of the dye solution at different wavelengths is determined through the calibration curve. The curve is based on the dye solution absorption data at different concentrations (**Fig. 13**).

Specifically, during the 1st cycle, when considering the value of the maximum absorption peak (519 nm) for each sample, it is observed that the concentration of the dye decreases regardless of its initial concentration. The reached concentrations are 0.00115% for GC 800, 0.00133% for GS 800 and 0.00074% for SOL65 despite the initial dye concentration value of 0,00185%. This means that the samples reduced the dye concentration of 38% (GC 800), 28% (GS 800) and 60% (SOL 65) in a time frame of 15 minutes. The SOL 65 sample is the more absorptive one, this is due to the fact that the content of NPs is higher (25% of the composition).

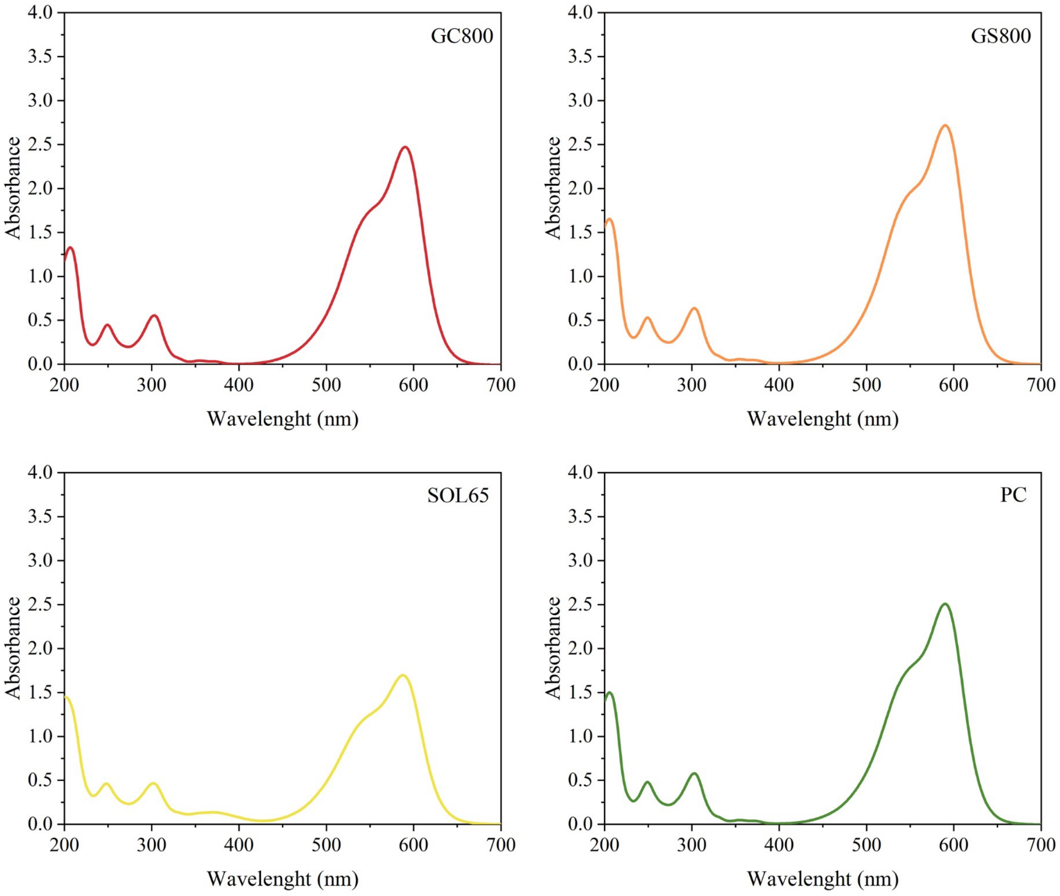

Fig. 11 - *Sunlight exposition UV-vis spectra (1st cycle)*

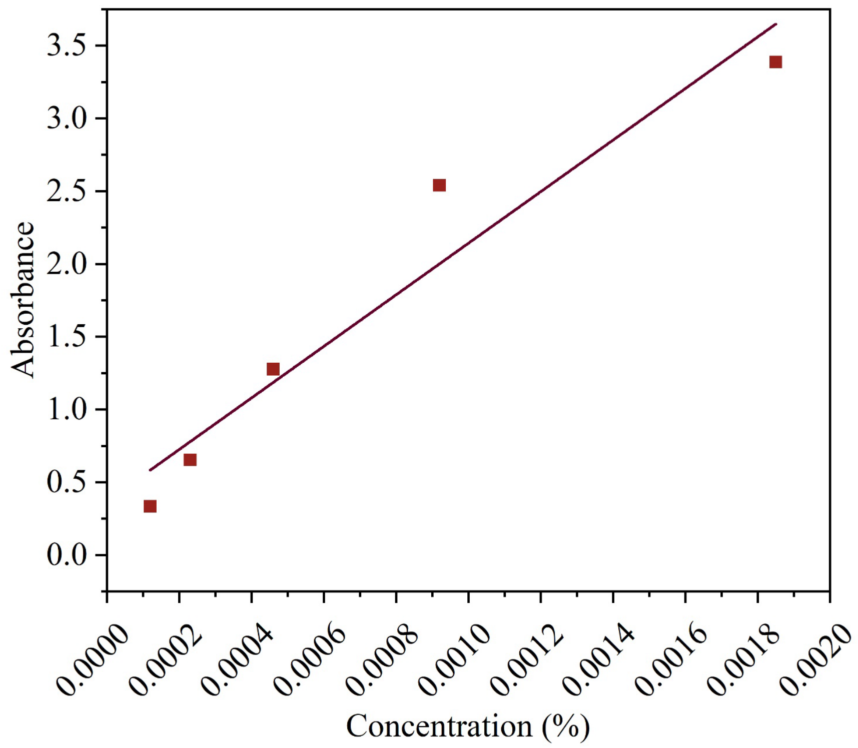

Fig. 12 - *Dye solution calibration curve*

Despite the high concentration, the exposure to sunlight demonstrates significant effectiveness in catalytically degrading the dye solution. The images below are obtained from image processing and show the colour changing of the specimens in a time frame that goes from 10 AM to 5 PM. The colour changing is index of the degradation of the dye present in the sample surface. The colour change is analysed in terms of RGB colour spectra. As can be seen in **Fig. 14**, the GC 800 and GS 800 specimens (1st cycle) exhibit remarkable degradation of the dye, as evidenced by the maximum colour intensity near 255 (white).

In this case, GC 800 and GS 800 samples show high efficiency in the removal of the dye through catalytic action. Whilst, SOL 65 specimen shows lower efficiency in terms of photocatalytic degradation of dye pigment. The commercial photocatalytic paint, Solarya 65, contains 25% TiO_2 nanoparticles [84]. In contrast, GC 800 and GS 800, which are mixed with 2 grams of paint, have an addition of 50 mg of nanoparticles, accounting for 2.5% of the overall mixture. Remarkably, despite having a nanoparticle content that is 10 times lower than the commercial product, GC 800 and GS 800 exhibit higher efficiency in removing dyes, as evidenced by the comparison of results.

The maximum intensities of the RGB values for each specimen are reported for every hour in the graph in **Fig. 15 (A)**. The data are analyzed also in logarithmical scale in the graph in **Fig. 15 (B)**.

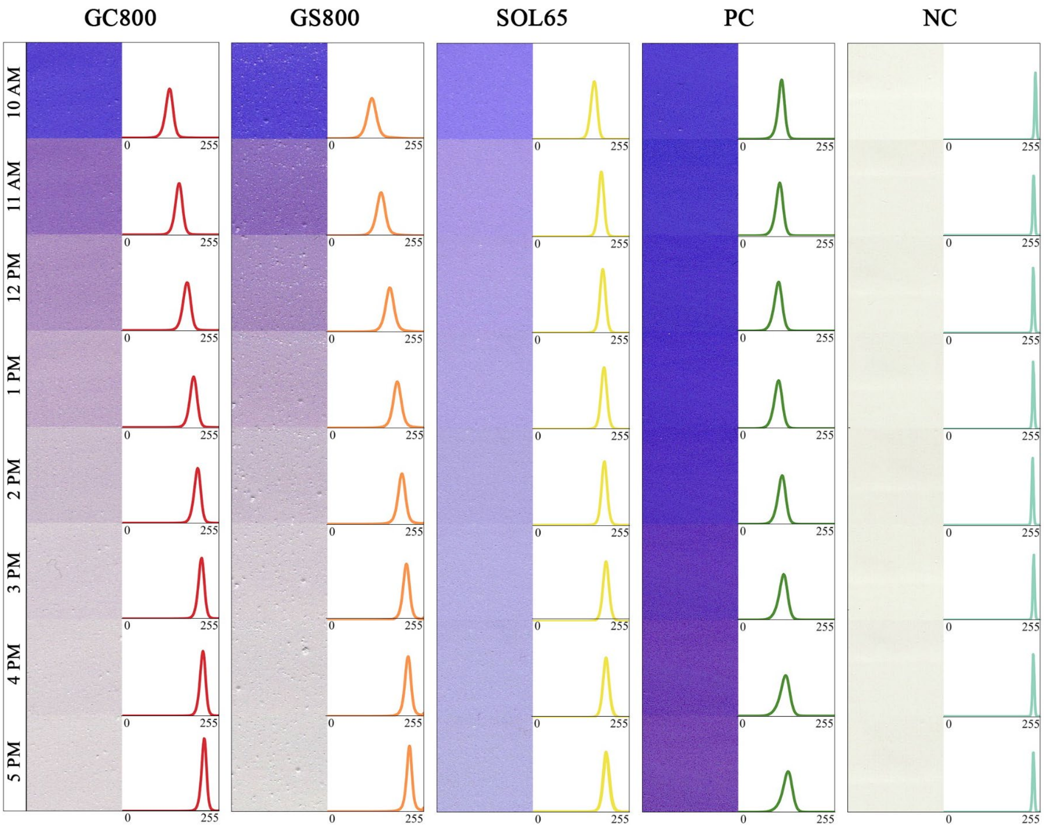

Fig. 13 - *Dye absorption through color spectra analysis – RGB intensity values (1st cycle)*

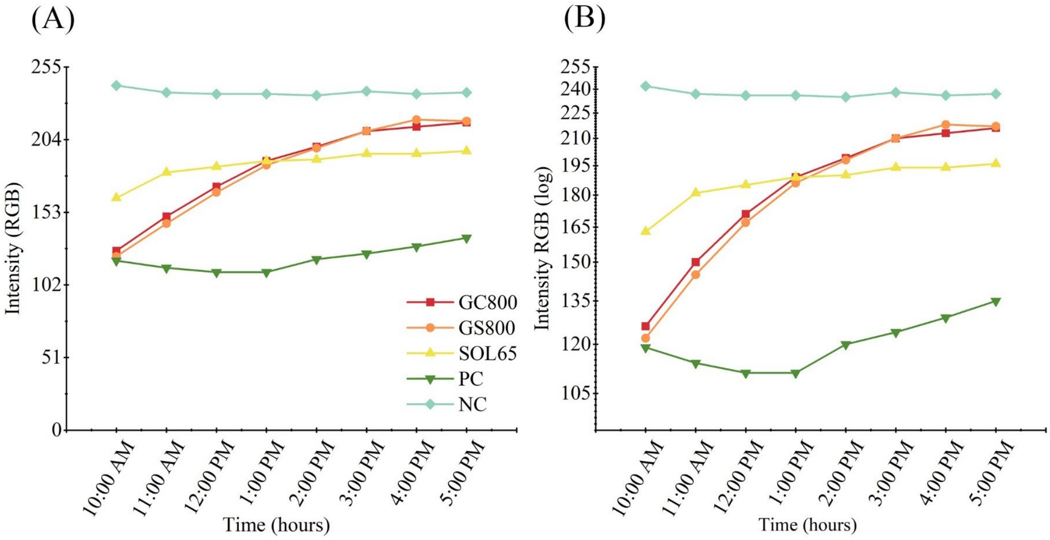

Fig. 14 - *(A) Maximum intensity of RGB spectra through hour range (1st cycle); (B) Maximum RGB intensity through hours in logarithmic scale (1st cycle)*

Regarding the 2nd cycle, as can be observed in the UV-vis spectra below, the specimens show higher absorption values because of the presence of the residue of dye solution from the first cycle of exposition. Among all the specimens, SOL 65 shows a marked difference between 1st and 2nd cycle due to the fact that the residue of dye on the surface is higher than in the case of GC 800 and GS 800 samples.

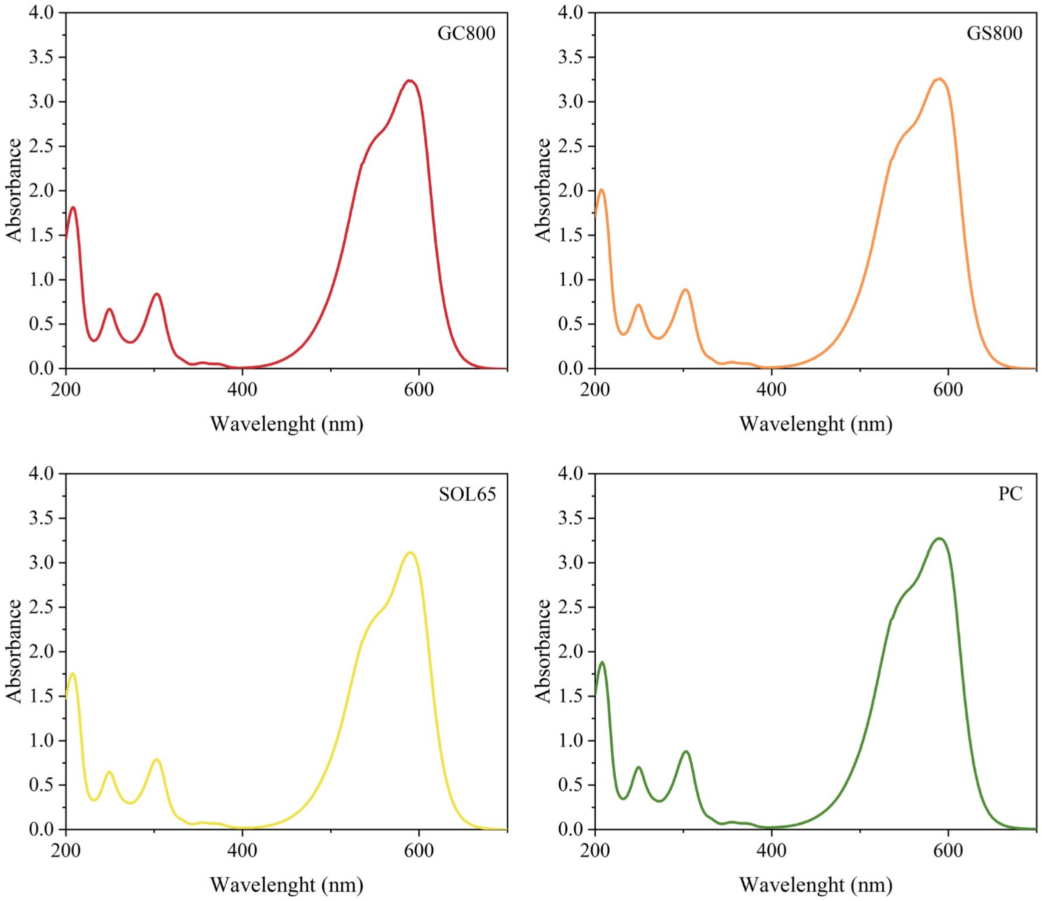

Fig. 15 - *Sunlight exposition UV-vis spectra (2nd cycle)*

The results of image processing are shown in **Fig. 17** and **Fig.18** below:

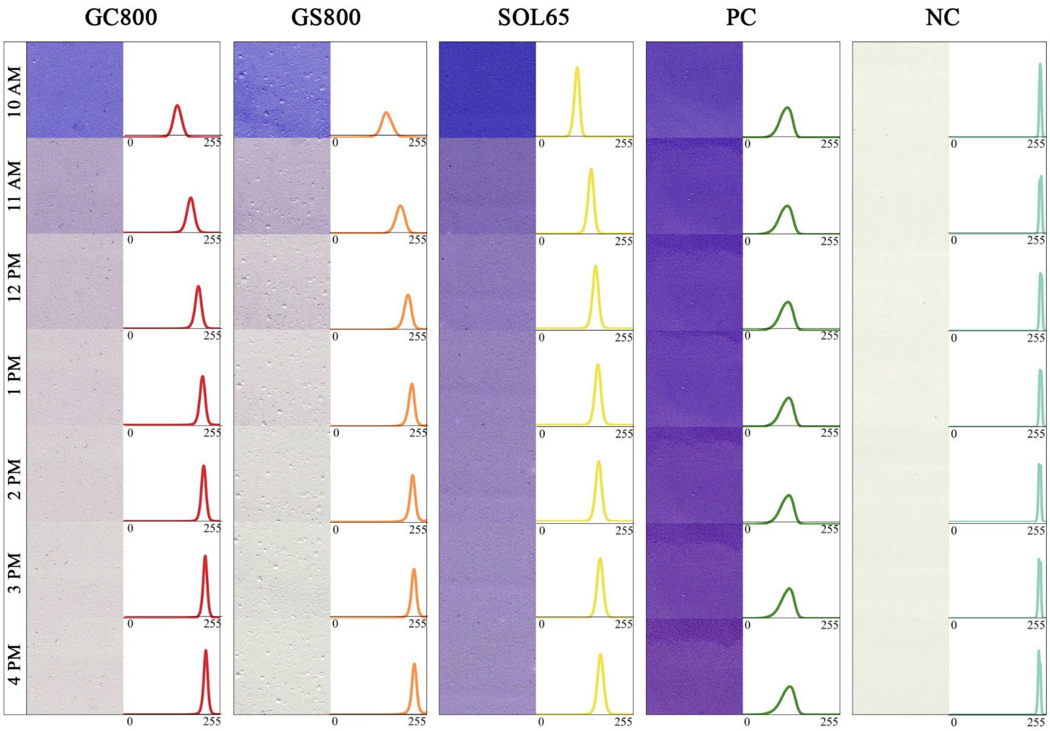

Fig. 16 - *Dye absorption through color spectra analysis (2nd cycle)*

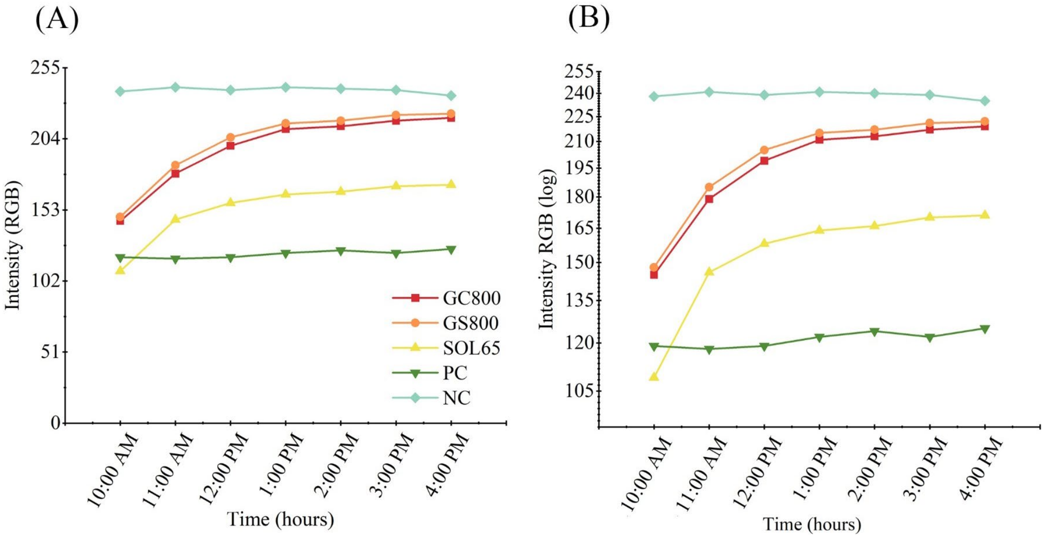

Fig. 17 - *(A) Maximum intensity of RGB spectra through hour range (2nd cycle); (B) Maximum RGB intensity through hours in logarithmic scale (2nd cycle)*

As it can be observed from **Fig. 18**, GC 800 and GS 800 show a growing trend that after 5 hours range is near the value of NC. Whilst, SOL 65 show a growth only in the first hour then the trend of intensity is nearly constant. This can be also seen from the RGB intensity spectra in **Fig. 17**. The curve of GC 800 and GS 800 intensity is near the NC one, while the SOL 65 curve shows a significant change only through the first hour.

As a result, SOL 65 demonstrates a loss of photocatalytic activity after the first cycle. In contrast, despite their lower nanoparticle content, GC 800 and GS 800 maintain effective photocatalytic degradation even during the second cycle. This suggests that GC 800 and GS 800 demonstrate superior efficiency for long-term applications due to their ability to maintain photocatalytic activity over time.

For the visible light exposition case the results of the experiment are shown in **Fig. 19**, **Fig. 20** and **Fig. 21**.

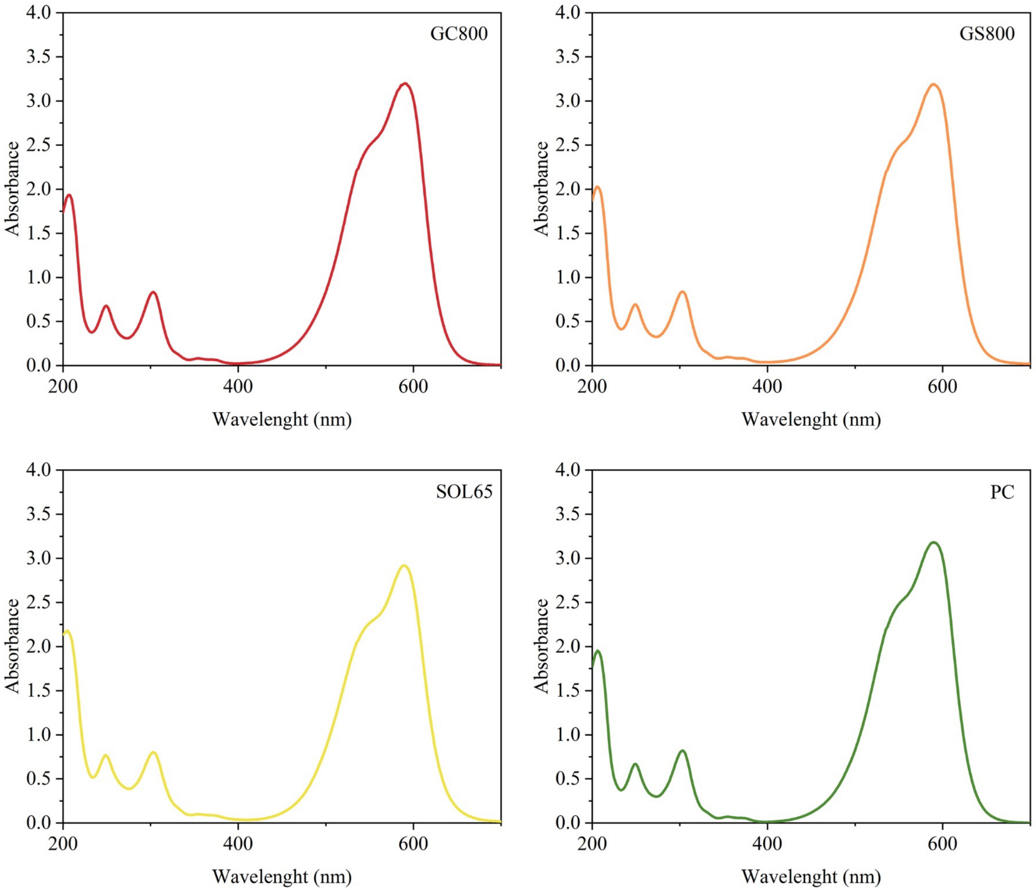

Fig. 18 - *UV-vis absorption spectra for visible light exposition*

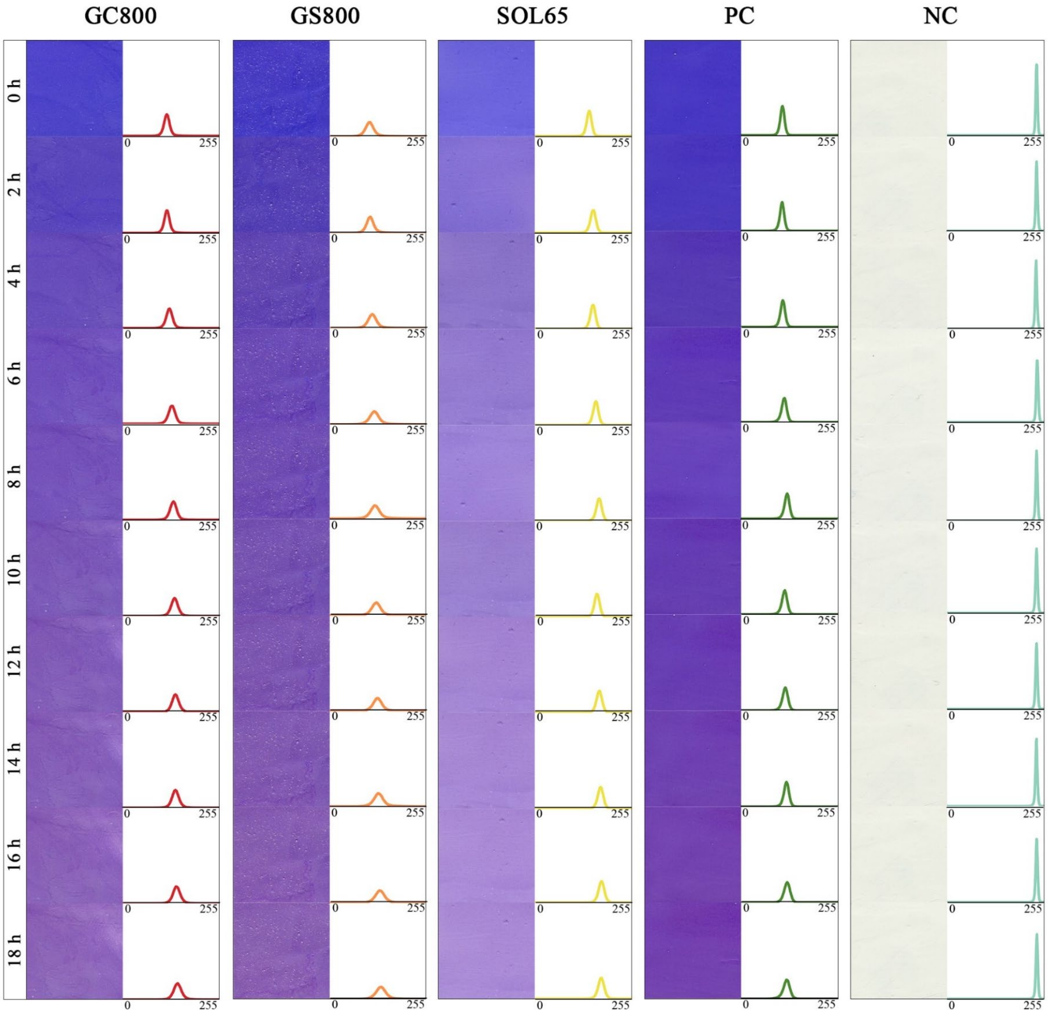

Fig. 19 - *GC800, GS800, SOL65, PC and NC dye absorption through color spectra analysis (visible light)*

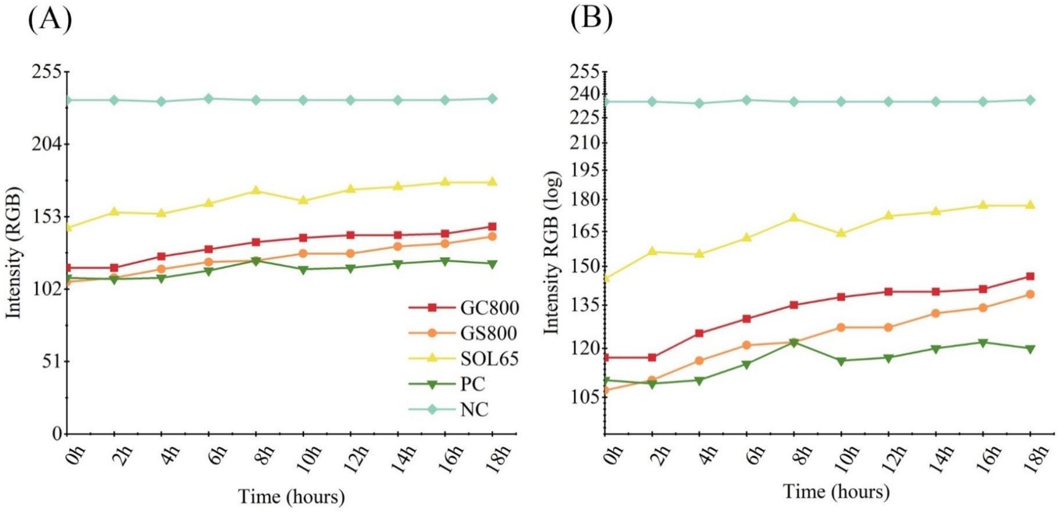

Fig. 20 - *(A) Maximum intensity RGB spectra for visible light exposition; (B) Maxiumum intensity RGB spectra for visible light exposition in logarithmic scale*

As can be seen from the **Fig. 20** and **Fig. 21** the specimens show a slower photocatalytic degradation compared to the first and second cycle of sunlight exposition. This phenomenon can be attributed to the slower reaction rate in visible light and the high concentration of CV (Crystal Violet) in the dye solution. By examining the maximum intensity RGB graph, it is observed that the values of maximum intensity after 18 hours are 177, 146, and 139, respectively, for SOL 65, GC 800, and GS 800. As a result, SOL 65 specimen is the one with major activity.

However, the NPs content of the specimens should be taken in account. The NC (reference sample) exhibits a maximum RGB intensity of 236. Interestingly, considering that SOL 65 contains 10 times the quantity of nanoparticles (NPs) [84], a straightforward calculation reveals that GC 800 and GS 800 demonstrate a more efficient photocatalytic degradation while utilizing fewer NPs.

6.1.6 Considerations

Indoor air quality (IAQ) is a growing concern as people spend a significant portion of their time indoors, whether at home, in offices, or other enclosed spaces. The presence of airborne pollutants, such as volatile organic compounds (VOCs), allergens, and bacteria, can have detrimental effects on human health and well-being. In recent years, the utilization of titanium dioxide nanoparticles (TiO_2 NPs) has emerged as a promising solution for enhancing IAQ.

TiO_2-NPs, with their unique properties and photocatalytic capabilities, have attracted considerable attention as a potential tool for improving IAQ. These nanoparticles can harness the power of light to initiate chemical reactions, leading to the degradation and removal of various airborne pollutants.

The application of TiO_2 nanoparticles for IAQ improvement extends to various indoor settings, including residential, commercial, and healthcare spaces. Moreover, the use of TiO_2 NPs for IAQ enhancement aligns with the growing emphasis on sustainable and eco-friendly solutions, as they do not introduce additional chemicals into the environment and can contribute to energy savings by reducing the need for traditional air purification methods.

Traditionally, titanium oxide NPs were primarily known for their photocatalytic activity under ultraviolet (UV) light, which constitutes only a small fraction of the solar spectrum. However, recent advancements have focused on enhancing their photocatalytic efficiency in the visible light range, which makes up a significant portion of natural sunlight.

Visible light-responsive nanoparticles have been developed through various strategies, such as modifying their structure, composition, and surface properties. These modifications enable TiO_2 NPs to harness visible light energy and utilize it for photocatalytic reactions. This expanded absorption range allows to be more effective in practical applications where visible light is abundant, such as indoor environments or under cloudy sky conditions.

In this research, the use of TiOP waste-derived nanoparticles is investigated for improving indoor air quality. The synthesized nanoparticles are used as additive for indoor paint comparing the results with a commercial paint.

From the comparation of the data it’s clear that challenges remain in implementing TiO_2 NPs for IAQ improvement, including addressing their potential health and safety concerns, optimizing their photocatalytic efficiency, and ensuring long-term durability in real-world indoor environments. Further research and development efforts are necessary to overcome these challenges and unlock the full potential of TiO_2 NPs for enhancing IAQ.

The present research had the aim to present the comparation between traditional methods of synthesis and two modified sustainable methods. For what has emerged from the results, it’s demonstrated that greener approaches can be used to provide new nanomaterials from waste matter. The “Green” TiO_2 NPs are proved to be advantageous compared to the commercial option in terms of efficiency, sustainability of the method and quantity of materials used for the experiment.

6.2 PAN-based electro-spun nanoweb for water filtration

6.2.1 SEM of PAN-based membranes with NCel additives

The figure below represents the SEM images of the PAN-based electro-spun membranes (**Fig. 22**).

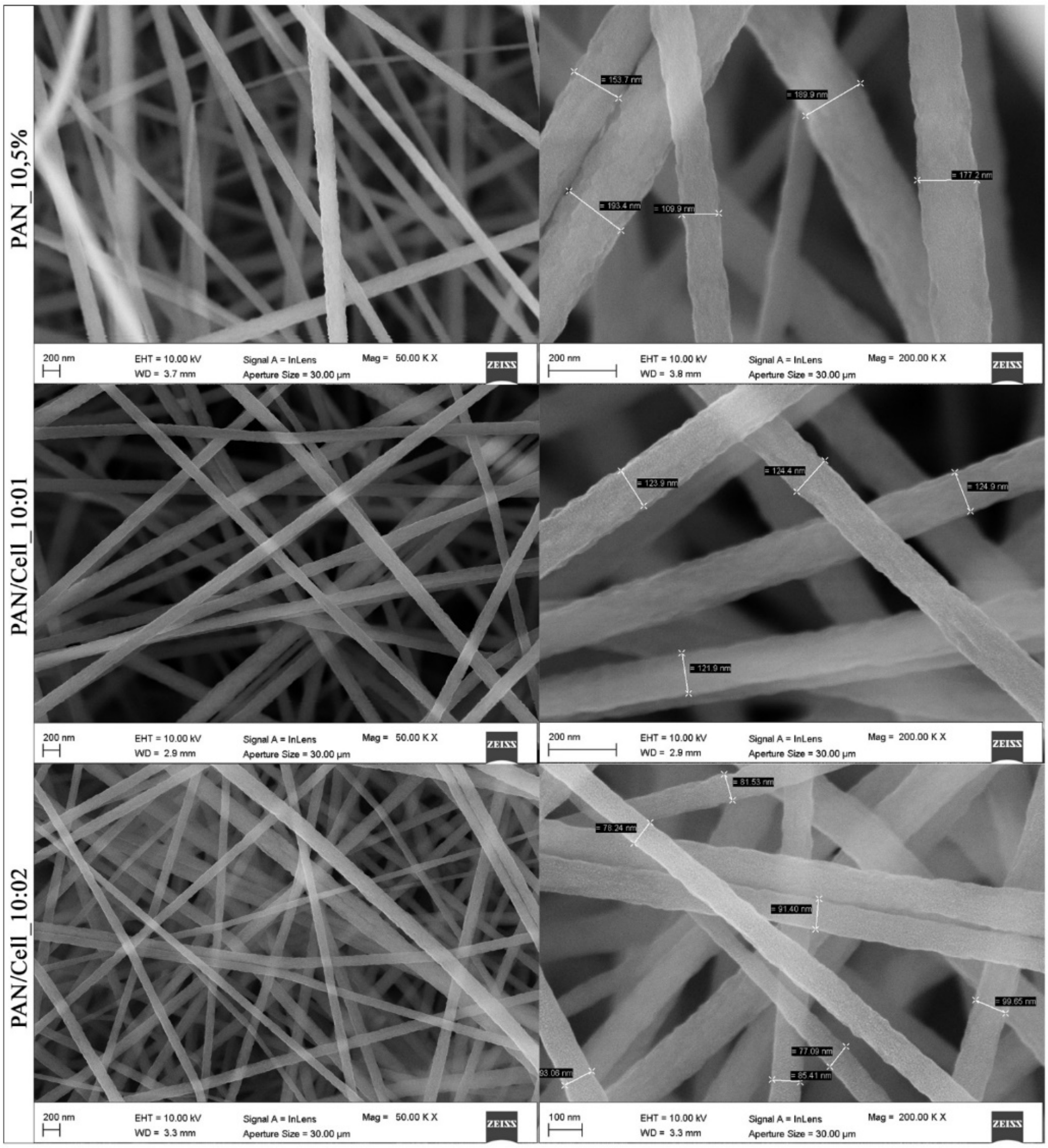

Fig. 21 - *SEM spectroscopy of PAN-based membranes*

The diameter of the fibers is found to be in the range of 100 − 200 nm for the specimens PAN_10.5% and PAN/NCel_10:01, while for PAN/NCel_10:02 the diameter range is between 75 − 150 nm. This diminution of the fibers diameter in this membrane can be justified for the presence of NCel in higher quantity. In all three cases, the surface of the fibers shows a rough surface.

6.2.2 Electro-spun PAN-based membrane absorption test – results

The assessment of absorption properties is crucial in evaluating the performance and effectiveness of various types of membranes used in diverse applications, including water treatment, gas separation, and drug delivery systems. Membrane absorption tests provide valuable insights into the capacity of a membrane to absorb specific substances or solutes, which is a critical factor in determining its suitability for a particular application.

The absorption test involves exposing the membrane to a specific solution or gas mixture under controlled conditions and monitoring the amount of material absorbed by the membrane over a defined period. This test allows to quantify the membrane's absorption capacity, as well as study the kinetics and mechanisms of the absorption process.

The results obtained from membrane absorption tests provide valuable information for optimizing membrane materials, modifying surface properties, and designing membranes with enhanced absorption capabilities. By understanding the absorption behaviour, researchers can tailor membranes to target specific substances, improve separation efficiency, and optimize performance in various applications.

The UV-Vis absorption values of the membranes over a 90-minute time span are represented in the figures below (**Fig. 24**) for each cycle (from 400 to 800 nm wavelengths). The spectra are represented in terms of concentration and wavelengths using the calibration curve in **Fig. 23**.

From the described images, it is evident that there is a notable reduction in the CV content in the solution throughout the 90-minute duration. This decrease is observed consistently across all performed cycles, indicating the membranes' potential and effectiveness over time.

Remarkably, all three membranes exhibit sustained absorption capacity even after the third cycle. Specifically, the PAN/NCel_10:02 membrane demonstrates enhanced absorption in the second cycle and maintains comparable absorption levels in the last cycle, similar to those observed in the initial cycle.

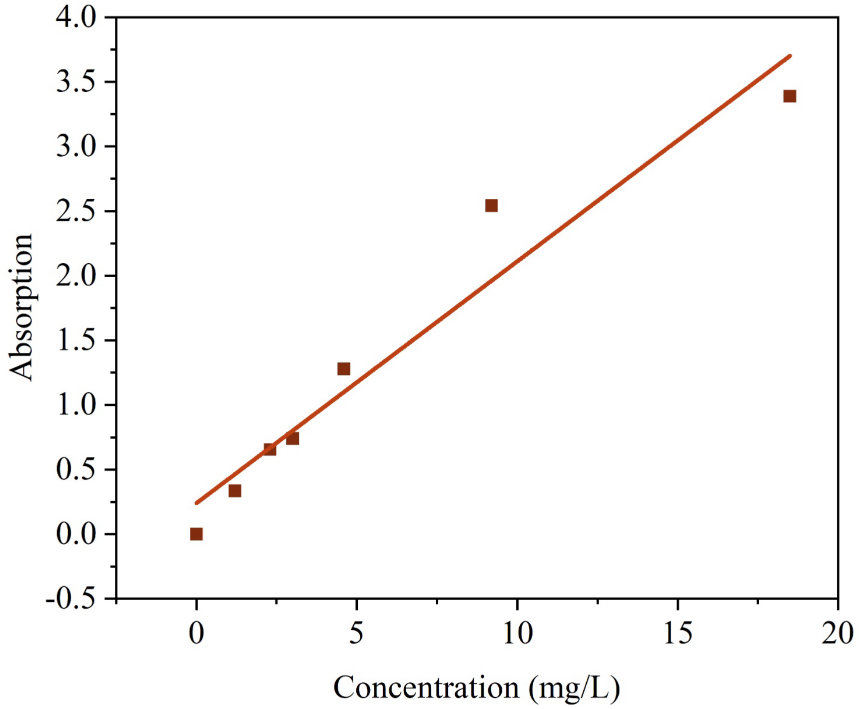

Fig. 22 - *Calibration curve; x-axis is concentration in mg/L, y-axis is absorbance*

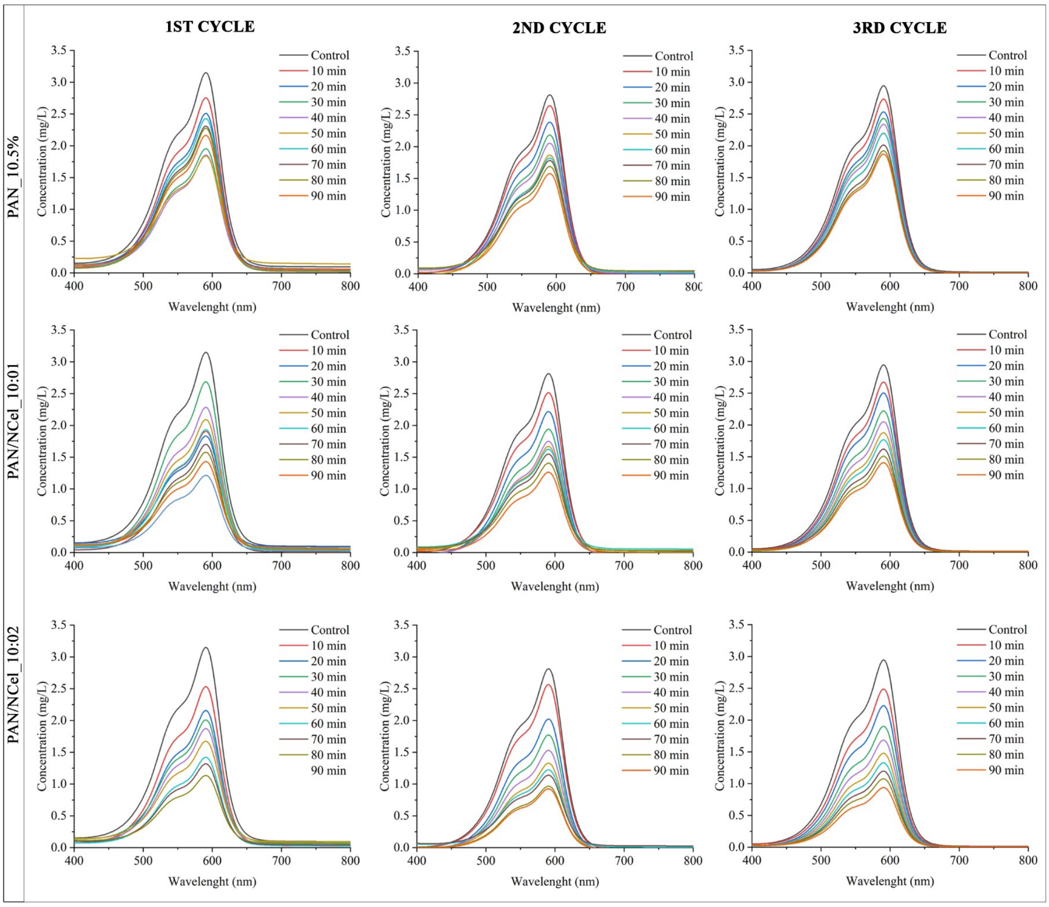

Fig. 23 - *UV-vis spectra of PAN_10.5%, PAN/NCel_10:01, PAN/NCel_10:02; x-axis is wavelength, y-axis is concentration*

This phenomenon can be further investigated observing the duration of contact between adsorbent materials and adsorbate (**Fig. 25**). This data is a crucial factor in adsorption experiments, as it significantly affects the removal of pollutants from aqueous solutions. The effect of contact time is decisive because it directly influences the rate at which the adsorbate molecules are transferred from the solution onto the surface of the adsorbent material. During the initial stages of the adsorption process, there is typically a rapid increase in the amount of adsorbate molecules being adsorbed as the adsorbent surface becomes available for adsorption. This phase is known as the "adsorption kinetics" or "adsorption uptake" stage.

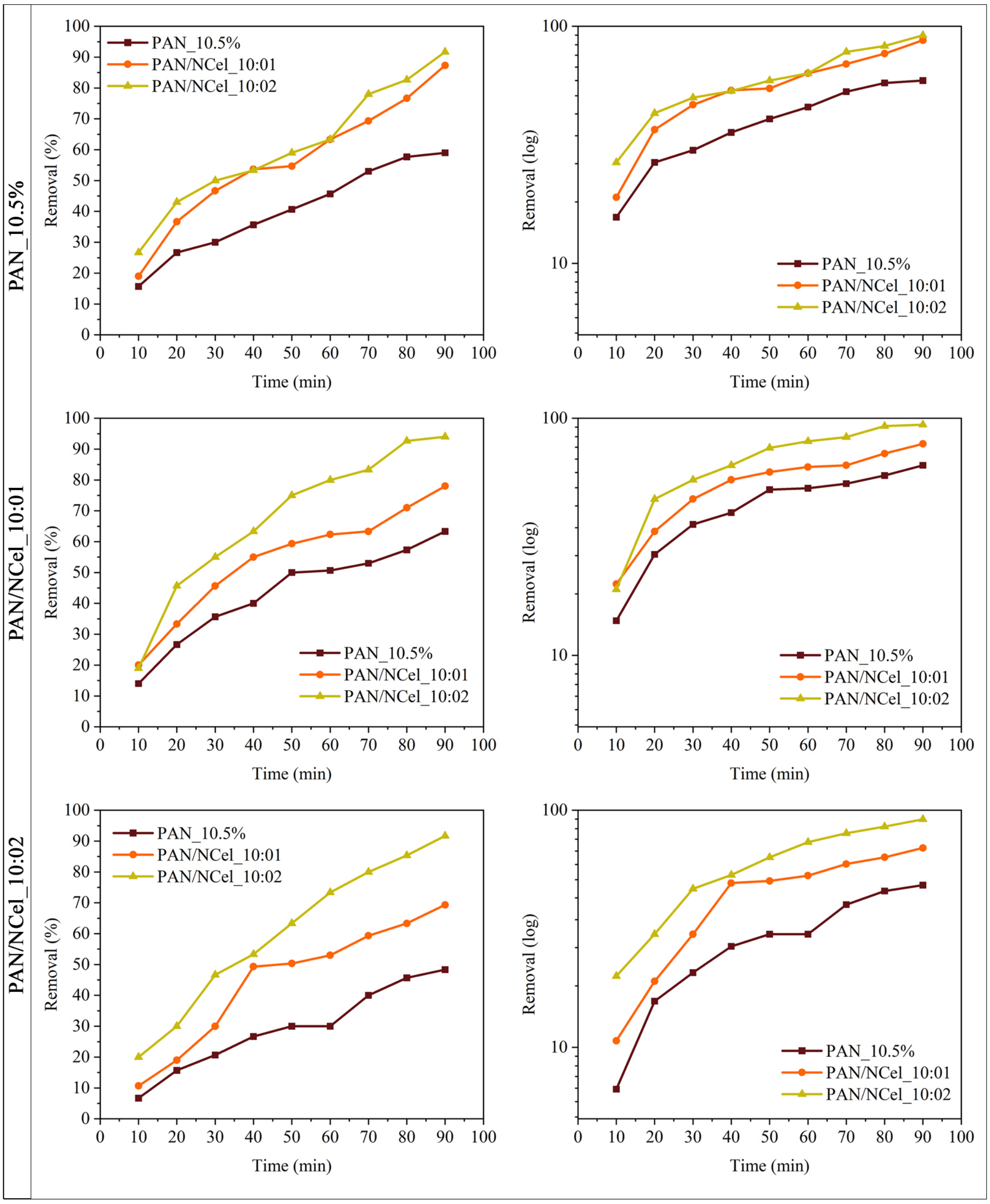

Fig. 24 - *Effect of contact time study: Percentage removal of CV dye through time.*

As the contact time progresses, the rate of adsorption gradually slows down, eventually reaching a point of equilibrium where the amount of adsorbate being adsorbed remains constant. This equilibrium point signifies that the adsorbent surface has reached its maximum adsorption capacity, and no further adsorption occurs.

Studying the effect of contact time in batch absorption experiments helps determine the optimal contact time required to achieve maximum adsorption efficiency. By monitoring the adsorption process at different time intervals, the point of equilibrium and the time needed for the adsorption system to stabilize are evaluated.

Additionally, the study of contact time provides insights into the adsorption kinetics and the overall rate of adsorption. It helps in understanding the adsorption mechanism, whether it follows a rapid initial adsorption phase or a slower, gradual adsorption process.

Moreover, the effect of contact time allows to evaluate the feasibility of using a particular adsorbent material in practical applications. If the adsorption process reaches equilibrium within a short contact time, it indicates that the adsorbent material is efficient and can be applied for rapid purification or separation processes. On the other hand, if a longer contact time is required to achieve equilibrium, it may imply that the adsorption process is relatively slower or that the adsorbent material needs further optimization [12].

The effect of contact time is measured considering the percentage of removal of CV dye through 90 minute time range. From the relative figure, it can be observed that the percentage removal of CV dye increases over time.

The highest removal rate, is shown by PAN/NCel_10:02 which reaches the maximum peak at 90 minutes with values of removal of 91.7 % (1st cycle), 94% (2nd cycle) and 91.7% (3rd cycle).

In contrast to PAN/NCel_10:02, PAN/NCel_10:01 exhibits a reduced removal rate across different cycles, indicating that the equilibrium point in subsequent cycles will be reached at a slower pace compared to the initial cycle. In fact, the final percentage of removal at 90 min is decreased of 32% during the second cycle and 45% during the third onee.

The PAN_10.5% membrane demonstrates the lowest removal values, with maximum percentages of removal reaching approximately 60% in the first and second cycles, which further decrease to 48% in the final cycle. This data may indicate the swelling of the membrane during the cleansing process.

The obtained results highlight the effectiveness of incorporating NCel into PAN-based membranes. The observed higher removal rate can be attributed to the increased quantity of functional groups present in the membranes, which is a direct result of the addition of NCel.

Adsorption kinetics study is a fundamental aspect of understanding the dynamics and rate at which adsorption processes occur. It involves investigating the interaction between adsorbate molecules and the adsorbent material over time. The kinetics of adsorption play a crucial role in determining the efficiency, effectiveness, and applicability of various adsorption processes in fields such as environmental remediation, water treatment, and gas separation.

Adsorption kinetics focuses on the examination of how the concentration of adsorbate changes with respect to time during the adsorption process. Various mathematical models, such as the pseudo-first-order and pseudo-second-order models, can be applied to describe the adsorption kinetics and predict the adsorption behaviour over time. These models provide insights into the adsorption mechanism, reaction rate constants, and equilibrium parameters.

Adsorption kinetics studies offer valuable information for understanding the factors influencing the adsorption process, including temperature, pH, initial concentration, and surface properties of the adsorbent material. They also provide a basis for evaluating the efficiency and feasibility of different adsorbents for specific applications [76].

The absorption is primarily evaluated through the relationship between the concentration of the adsorbate (C) relative to its initial concentration (C_0) and the elapsed time during the adsorption process. The graphs are plotted also in logarithmic scale as shown in **Fig. 26**.

The behaviour of the (C/C_0) versus time graph can provide insights into the adsorption process. Generally, at the beginning of the adsorption process, (C/C_0) is high as the concentration of the adsorbate in the solution is relatively high compared to its initial concentration. As time progresses, the (C/C_0) value decreases, indicating the adsorbate's removal from the solution.

The shape of the graph can vary depending on the specific adsorption kinetics and equilibrium characteristics. In some cases, (C/C_0) may decrease rapidly initially and then level off as the adsorption approaches equilibrium. In other cases, (C/C_0) may decrease gradually over time until it reaches a steady-state or equilibrium value.

The $ln(C/C_0)$ value is a common representation used in adsorption studies to assess the extent of adsorption and the kinetics of the process. A steeper slope indicates a more rapid adsorption process, while a shallower slope suggests a slower rate of adsorption. The slope can also provide insights into the order of the adsorption kinetics, as different kinetic models exhibit distinct slope characteristics. Furthermore, the intercept of the line with the y-axis represents the equilibrium point or the point at which the adsorption process reaches a steady state.

The value of *ln*(C/C$_0$) at this intercept corresponds to the equilibrium concentration of the adsorbate. Overall, the graph provides a visual representation of the adsorption kinetics, enabling the determination of the rate, order, and equilibrium of the adsorption process.

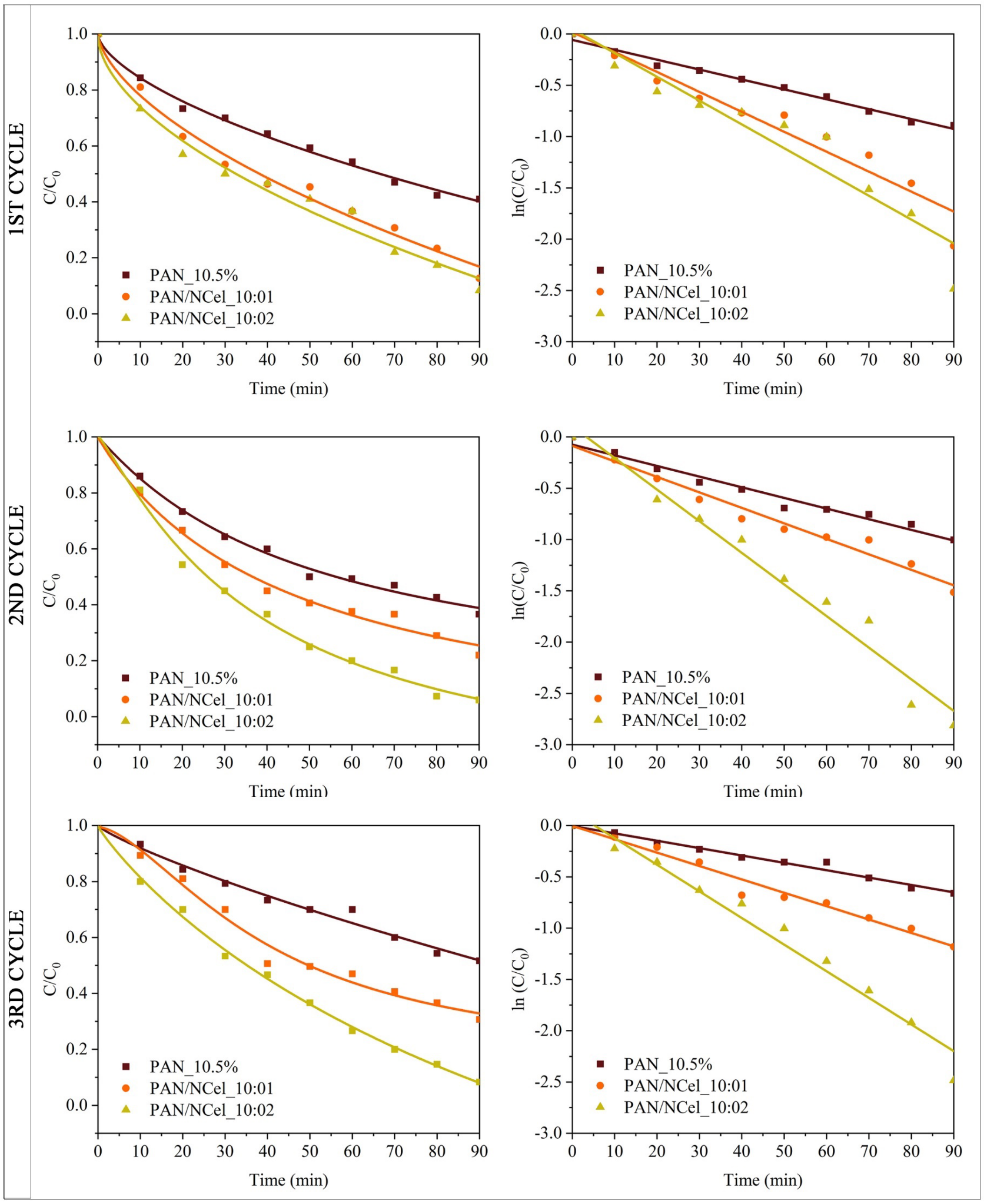

Fig. 26 - *Behavior of the (C/C$_0$) versus time graph*

As can be seen from the figures (**Fig. 27**), the second order kinetics model of the PAN-based membrane is more suitable to represent the absorption. The correlation coefficient (R^2) for the pseudo-second order kinetics model surpasses that of the pseudo-first order kinetics model, indicating a stronger agreement between the adsorption kinetics and the pseudo-second order model compared to the pseudo-first order model. Furthermore, the parameters of the non-linear pseudo-second order kinetic model for CV are summarized in **Tab. 3**.

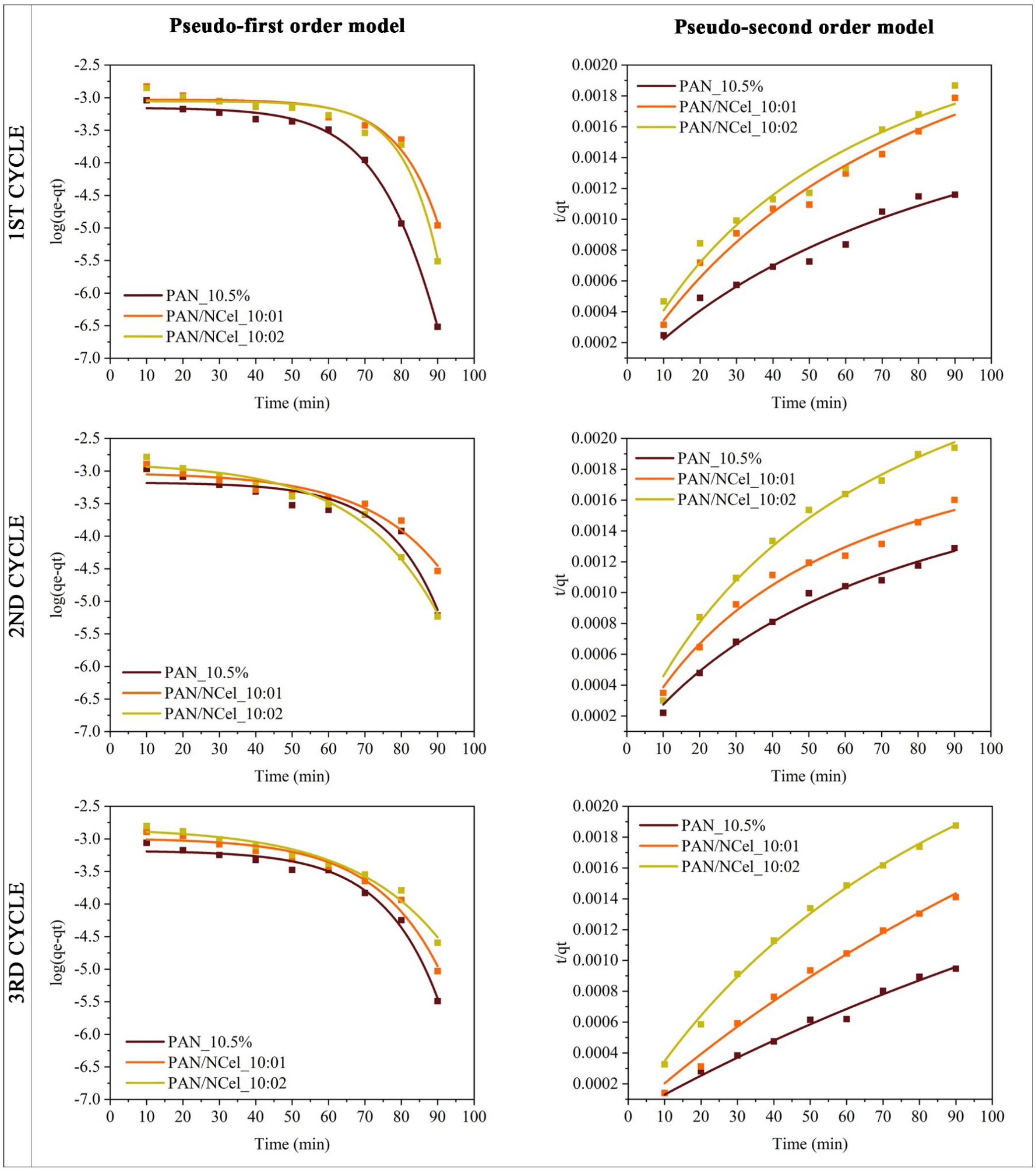

Fig. 25 - *Pseudo-first order and pseudo-second order kinetics models*

1st cycle		*2nd cycle*		*3rd cycle*	
PAN_10.5%					
q_e (mg/g)	0.00418 ± 2.46441E-4	**q_e** (mg/g)	0.00244 ± 1.82439E-4	**q_e** (mg/g)	0.00418 ± 2.46441E-4
k_2 (g* mg−1*min−1)	2.17452 ± 0.33022	**k_2** (g* mg−1*min−1)	7.70268 ± 1.7658	**k_2** (g* mg−1*min−1)	2.17452 ± 0.33022
R^2	0.99731	**R^2**	0.98341	**R^2**	0.99731
PAN/NCel_10:01					
q_e (mg/g)	0.0059 ± 0.00162	**q_e** (mg/g)	0.00233 ± 1.9505E-4	**q_e** (mg/g)	0.0059 ± 0.00162
k_2 (g* mg−1*min−1)	0.60613 ± 0.37495	**k_2** (g* mg−1*min−1)	5.73064 ± 1.34508	**k_2** (g* mg−1*min−1)	0.60613 ± 0.37495
R^2	0.99073	**R^2**	0.9892	**R^2**	0.99073
PAN/NCel_10:02					
q_e (mg/g)	0.00464 ± 0.00194	**q_e** (mg/g)	0.00338 ± 2.85851E-4	**q_e** (mg/g)	0.00464 ± 0.00194
k_2 (g* mg−1*min−1)	0.6221 ± 0.5724	**k_2** (g* mg−1*min−1)	4.63328 ± 1,14393	**k_2** (g* mg−1*min−1)	0.6221 ± 0.5724
R^2	0.98531	**R^2**	0.9857	**R^2**	0.98531

Tab. 3 - *Kinetic parameters for pseudo-second order adsorption model*

Adsorption isotherm studies provide valuable insights into the equilibrium relationship between the concentration of the adsorbate in the solution and its concentration on the surface of the adsorbent material.

The primary objective of adsorption isotherm studies is to determine the adsorption capacity, adsorption efficiency, and the nature of the adsorption process.

Various mathematical models and equations have been developed to describe adsorption isotherms, such as the Langmuir isotherm, Freundlich isotherm, BET isotherm, and others.

These models allow researchers to quantify the adsorption capacity, assess the homogeneity or heterogeneity of the adsorption sites, and understand the mechanism of the adsorption process.

In this research the isotherm study is carried out using the Langmuir isotherm representation (**Fig. 28**).

The Langmuir model assumes adsorption homogeneity, implying that all adsorption sites are equally available for the adsorbate.

It also assumes the formation of a monolayer of adsorbate on the surface, with no interaction between the adsorbed species.

The maximum adsorption capacity corresponds to the point at which a saturated monolayer of the adsorbate (CV dye) is formed on the surface of the adsorbent [12].

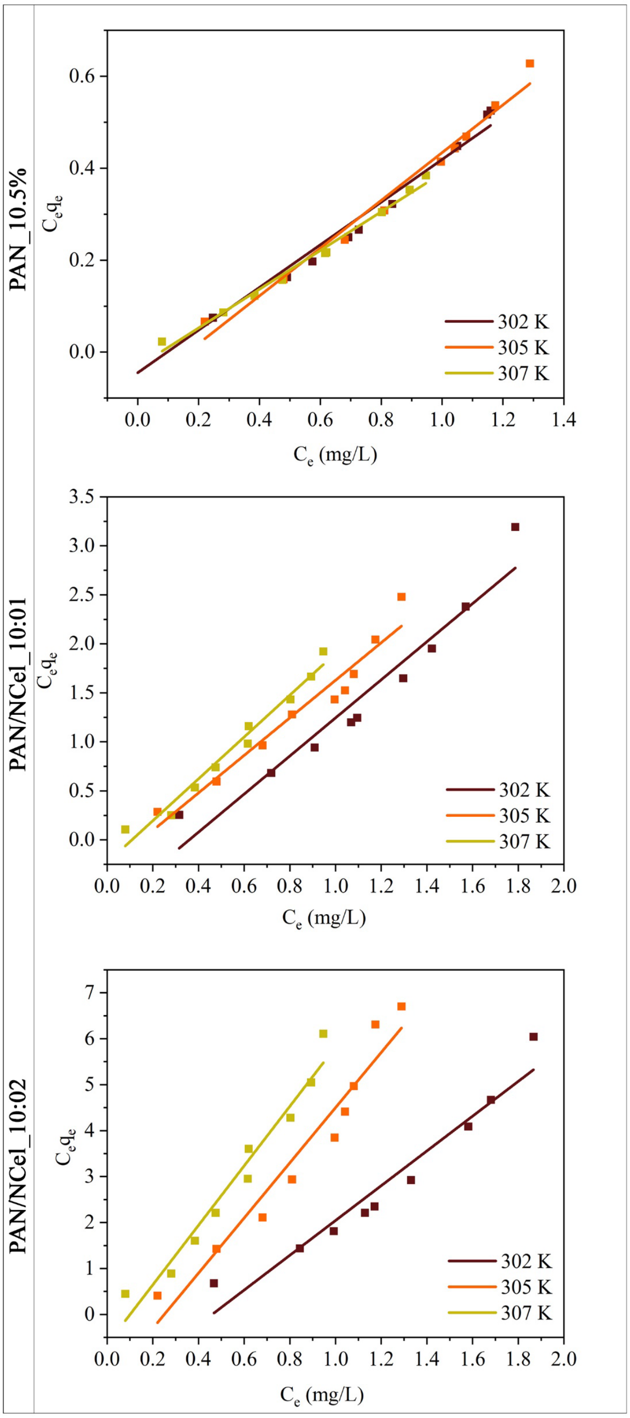

Fig. 26 - *Langmuir isotherm model*

Another factor that is investigated is the effect of initial concentration of NCel in PAN. The graphs in figure **Fig. 29** shows how varying the concentration of NCel in the PAN membranes can influence the absorption removal.

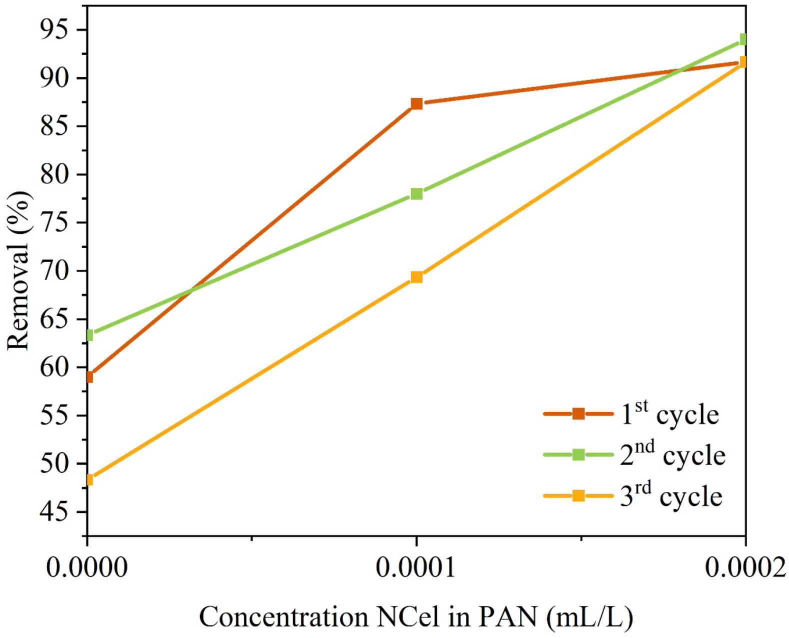

Fig. 27 - *Effect of initial concentration of NCel in PAN*

The membranes are also evaluated in terms of "Performance efficient on reusability" graph in **Fig. 30**.

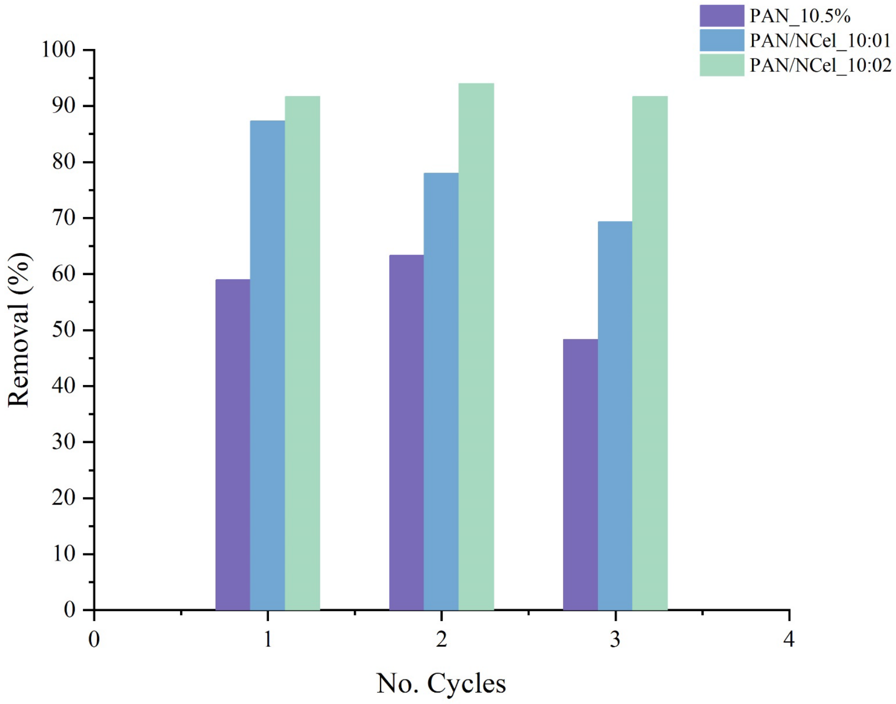

Fig. 28 - *Performance efficient on reusability*

This graph represents how the removal is influenced by consecutive cycles. As can be observed, the performance of removal of PAN/NCel_10:02 emerged to be nearly the same through the three cycles, with a sensible increment in the second cycle. On the contrary, the lowest value of efficiency is attributable to PAN_10.5%. While, PAN/NCel_10:01 shows an intermediate behavior, with a constant reduction of efficiency through the cycles.

In **Tab. 4** are showed different existing materials applied for dye removal through absorption and filtration in wastewater treatment.

Material description	**Synthesis procedure**	**Organic pollutant targeted**	**Adsorbent Analyte**	**Removal efficiency**	**Working pH**	**Ref.**
PANI/PEO membrane	casting	MO	2 g/L 5 mg/L	93.3% 40 min	6.5	[77]
Chitosan/CNCs membrane	casting	Victoria Blue 2B	30x20 mm 1 mg/L	98% 24h	5.01	[78]
Hybrid carbon nanofibers-TiO$_2$ (6 wt.%)-PAN (7 wt.%)	electrospinning	MB	3 × 4 cm^2 2 mg/L	84% 60 min	-	[79]
PVDF membrane	casting	EBT	6.16 cm^2 20 mg/L	83.5% 120 min	7.3	[80]
PAN/biogenic silica	electrospinning	MG	15 mg 10 mg/L	100% 10 min	7.1	[81]
PAN/PVIF	electrospinning	Basic blue 41	0.015 mg/L 10 mg/L	80% 100 min	6	[82]
Graphene oxide/MIL-101(Fe)/PAN-co-maleic acid)	electrospinning	RB	4 mg 5.061mg/20 mL	100% 60 min	4.2	[83]
PAN_10.5%	electrospinning	CV	65x65 mm 0.05 g 3 mg/L	59% 90 min	7	This study
PAN/NCel_10:01	electrospinning	CV	65x65 mm 0.13 g 3 mg/L	87.3% 90 min	7	This study
PAN/NCel_10:02	electrospinning	CV	65x65 mm 0.22 g 3 mg/L	91.7% 90 min	7	This study

Tab. 4 - *Comparative table with existing dye removal methods*

6.2.3 Considerations

The results of the CV dye absorption analysis revealed that the incorporation of NC into the electro-spun PAN membrane led to an improvement in the membrane surface characteristics. The enhancement observed in the membrane surface suggests that the incorporation of NCel could potentially improve the performance and functionality of the membrane for water purification application.

This aspect is highlighted in the results as at higher concentration of NCel in the membranes correspond higher capacity of removal and reusability performance. Therefore, the addition of NCel contributes to the mechanical stability, thermal resistance, and chemical resistance of the polymeric membranes, making them more robust and durable also through different cycles.

Moreover, the effectiveness of the addition of nano-cellulose to PAN-membranes has the advantages of providing an eco-friendlier method to enhance the polymer membranes. This is due to the fact that the synthesized semi-crystalline nano-cellulose is obtained from tissue paper waste and doesn’t present harmful effects on the environment. The importance of this research lies precisely in the concept of sustainability of the synthesis processes and the materials used.

Conclusions

Due to the expanding urbanization and growing population, pollution has emerged as the primary environmental obstacle. Additionally, advancements in technology have introduced new pollutants that are multiplying rapidly and surpassing the environment's natural ability to heal itself. It is crucial to urgently discover technologies that can swiftly and effortlessly lower these pollution levels to a safe state.

The presence of pollutants in the atmosphere and environment is causing can have detrimental effects on human health, ecosystems, and the overall quality of the environment. According to the World Health Organization (WHO), outdoor air pollution is responsible for contributing approximately 0.6 to 1.4 percent of the disease burden in developing regions. Additionally, other forms of pollution, such as lead in water, air, and soil, may contribute around 0.9 percent (World Health Organization, 2002). Moreover, the scarcity of clean water due to contamination of several aquatic sites is a growing issue. The environmental pollution is affecting the natural resources as well as ecosystems.

In this situation of growing concern, nanotechnology is currently being investigated as a potential solution for environmental cleaning and enhancing the effectiveness of traditional approaches. It is also being explored as a means to combat pollution by minimizing the release or inhibiting the formation of pollutants.

Undoubtedly, nanotechnology, especially NPs and organic biopolymers, will bring significant benefits to various areas of environmental technology. However, a major constraint arises from the limited knowledge regarding the toxicity of engineered nanoparticles. The main concerns remain on the disposal and reusability of these materials.

It is clear that that the exploration of the environmental sustainability of nanomaterials is an ongoing process and still requires further investigation. While NCel and TiO_2 NPs hold promise as sustainable and biodegradable nanomaterials, continued research is necessary to fully understand and mitigate any potential risks associated with both. Moreover, further analysis should be undertaken to assess the feasibility of the proposed synthesis methods in terms of costs and standardization of the processes.

However, the reported results show high potential and efficiency in the field of environmental remediation and sustainability providing a method to simultaneously recycle materials and reduce pollution.

Indeed, the importance of the research lies specially in the possibility of transformation and reuse of waste-material to synthesized these valuable “Green” nanomaterials. By valorising industrial and organic waste, more economically convenient ways to contrast pollution can be provided. The opportunity to recycle industrial organic and inorganic waste should be taken in consideration as a concrete option to assess the environmental crisis.

Moreover, the development and utilization of waste-derived nanomaterials also foster innovation and economic growth. It provides opportunities for new industries and businesses to emerge, creating jobs and driving economic development. The integration of waste-derived nanomaterials in various sectors can lead to the development of sustainable and cost-effective solutions, thus improving overall efficiency and reducing the reliance on traditional, resource-intensive processes.

In conclusion, waste-derived nanomaterials offer high potential in addressing various environmental and technological challenges of our time. By harnessing the intrinsic properties of waste materials and transforming them into nanoscale structures, we can unlock a myriad of applications across diverse fields.

However, as any emerging technology, potential environmental and health risks need to be thoroughly assessed and managed. Adequate regulations, standardized protocols, and responsible practices are necessary to ensure the safe and sustainable implementation of waste-derived nanomaterials.

The present research represents one of the numerous possibilities for the application of waste-derived sustainable nanomaterials to mitigate the current environmental emergency.

Bibliography

[1] J. E. Post and B. W. Altma, “Managing the Environmental Change Process: Barriers and Opportunities,” *Journal of Organizational Change Management*, vol. 7, no. 4, pp. 64–81, Aug. 1994, doi: 10.1108/09534819410061388.

[2] X. Ma, T. Zhang, C. Ji, Y. Zhai, X. Shen, and J. Hong, “Threats to human health and ecosystem: Looking for air-pollution related damage since 1990,” *Renewable and Sustainable Energy Reviews*, vol. 145, p. 111146, Jul. 2021, doi: 10.1016/j.rser.2021.111146.

[3] Z. KILIÇ, “Water Pollution: Causes, Negative Effects and Prevention Methods,” *İstanbul Sabahattin Zaim Üniversitesi Fen Bilimleri Enstitüsü Dergisi*, vol. 3, no. 2, pp. 129–132, Aug. 2021, doi: 10.47769/izufbed.862679.

[4] S. Wong *et al.*, “Adsorption of anionic dyes on spent tea leaves modified with polyethyleneimine (PEI-STL),” *J Clean Prod*, vol. 206, pp. 394–406, Jan. 2019, doi: 10.1016/j.jclepro.2018.09.201.

[5] C. Bhattacharjee, S. Dutta, and V. K. Saxena, “A review on biosorptive removal of dyes and heavy metals from wastewater using watermelon rind as biosorbent,” *Environmental Advances*, vol. 2, p. 100007, Dec. 2020, doi: 10.1016/j.envadv.2020.100007.

[6] S. Ortiz-Monsalve, J. Dornelles, E. Poll, M. Ramirez-Castrillón, P. Valente, and M. Gutterres, “Biodecolourisation and biodegradation of leather dyes by a native isolate of Trametes villosa,” *Process Safety and Environmental Protection*, vol. 109, pp. 437–451, Jul. 2017, doi: 10.1016/j.psep.2017.04.028.

[7] J. Zhu *et al.*, “Adsorption of phosphate and photodegradation of cationic dyes with BiOI in phosphate-cationic dye binary system,” *Sep Purif Technol*, vol. 223, pp. 196–202, Sep. 2019, doi: 10.1016/j.seppur.2019.04.079.

[8] G. Ramírez, F. J. Recio, P. Herrasti, C. Ponce-de-León, and I. Sirés, “Effect of RVC porosity on the performance of PbO2 composite coatings with titanate nanotubes for the electrochemical oxidation of azo dyes,” *Electrochim Acta*, vol. 204, pp. 9–17, Jun. 2016, doi: 10.1016/j.electacta.2016.04.054.

[9] M. R. F. Silva, M. A. O. Lourenço, D. M. Tobaldi, C. F. da Silva, M. P. Seabra, and P. Ferreira, “Carbon-modified titanium oxide materials for photocatalytic water and air decontamination,” *Chemical Engineering Journal*, vol. 387, p. 124099, May 2020, doi: 10.1016/J.CEJ.2020.124099.

[10] Y. jie Song *et al.*, "TiO2/carbon composites from waste sawdust for methylene blue photodegradation," *Diam Relat Mater*, vol. 136, p. 109918, Jun. 2023, doi: 10.1016/J.DIAMOND.2023.109918.

[11] I. Khan, K. Saeed, and I. Khan, "Nanoparticles: Properties, applications and toxicities," *Arabian Journal of Chemistry*, vol. 12, no. 7, pp. 908–931, Nov. 2019, doi: 10.1016/j.arabjc.2017.05.011.

[12] S. Patel and G. Hota, "Synthesis of novel surface functionalized electrospun PAN nanofibers matrix for efficient adsorption of anionic CR dye from water," *J Environ Chem Eng*, vol. 6, no. 4, pp. 5301–5310, Aug. 2018, doi: 10.1016/j.jece.2018.08.013.

[13] T. Fleischer and A. Grunwald, "Making nanotechnology developments sustainable. A role for technology assessment?," *J Clean Prod*, vol. 16, no. 8–9, pp. 889–898, May 2008, doi: 10.1016/J.JCLEPRO.2007.04.018.

[14] D. Gupta, A. Boora, A. Thakur, and T. K. Gupta, "Green and sustainable synthesis of nanomaterials: Recent advancements and limitations," *Environ Res*, vol. 231, p. 116316, Aug. 2023, doi: 10.1016/J.ENVRES.2023.116316.

[15] I. Corsi *et al.*, "Ecofriendly nanotechnologies and nanomaterials for environmental applications: Key issue and consensus recommendations for sustainable and ecosafe nanoremediation," *Ecotoxicol Environ Saf*, vol. 154, pp. 237–244, Jun. 2018, doi: 10.1016/J.ECOENV.2018.02.037.

[16] J. Zambrano, R. Irusta-Mata, J. J. Jiménez, S. Bolado, and P. A. García-Encina, "Photocatalytic removal of emerging contaminants in water and wastewater treatments: a review," in *Development in Wastewater Treatment Research and Processes*, Elsevier, 2022, pp. 543–572. doi: 10.1016/B978-0-323-85583-9.00023-5.

[17] A. C. Mecha, M. S. Onyango, A. Ochieng, T. S. Jamil, C. J. S. Fourie, and M. N. B. Momba, "UV and solar light photocatalytic removal of organic contaminants in municipal wastewater," *Sep Sci Technol*, vol. 51, no. 10, pp. 1765–1778, Jul. 2016, doi: 10.1080/01496395.2016.1178290.

[18] M. J. Mattle and K. R. Thampi, "Photocatalytic degradation of Remazol Brilliant Blue® by sol–gel derived carbon-doped TiO2," *Appl Catal B*, vol. 140–141, pp. 348–355, Aug. 2013, doi: 10.1016/J.APCATB.2013.04.020.

[19] Momina and K. Ahmad, "Feasibility of the adsorption as a process for its large scale adoption across industries for the treatment of wastewater: Research gaps and economic assessment," *J Clean Prod*, vol. 388, p. 136014, Feb. 2023, doi: 10.1016/j.jclepro.2023.136014.

[20] B. S. Muthukrishnan S, S. M. Muthukumar M, and S. K. T. Rao MV, "Catalytic Degradation of Organic Dyes using Synthesized Silver Nanoparticles: A Green Approach," *J Bioremediat Biodegrad*, vol. 06, no. 05, 2015, doi: 10.4172/2155-6199.1000312.

[21] A. Bhatnagar, W. Hogland, M. Marques, and M. Sillanpää, "An overview of the modification methods of activated carbon for its water treatment applications," *Chemical Engineering Journal*, vol. 219, pp. 499–511, Mar. 2013, doi: 10.1016/j.cej.2012.12.038.

[22] A. Bhatnagar, M. Sillanpää, and A. Witek-Krowiak, "Agricultural waste peels as versatile biomass for water purification – A review," *Chemical Engineering Journal*, vol. 270, pp. 244–271, Jun. 2015, doi: 10.1016/J.CEJ.2015.01.135.

[23] I. Corsi, I. Venditti, F. Trotta, and C. Punta, "Environmental safety of nanotechnologies: The eco-design of manufactured nanomaterials for environmental remediation," *Science of The Total Environment*, vol. 864, p. 161181, Mar. 2023, doi: 10.1016/J.SCITOTENV.2022.161181.

[24] R. V. Bordiwala, "Green synthesis and Applications of Metal Nanoparticles.- A Review Article," *Results Chem*, vol. 5, p. 100832, Jan. 2023, doi: 10.1016/j.rechem.2023.100832.

[25] *Advanced Materials for Sustainable Environmental Remediation*. Elsevier, 2022. doi: 10.1016/C2020-0-03311-6.

[26] K. Scida, P. W. Stege, G. Haby, G. A. Messina, and C. D. García, "Recent applications of carbon-based nanomaterials in analytical chemistry: Critical review," *Anal Chim Acta*, vol. 691, no. 1–2, pp. 6–17, Apr. 2011, doi: 10.1016/j.aca.2011.02.025.

[27] J. Jordan, K. I. Jacob, R. Tannenbaum, M. A. Sharaf, and I. Jasiuk, "Experimental trends in polymer nanocomposites—a review," *Materials Science and Engineering: A*, vol. 393, no. 1–2, pp. 1–11, Feb. 2005, doi: 10.1016/j.msea.2004.09.044.

[28] Vishal J. Lingayat, Nilesh S. Zarekar, and Rajan S. Shendge, "Solid Lipid Nanoparticles: A Review", doi: 10.12691/nnr-4-2-5.

[29] A. A. H. Abdellatif and A. F. Alsowinea, "Approved and marketed nanoparticles for disease targeting and applications in COVID-19," *Nanotechnol Rev*, vol. 10, no. 1, pp. 1941–1977, Nov. 2021, doi: 10.1515/ntrev-2021-0115.

[30] N. Abid *et al.*, "Synthesis of nanomaterials using various top-down and bottom-up approaches, influencing factors, advantages, and disadvantages:

A review," *Adv Colloid Interface Sci*, vol. 300, p. 102597, Feb. 2022, doi: 10.1016/j.cis.2021.102597.

[31] G. M. Nair, T. Sajini, and B. Mathew, "Advanced green approaches for metal and metal oxide nanoparticles synthesis and their environmental applications," *Talanta Open*, vol. 5, p. 100080, Aug. 2022, doi: 10.1016/J.TALO.2021.100080.

[32] M. Bundschuh *et al.*, "Nanoparticles in the environment: where do we come from, where do we go to?," *Environ Sci Eur*, vol. 30, no. 1, p. 6, Dec. 2018, doi: 10.1186/s12302-018-0132-6.

[33] P. Anastas and N. Eghbali, "Green Chemistry: Principles and Practice," *Chem. Soc. Rev.*, vol. 39, no. 1, pp. 301–312, 2010, doi: 10.1039/B918763B.

[34] I. T. Horváth and P. T. Anastas, "Innovations and Green Chemistry," *Chem Rev*, vol. 107, no. 6, pp. 2169–2173, Jun. 2007, doi: 10.1021/cr078380v.

[35] S. Ying *et al.*, "Green synthesis of nanoparticles: Current developments and limitations," *Environ Technol Innov*, vol. 26, p. 102336, May 2022, doi: 10.1016/j.eti.2022.102336.

[36] J. Virkutyte and R. S. Varma, "Green Synthesis of Nanomaterials: Environmental Aspects," 2013, pp. 11–39. doi: 10.1021/bk-2013-1124.ch002.

[37] N. A. I. Md Ishak, S. K. Kamarudin, and S. N. Timmiati, "Green synthesis of metal and metal oxide nanoparticles via plant extracts: an overview," *Mater Res Express*, vol. 6, no. 11, p. 112004, Oct. 2019, doi: 10.1088/2053-1591/ab4458.

[38] J. C. Védrine, "Metal Oxides in Heterogeneous Oxidation Catalysis: State of the Art and Challenges for a More Sustainable World," *ChemSusChem*, vol. 12, no. 3, pp. 577–588, Feb. 2019, doi: 10.1002/cssc.201802248.

[39] E. Roduner, "Understanding catalysis," *Chem. Soc. Rev.*, vol. 43, no. 24, pp. 8226–8239, 2014, doi: 10.1039/C4CS00210E.

[40] S. B. Kalidindi and B. R. Jagirdar, "Nanocatalysis and Prospects of Green Chemistry," *ChemSusChem*, vol. 5, no. 1, pp. 65–75, Jan. 2012, doi: 10.1002/cssc.201100377.

[41] W. S. Koe, J. W. Lee, W. C. Chong, Y. L. Pang, and L. C. Sim, "An overview of photocatalytic degradation: photocatalysts, mechanisms, and development of photocatalytic membrane," *Environmental Science and Pollution Research*, vol. 27, no. 3, pp. 2522–2565, Jan. 2020, doi: 10.1007/s11356-019-07193-5.

[42] E. Pelizzetti and N. Serpone, Eds., *Homogeneous and Heterogeneous Photocatalysis*. Dordrecht: Springer Netherlands, 1986. doi: 10.1007/978-94-009-4642-2.

[43] R. M. Navarro, M. C. Sánchez-Sánchez, M. C. Alvarez-Galvan, F. del Valle, and J. L. G. Fierro, "Hydrogen production from renewable sources: biomass and photocatalytic opportunities," *Energy Environ. Sci.*, vol. 2, no. 1, pp. 35–54, 2009, doi: 10.1039/B808138G.

[44] N. Serpone, "Photocatalysis," in *Kirk-Othmer Encyclopedia of Chemical Technology*, Hoboken, NJ, USA: John Wiley & Sons, Inc., 2000. doi: 10.1002/0471238961.1608152019051816.a01.

[45] *Advanced Oxidation Processes for Waste Water Treatment*. Elsevier, 2018. doi: 10.1016/C2016-0-00384-4.

[46] P. Singh Jassal, D. Kaur, R. Prasad, and J. Singh, "Green synthesis of titanium dioxide nanoparticles: Development and applications," *J Agric Food Res*, vol. 10, p. 100361, Dec. 2022, doi: 10.1016/j.jafr.2022.100361.

[47] H. Mahmoudi *et al.*, "A review of Fischer Tropsch synthesis process, mechanism, surface chemistry and catalyst formulation," *Biofuels Engineering*, vol. 2, no. 1, pp. 11–31, Dec. 2017, doi: 10.1515/bfuel-2017-0002.

[48] D. Martín-Yerga, J. Carrasco-Rodríguez, J. L. G. Fierro, F. J. García Alonso, and A. Costa-García, "Copper-modified titanium phosphate nanoparticles as electrocatalyst for glucose detection," *Electrochim Acta*, vol. 229, pp. 102–111, Mar. 2017, doi: 10.1016/j.electacta.2017.01.143.

[49] S. Guo, S. Han, B. Chi, J. Pu, and J. Li, "Synthesis of shape-controlled mesoporous titanium phosphate nanocrystals: The hexagonal titanium phosphate with enhanced hydrogen generation from water splitting," *Int J Hydrogen Energy*, vol. 39, no. 6, pp. 2446–2453, Feb. 2014, doi: 10.1016/j.ijhydene.2013.12.007.

[50] L. Kőrösi and I. Dékány, "Preparation and investigation of structural and photocatalytic properties of phosphate modified titanium dioxide," *Colloids Surf A Physicochem Eng Asp*, vol. 280, no. 1–3, pp. 146–154, Jun. 2006, doi: 10.1016/j.colsurfa.2006.01.052.

[51] P. Phanthong, P. Reubroycharoen, X. Hao, G. Xu, A. Abudula, and G. Guan, "Nanocellulose: Extraction and application," *Carbon Resources Conversion*, vol. 1, no. 1, pp. 32–43, Apr. 2018, doi: 10.1016/j.crcon.2018.05.004.

[52] A. Q. Almashhadani, C. P. Leh, S.-Y. Chan, C. Y. Lee, and C. F. Goh, "Nanocrystalline cellulose isolation via acid hydrolysis from non-woody

biomass: Importance of hydrolysis parameters," *Carbohydr Polym*, vol. 286, p. 119285, Jun. 2022, doi: 10.1016/j.carbpol.2022.119285.

[53] V. A. Barbash, O. V. Yashchenko, and O. A. Vasylieva, "Preparation and Properties of Nanocellulose from *Miscanthus x giganteus*," *J Nanomater*, vol. 2019, pp. 1–8, Nov. 2019, doi: 10.1155/2019/3241968.

[54] A. Dufresne, "Nanocellulose: a new ageless bionanomaterial," *Materials Today*, vol. 16, no. 6, pp. 220–227, Jun. 2013, doi: 10.1016/j.mattod.2013.06.004.

[55] A. Dufresne, "Nanocellulose: a new ageless bionanomaterial," *Materials Today*, vol. 16, no. 6, pp. 220–227, Jun. 2013, doi: 10.1016/j.mattod.2013.06.004.

[56] Q. Li, S. McGinnis, C. Sydnor, A. Wong, and S. Renneckar, "Nanocellulose Life Cycle Assessment," *ACS Sustain Chem Eng*, vol. 1, no. 8, pp. 919–928, Aug. 2013, doi: 10.1021/sc4000225.

[57] A. Gul, J. Hruza, L. Dvorak, and F. Yalcinkaya, "Chemical Cleaning Process of Polymeric Nanofibrous Membranes," *Polymers (Basel)*, vol. 14, no. 6, p. 1102, Mar. 2022, doi: 10.3390/polym14061102.

[58] V. Mangematin and S. Walsh, "The future of nanotechnologies," *Technovation*, vol. 32, no. 3–4, pp. 157–160, Mar. 2012, doi: 10.1016/j.technovation.2012.01.003.

[59] N. A. A. M. Amin, M. A. Mokhter, N. Salamun, M. F. bin Mohamad, and W. M. A. W. Mahmood, "Anti-fouling electrospun organic and inorganic nanofiber membranes for wastewater treatment," *S Afr J Chem Eng*, vol. 44, pp. 302–317, Apr. 2023, doi: 10.1016/j.sajce.2023.02.002.

[60] N. Bhardwaj and S. C. Kundu, "Electrospinning: A fascinating fiber fabrication technique," *Biotechnol Adv*, vol. 28, no. 3, pp. 325–347, May 2010, doi: 10.1016/j.biotechadv.2010.01.004.

[61] W. S. Khan, R. Asmatulu, M. Ceylan, and A. Jabbarnia, "Recent progress on conventional and non-conventional electrospinning processes," *Fibers and Polymers*, vol. 14, no. 8, pp. 1235–1247, Aug. 2013, doi: 10.1007/s12221-013-1235-8.

[62] X. Shi, G. Tal, N. P. Hankins, and V. Gitis, "Fouling and cleaning of ultrafiltration membranes: A review," *Journal of Water Process Engineering*, vol. 1, pp. 121–138, Apr. 2014, doi: 10.1016/j.jwpe.2014.04.003.

[63] S. K. Nataraj, K. S. Yang, and T. M. Aminabhavi, "Polyacrylonitrile-based nanofibers—A state-of-the-art review," *Prog Polym Sci*, vol. 37, no. 3, pp. 487–513, Mar. 2012, doi: 10.1016/j.progpolymsci.2011.07.001.

[64] A. Mohamed, T. A. Osman, M. S. Toprak, M. Muhammed, and A. Uheida, "Surface functionalized composite nanofibers for efficient removal of arsenic from aqueous solutions," *Chemosphere*, vol. 180, pp. 108–116, Aug. 2017, doi: 10.1016/j.chemosphere.2017.04.011.

[65] D. Wang *et al.*, "Composite membranes of polyacrylonitrile cross-linked with cellulose nanocrystals for emulsion separation and regeneration," *Compos Part A Appl Sci Manuf*, vol. 164, p. 107300, Jan. 2023, doi: 10.1016/j.compositesa.2022.107300.

[66] A. P. Jones, "Indoor air quality and health," *Atmos Environ*, vol. 33, no. 28, pp. 4535–4564, Dec. 1999, doi: 10.1016/S1352-2310(99)00272-1.

[67] Y. Gu, K. Xia, D. Wu, J. Mou, and S. Zheng, "Technical Characteristics and Wear-Resistant Mechanism of Nano Coatings: A Review," *Coatings*, vol. 10, no. 3, p. 233, Mar. 2020, doi: 10.3390/coatings10030233.

[68] P. Nguyen-Tri *et al.*, "Recent progress in the preparation, properties and applications of superhydrophobic nano-based coatings and surfaces: A review," *Prog Org Coat*, vol. 132, pp. 235–256, Jul. 2019, doi: 10.1016/j.porgcoat.2019.03.042.

[69] J. Auvinen and L. Wirtanen, "The influence of photocatalytic interior paints on indoor air quality," *Atmos Environ*, vol. 42, no. 18, pp. 4101–4112, Jun. 2008, doi: 10.1016/j.atmosenv.2008.01.031.

[70] L. Hochmannova and J. Vytrasova, "Photocatalytic and antimicrobial effects of interior paints," *Prog Org Coat*, vol. 67, no. 1, pp. 1–5, Jan. 2010, doi: 10.1016/j.porgcoat.2009.09.016.

[71] S. Banerjee, D. D. Dionysiou, and S. C. Pillai, "Self-cleaning applications of TiO2 by photo-induced hydrophilicity and photocatalysis," *Appl Catal B*, vol. 176–177, pp. 396–428, Oct. 2015, doi: 10.1016/j.apcatb.2015.03.058.

[72] X. Zhang *et al.*, "Superhydrophobic TiO $_2$ Surfaces: Preparation, Photocatalytic Wettability Conversion, and Superhydrophobic−Superhydrophilic Patterning," *The Journal of Physical Chemistry C*, vol. 111, no. 39, pp. 14521–14529, Oct. 2007, doi: 10.1021/jp0744432.

[73] V. Etacheri, C. Di Valentin, J. Schneider, D. Bahnemann, and S. C. Pillai, "Visible-light activation of TiO2 photocatalysts: Advances in theory and experiments," *Journal of Photochemistry and Photobiology C:*

Photochemistry Reviews, vol. 25, pp. 1–29, Dec. 2015, doi: 10.1016/j.jphotochemrev.2015.08.003.

[74] Q. Maqbool, G. Barucca, S. Sabbatini, M. Parlapiano, M. L. Ruello, and F. Tittarelli, “Transformation of industrial and organic waste into titanium doped activated carbon – cellulose nanocomposite for rapid removal of organic pollutants,” *J Hazard Mater*, vol. 423, p. 126958, Feb. 2022, doi: 10.1016/j.jhazmat.2021.126958.

[75] R. Hashaikeh and H. Abushammala, “Acid mediated networked cellulose: Preparation and characterization,” *Carbohydr Polym*, vol. 83, no. 3, pp. 1088–1094, Jan. 2011, doi: 10.1016/j.carbpol.2010.08.081.

[76] H. Qiu, L. Lv, B. Pan, Q. Zhang, W. Zhang, and Q. Zhang, “Critical review in adsorption kinetic models,” *Journal of Zhejiang University-SCIENCE A*, vol. 10, no. 5, pp. 716–724, May 2009, doi: 10.1631/jzus.A0820524.

[77] E. S. Mansor, H. Ali, and A. Abdel-Karim, “Efficient and reusable polyethylene oxide/polyaniline composite membrane for dye adsorption and filtration,” *Colloid Interface Sci Commun*, vol. 39, p. 100314, Nov. 2020, doi: 10.1016/j.colcom.2020.100314.

[78] Z. Karim, A. P. Mathew, M. Grahn, J. Mouzon, and K. Oksman, “Nanoporous membranes with cellulose nanocrystals as functional entity in chitosan: Removal of dyes from water,” *Carbohydr Polym*, vol. 112, pp. 668–676, Nov. 2014, doi: 10.1016/j.carbpol.2014.06.048.

[79] P. S. Kumar, K. Venkatesh, E. L. Gui, S. Jayaraman, G. Singh, and G. Arthanareeswaran, “Electrospun carbon nanofibers/TiO2-PAN hybrid membranes for effective removal of metal ions and cationic dye,” *Environ Nanotechnol Monit Manag*, vol. 10, pp. 366–376, Dec. 2018, doi: 10.1016/j.enmm.2018.08.006.

[80] T. T. Van Tran, S. R. Kumar, and S. J. Lue, “Separation mechanisms of binary dye mixtures using a PVDF ultrafiltration membrane: Donnan effect and intermolecular interaction,” *J Memb Sci*, vol. 575, pp. 38–49, Apr. 2019, doi: 10.1016/j.memsci.2018.12.070.

[81] A. Mohamed, M. M. Ghobara, M. K. Abdelmaksoud, and G. G. Mohamed, “A novel and highly efficient photocatalytic degradation of malachite green dye via surface modified polyacrylonitrile nanofibers/biogenic silica composite nanofibers,” *Sep Purif Technol*, vol. 210, pp. 935–942, Feb. 2019, doi: 10.1016/j.seppur.2018.09.014.

[82] Z. Mokhtari-Shourijeh, L. Montazerghaem, and M. E. Olya, “Preparation of Porous Nanofibers from Electrospun Polyacrylonitrile/Polyvinylidene

Fluoride Composite Nanofibers by Inexpensive Salt Using for Dye Adsorption," *J Polym Environ*, vol. 26, no. 9, pp. 3550–3563, Sep. 2018, doi: 10.1007/s10924-018-1238-z.

[83] P. G. Abadi, M. Irani, and L. R. Rad, "Mechanisms of the removal of the metal ions, dyes, and drugs from wastewaters by the electrospun nanofiber membranes," *J Taiwan Inst Chem Eng*, vol. 143, p. 104625, Feb. 2023, doi: 10.1016/j.jtice.2022.104625.

[84] https://www.boero.it/prodotto/pittura-autopulente-fotocatalitica-silossanica-solarya-65/

Acknowledgements

I would like to begin by expressing my gratitude to my supervisor, Professor Francesca Tittarelli, for their invaluable guidance and unwavering patience in assisting me with the preparation of this paper.

Equally significant was the support and timely advice provided by my co-supervisor, Dr. Qaisar Maqbool, who offered constructive criticism that greatly contributed to the refinement of my work.

In primo luogo vorrei ringraziare mia madre Chiara, mio padre Paride e i miei due fratelli Alan e Riccardo, per l'affetto e l'appoggio ricevuto in questi anni in ogni scelta corretta o sbagliata che ha accompagnato questo percorso.

Un ringraziamento particolare va anche a mio zio Enrico e mio nonno Domenico che con la loro saggezza e bontà d'animo hanno contribuito a crescermi fin da quando ero bambina.

Un grazie anche a mia nonna, Luisa, che anche se non è qui per condividere questo traguardo mi ha insegnato tanto della vita.

Un ringraziamento a tutta la mia famiglia, ai miei zii e numerosi cugini che mi hanno dimostrato affetto e hanno partecipato dal primo giorno a questa esperienza.

Vorrei anche ringraziare il mio fidanzato, Dario, per aver creduto in me durante la parte più complicata del mio percorso e per il continuo incoraggiamento a dare sempre il meglio di me stessa.

Un grazie alla mia amica di sempre, Eleonora, che mi accompagna da tutta la vita e che ha alleggerito i miei momenti più pesanti con la sua spensieratezza e voglia di vivere.

Un ringraziamento sentito va anche alle due persone che hanno intrapreso con me questa avventura.

Eleonora, che mi ha supportata e sopportata in tutto, la mia compagna di banco dai primi momenti ma anche un'amica.

Barbara, che con la sua positività e voglia di fare mi ha spronata a dare il meglio e ha alleggerito le giornate di studio "matto e disperatissimo".

Infine, un grazie generale va a tutti le persone e gli amici, lontani e vicini, che mi hanno sostenuta, accompagnata e soprattutto sopportata in questi anni rendendo la strada verso il traguardo più semplice e meno in salita.